Lecture 13: Glass Finishing (Grinding & Polishing)

Glass Processing Course (Lehigh University; Spring 2015)
International Materials Institute for New Functionality in Glass (IMI-NFG)
March 5, 2015 1:00 -2:15 pm (EST)

Tayyab Suratwala suratwala1@llnl.gov

Lawrence Livermore National Laboratory

LLNL-PRES-668080
This work was performed under the auspices of the U.S. Department of Energy by Lawrence Livermore National Laboratory under Contract DE-AC52-07NA27344. Lawrence Livermore National Security, LLC

Useful Reading Material

H. Karow, “Fabrication Methods of Precision Optics” John Wiley & Sons (1993)

N. Brown, “Optical Fabrication” LLNL Report MISC4476 (August 1989)

L. Cook, “Chemical Processes in Glass Polishing” Journal of Non-Crystalline Solids 120 (1990) 152-171

T. Izumatani, “Optical Glass” (Kyoritsu Shuppan Company, Tokyo 1984; Lawrence Livermore National Laboratory (USA); American Institute of Physics (New York 1986)

D. Anderson, J. Burge, “The Handbook of Optical Engineering: Chapter 28: Optical Fabrication”

D. Malacara, “Optical Shot Testing” Wiley-Interscience (2007)

Other references quoted through the presentation

What is optical fabrication?

The objective of optical fabrication is to manufacture an optical element (e.g., lense, flat, mirror, active optic) which is often made of glass

Key Requirements

1) Surface Figure (affects wavefront)

2) Surface Quality (affects scatter and laser damage resistance)
   a) Roughness
   b) Sub-surface damage (scratch/dig)

An example of specifying the requirements of an optic

Power Spectral Density for Optic Surface

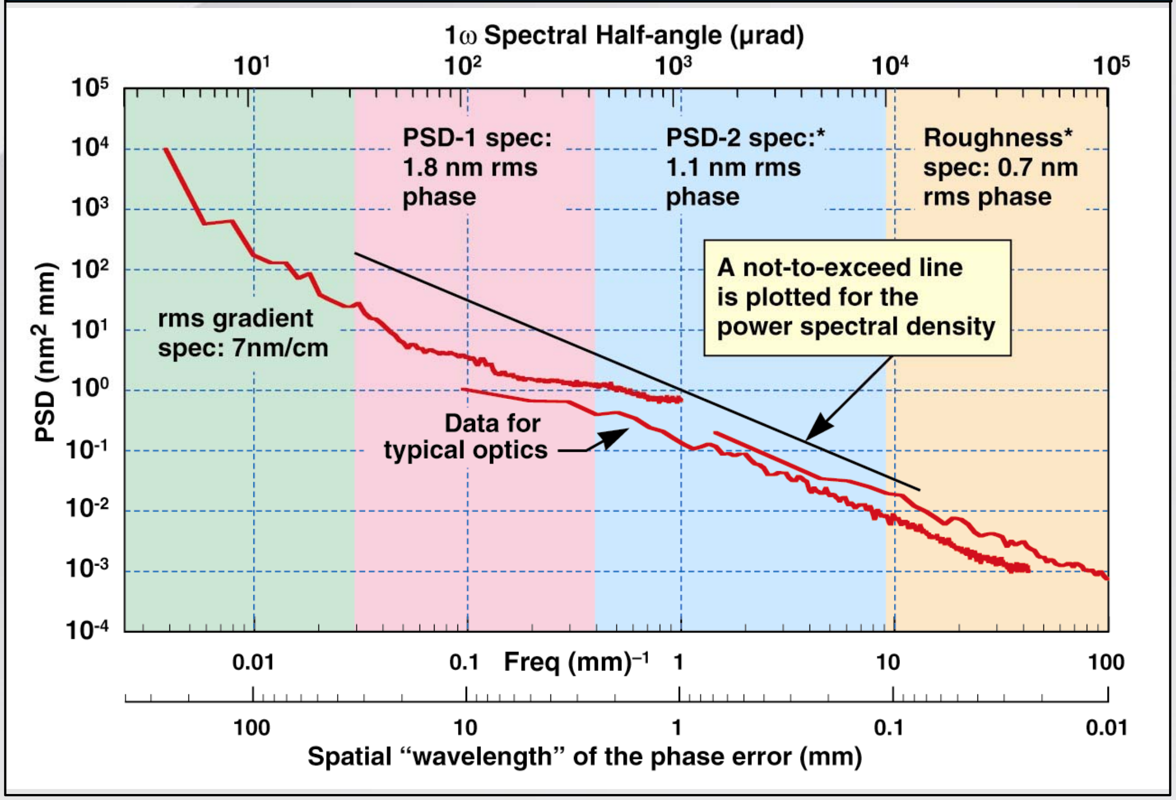

High Level Requirements[1]

Surface

Peak-to-Valley	211 nm (λ/3)
Gradient	<7 nm/cm
PSD1	1.8 nm
PSD2	1.1 nm
Roughness	4-10 Ang
Scratch/Dig[2]	20/10

Bulk

Homogeniety	<5 ppm
Inclusions(>5um)	0
Lenslets	0

[1] For typical 3ω NIF optics; [2] Post-etch with number of scratches (width>8μm) <12-50

Typical steps of an optical fabrication process

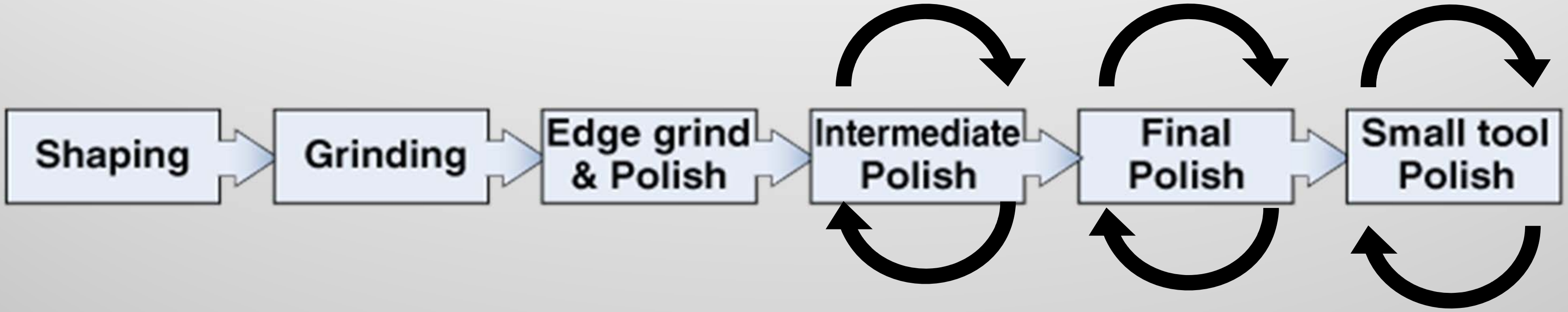

Shaping

Grinding

Edge grind & Polish

Intermediate Polish

Final Polish

Small tool Polish

Examples of grinding techniques

Examples of polishing techniques

The materials science behind grinding & polishing

1. Sub-surface Damage (scratch/dig)
2. Roughness
3. Surface Figure

There are numerous mechanical, structural and chemical effects on the glass surface during grinding and polishing

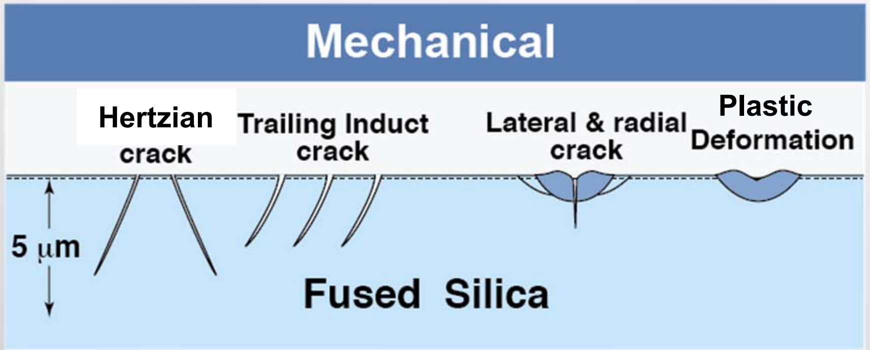

There are numerous mechanical, structural and chemical effects on the glass surface during grinding and polishing

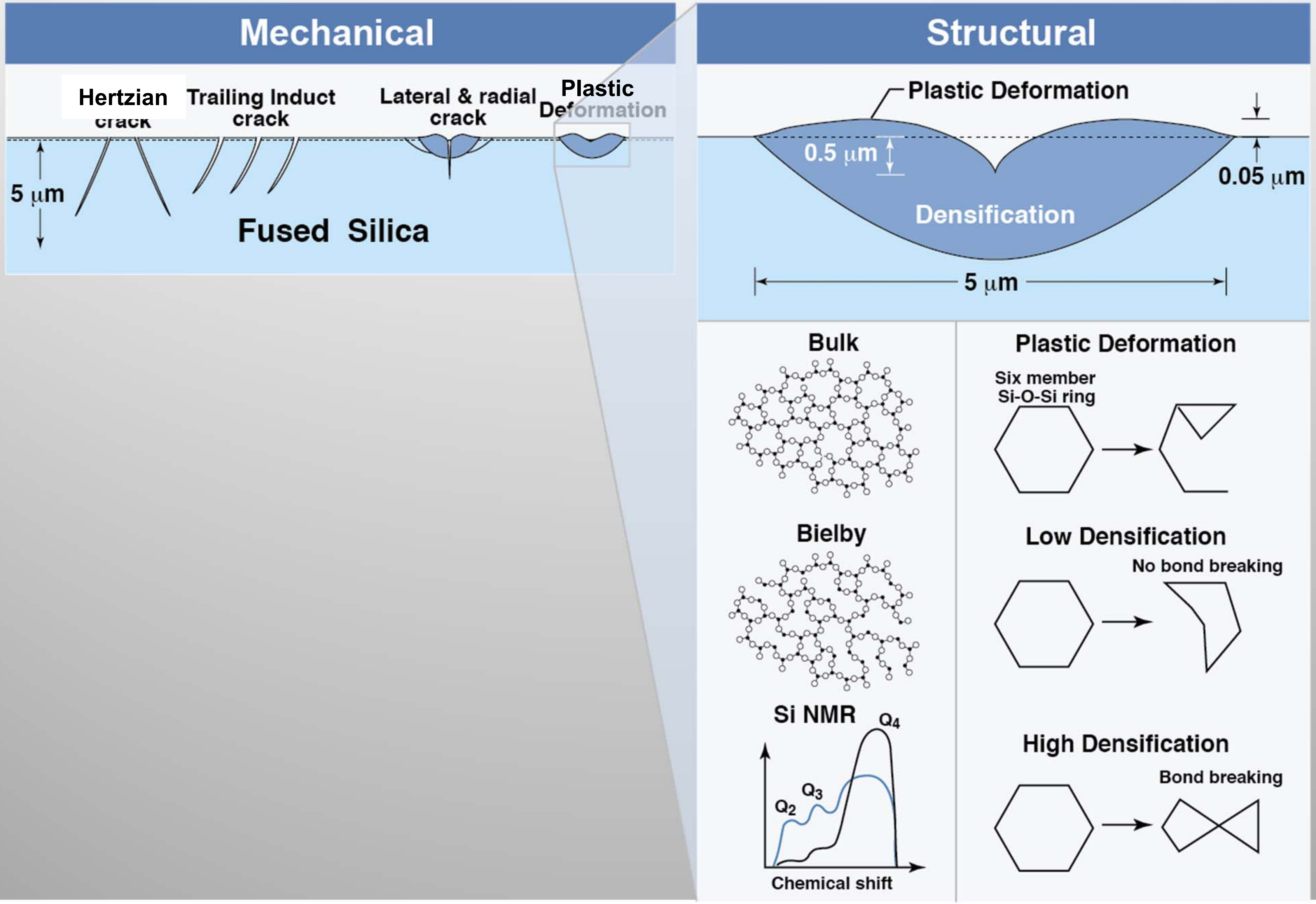

There are numerous mechanical, structural and chemical effects on the glass surface during grinding and polishing

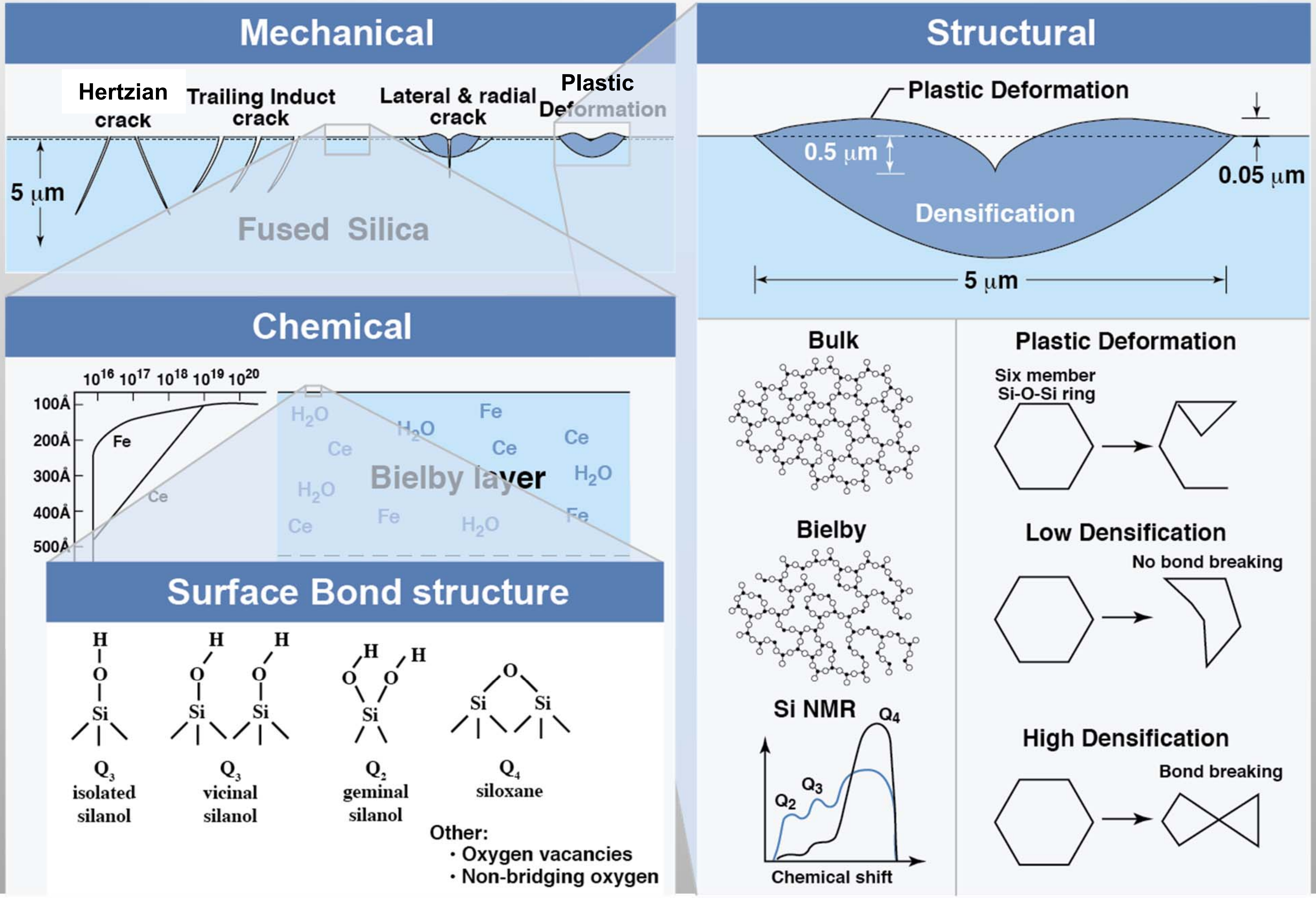

The load/particle determines the removal mechanism

Brittle Removal
Grinding or scratching

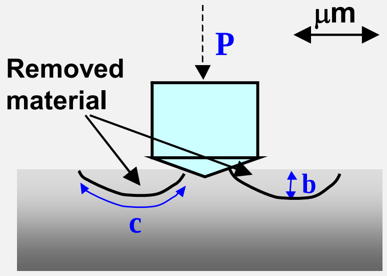

$P_{crit} > 0.1$ N

- Material within lateral cracks are removed (grinding process)
- Leads to scratches

Plastic Removal
Ductile Polishing

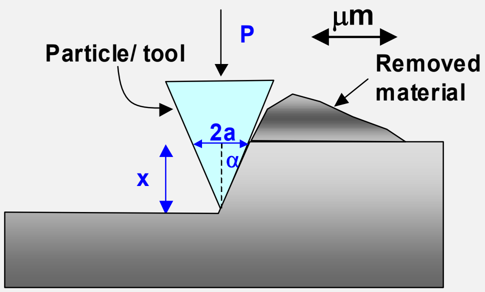

$P_{crit} > 5x10^{-5}$ N

- Portion of deformed material removed
- Leads to plastic scratches or sleeks
- Determined removal amount ~1 nm

Chemical removal
Chemical Polishing

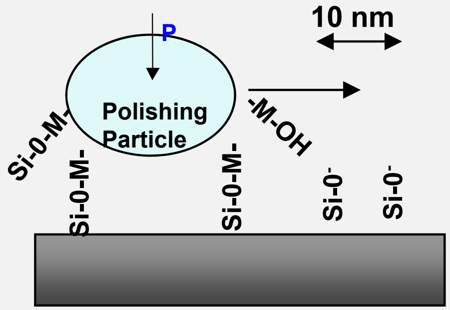

$P_{crit} < 5x10^{-5}$ N

- Removal at the molecular level ($Si(OH)_4$) by condensation & hydrolysis
- Creates smooth surface
- Determined removal amount ~0.04 nm

Approach for the management of sub-surface fractures (i.e. scratches/digs)

Schematic of material removal during various steps of the grinding/polishing process illustrating surface fracture removal

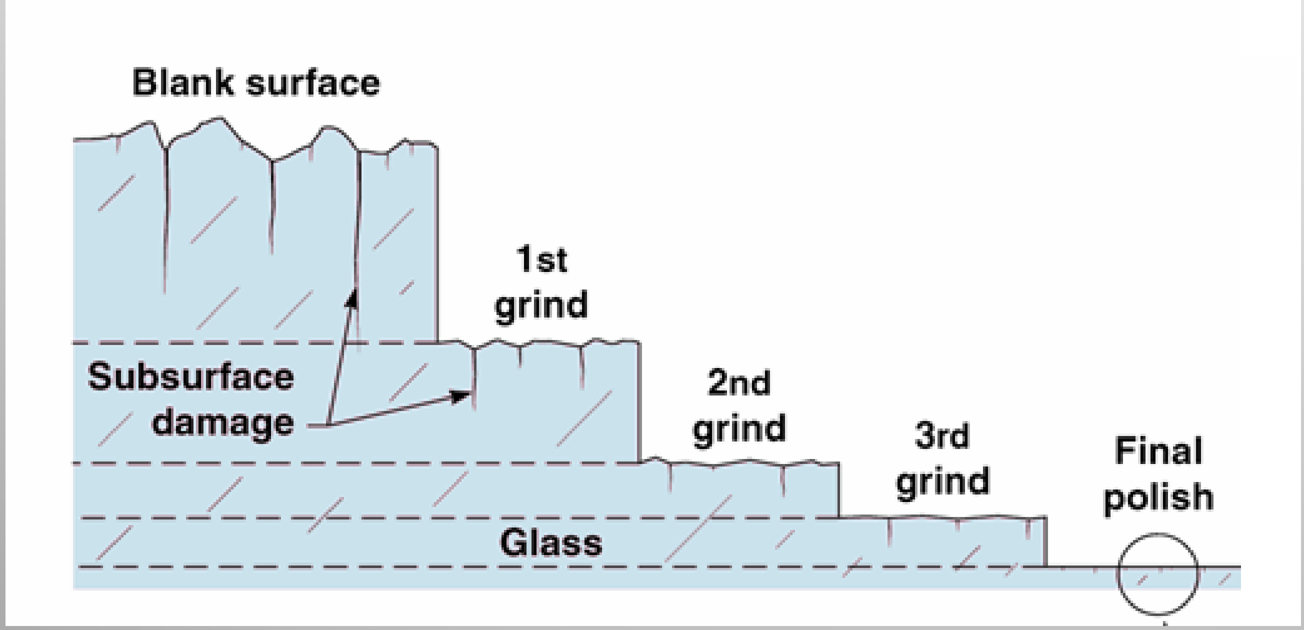

- Removal at each step is aimed at removal of deepest damage decreasing it to the level of deepest damage expected at current step (most economical design)
- Note each subsequent step has much lower removal rate
- This approach has been generally followed for hundreds of years

*Preston (1921), Aleinikov (1957), Edwards & Hed (1987), Brown (1980), Lambropoulos (1996)

There are five major areas of effort that have aided in managing sub-surface fractures

GRINDING

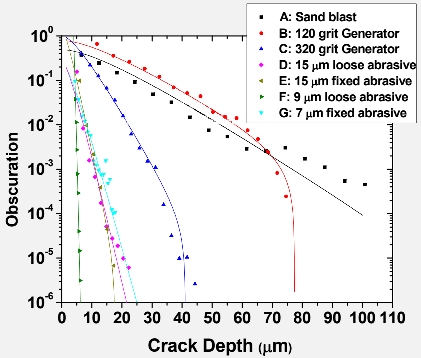

1. Developed fracture mechanics understanding of sub-surface fracture distributions

POLISHING

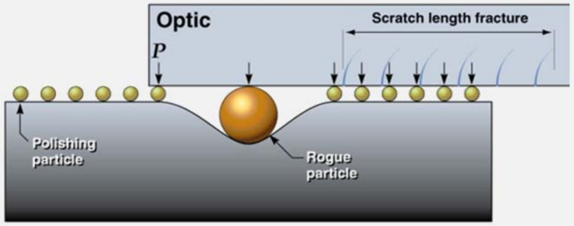

2. Identified/characterized behavior of rogue particles causing sub-surface fractures

CHEMICAL ETCHING

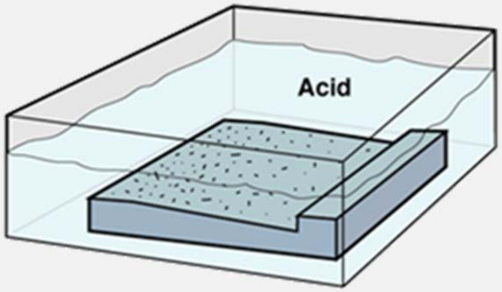

3. Established techniques using etching to reveal and remove subsurface fractures

SCRATCH FORENSICS

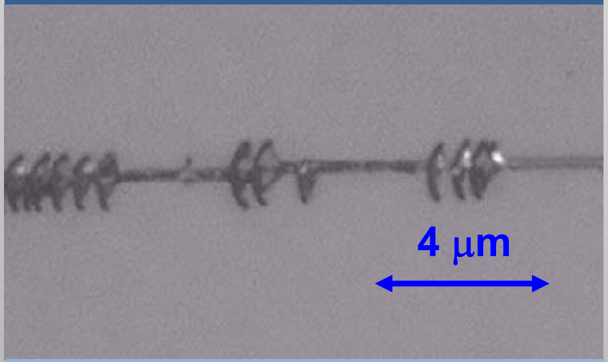

4. Developed quantitative rules for post-diagnosis of cause of surface fractures

LASER DAMAGE

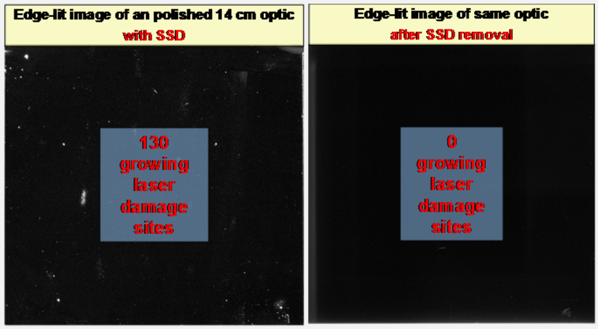

5. Showed link between sub-surface fracture removal & improved laser resistance

There are five major areas of effort that have aided in managing sub-surface fractures

GRINDING

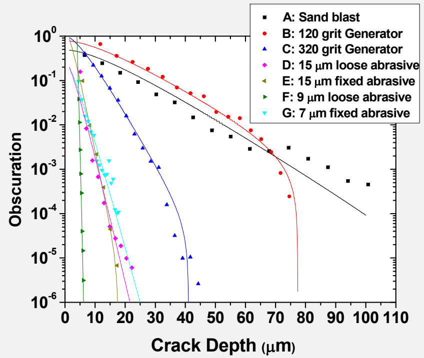

1. Developed fracture mechanics understanding of sub-surface fracture distributions

POLISHING

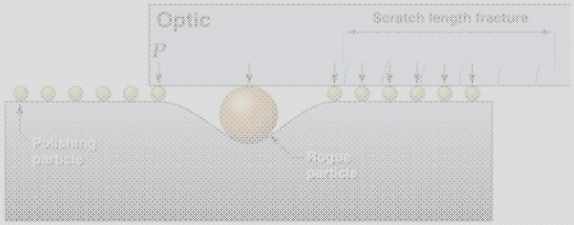

2. Identified/characterized behavior of rogue particles causing sub-surface fractures

CHEMICAL ETCHING

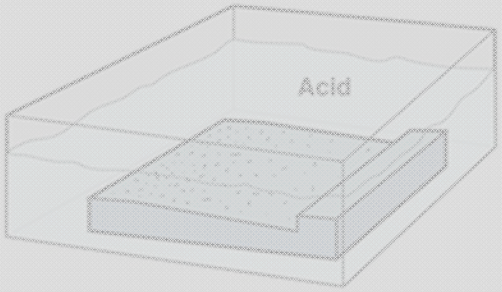

3. Established techniques using etching to reveal and remove subsurface fractures

SCRATCH FORENSICS

4. Developed quantitative rules for post-diagnosis of cause of surface fractures

LASER DAMAGE

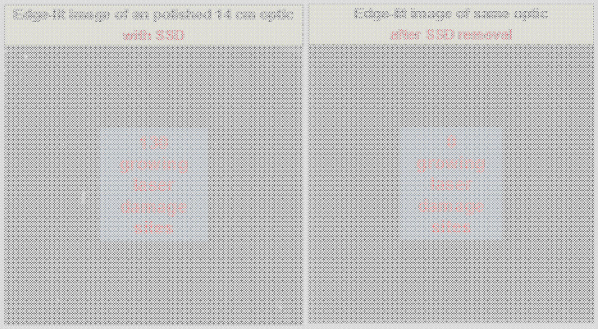

Edge-lit image of an polished 14 cm optic with SSD

Edge-lit image of same optic after SSD removal

5. Showed link between sub-surface fracture removal & improved laser resistance

There are three basic types of cracks created by static brittle indentation

	Hertzian Cracks[1] (blunt)	**Radial Cracks[1] (sharp)**	**Lateral Cracks[2] (sharp)**
	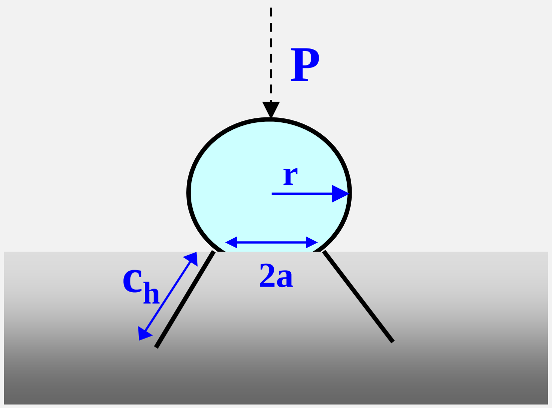	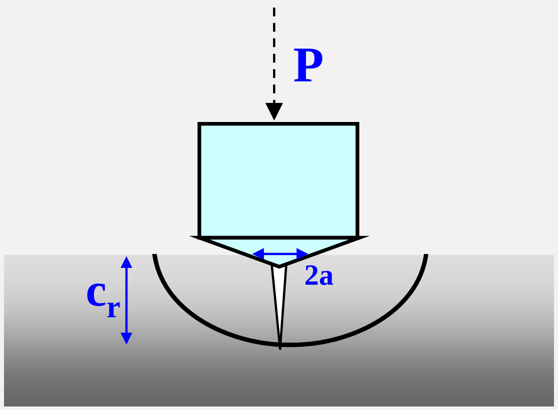	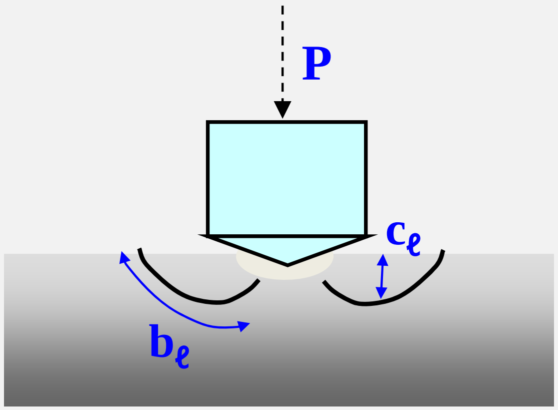
Initiation	$P_c = A r$	$P_c = \alpha_r \frac{K_{Ic}^4}{H^3}$	$P_c = P_{c\ell}$
Growth	$c_h = \left(\frac{\chi_h P}{K_{Ic}}\right)^{2/3}$	$c_r = \left(\frac{\chi_r P}{K_{Ic}}\right)^{2/3}$	$b_\ell = \frac{\chi_\ell \left(\frac{E}{H}\right)^{3/5} P^{5/8}}{K_{Ic}^{1/2} H^{1/8}}$ $c_\ell = \frac{\chi_{\ell 2} \left(\frac{E}{H}\right)^{2/5} P^{1/2}}{H^{1/2}}$
	Leads to subsurface damage	**Leads to subsurface damage**	**Leads to material removal**

---

[1] B. Lawn, "Fracture of Brittle Materials" (1993)

[2] I. Hutchings "Tribology:Friction and Wear of Engineering Materials" (1992)

The fracture initiation and growth constants need to be known to quantitatively use these relationships

Hertzian Cracks[1] (blunt)

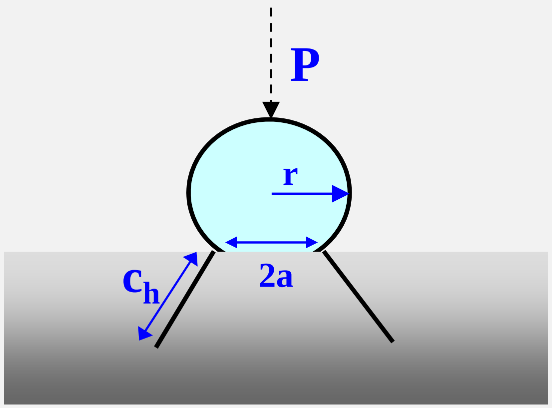

Radial Cracks[1] (sharp)

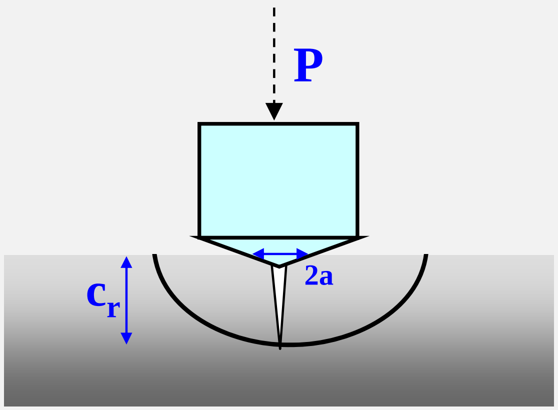

Lateral Cracks[2] (sharp)

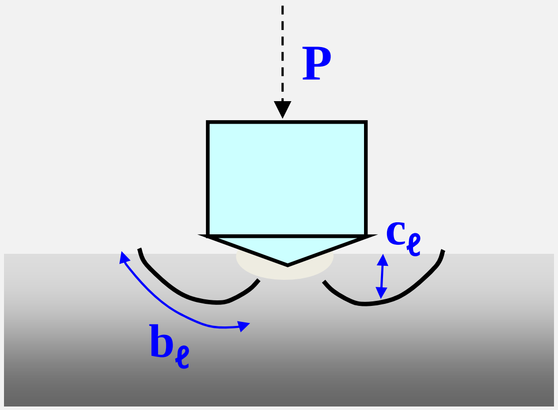

	Hertzian Cracks[1] (blunt)	Radial Cracks[1] (sharp)	Lateral Cracks[2] (sharp)
Initiation	$P_c = A r$	$P_c = \alpha_r \frac{K_{Ic}^{4}}{H^{3}}$	$P_c = P_{c\ell}$
Growth	$c_h = \left(\frac{\chi_h P}{K_{Ic}}\right)^{2/3}$	$c_r = \left(\frac{\chi_r P}{K_{Ic}}\right)^{2/3}$	$b_\ell = \frac{\chi_\ell \left(\frac{E}{H}\right)^{3/5} P^{5/8}}{K_{Ic}^{1/2} H^{1/8}}$ $c_\ell = \frac{\chi_{\ell 2} \left(\frac{E}{H}\right)^{2/5} P^{1/2}}{H^{1/2}}$
	Leads to subsurface damage	**Leads to subsurface damage**	**Leads to material removal**

---

[1] B. Lawn, "Fracture of Brittle Materials" (1993)

[2] I. Hutchings "Tribology:Friction and Wear of Engineering Materials" (1992)

Friction strongly influences fracture initiation for a sliding particle indentation (i.e. scratching)

Static Sphere[1]

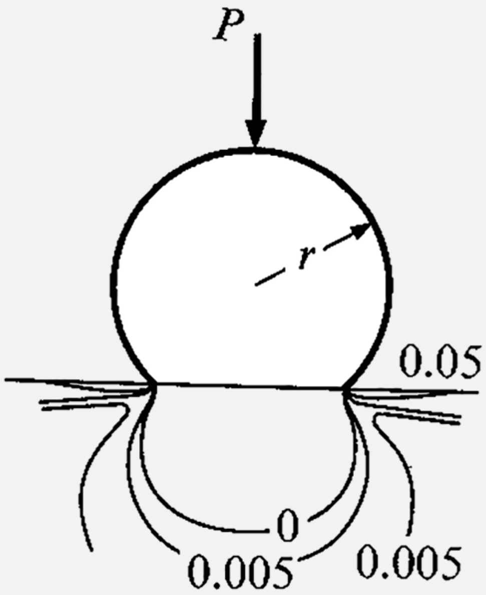

Initiation

$$P_c = A\,r$$

Growth

$$P = \frac{K_{Ic}}{\chi_h} c^{3/2}$$

Sliding Sphere[1,2]

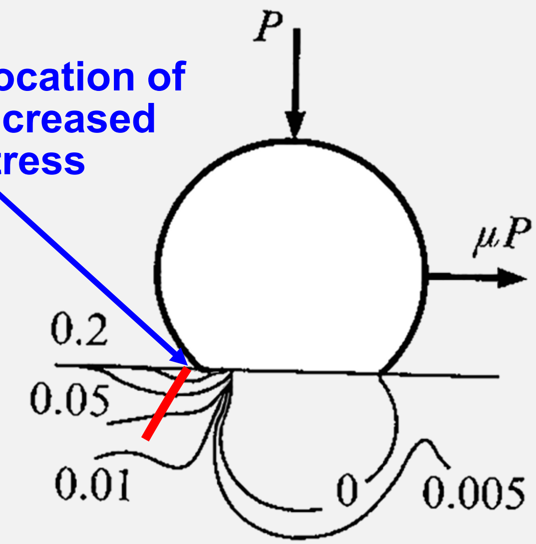

Location of increased stress

$$P_c = \frac{Ar}{(1+B\mu)^2}$$

$$P_c = \frac{C\,r^2}{(1+B\mu)^3}$$

$$P = \frac{K_{Ic}}{\chi_h (1+\mu^2)^2} c^{3/2}$$

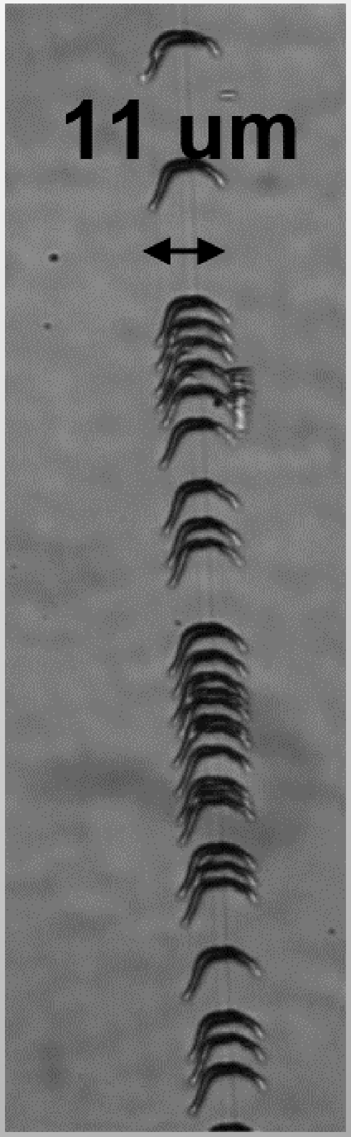

[1] Lawn, Fracture of Brittle Solids (1993)

[2] Lawn, Indentation Fracture: Principles and Applications (1975)

The effect of load on the fracture behavior of scratches has been measured

Schematic description of fractures associated with a scratch

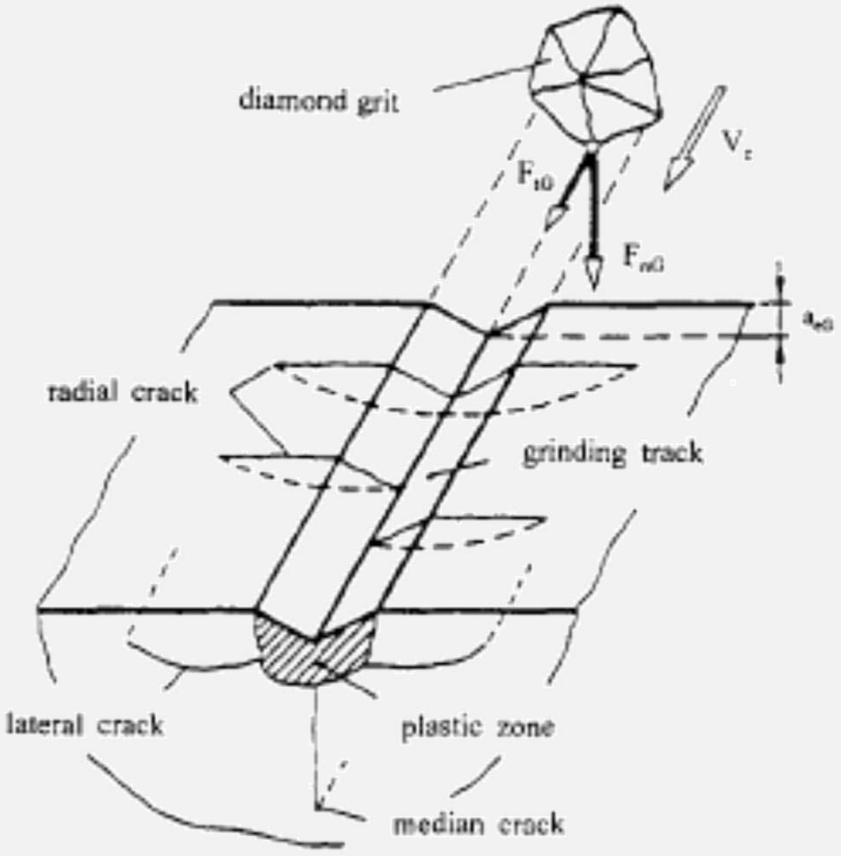

- **At low loads (P<0.1 N),** **no cracking is observed just a ductile track**
- **At intermediate loads (0.1 N< P < 5 N),** **well defined median and lateral cracks form**
- **At high loads (P> 5N),** **the plastically observed track appears to shatter and the median and lateral crack are not as extending as in the higher end of the intermediate loads**

Refs: Review: K. Li, Journal of Materials Processing Technology 57 (1996) 206
Review:M. Swain, Proc. R. Soc. London A, 366 (1979) 575

A wedge or taper polishing* technique was developed to directly measure the SSD distribution

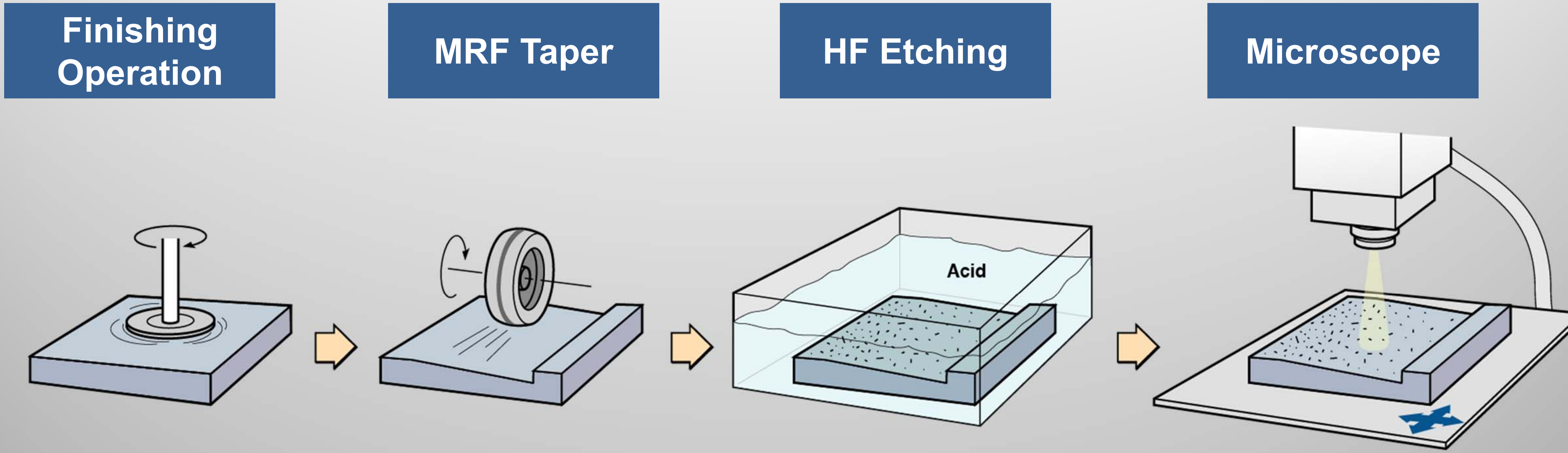

Finishing Operation → MRF Taper → HF Etching → Microscope

*J. Menapace, SPIE 2005, Boulder Damage Symposium;
Based on tapering technique used by Hed & Edwards (1987)

GRINDING

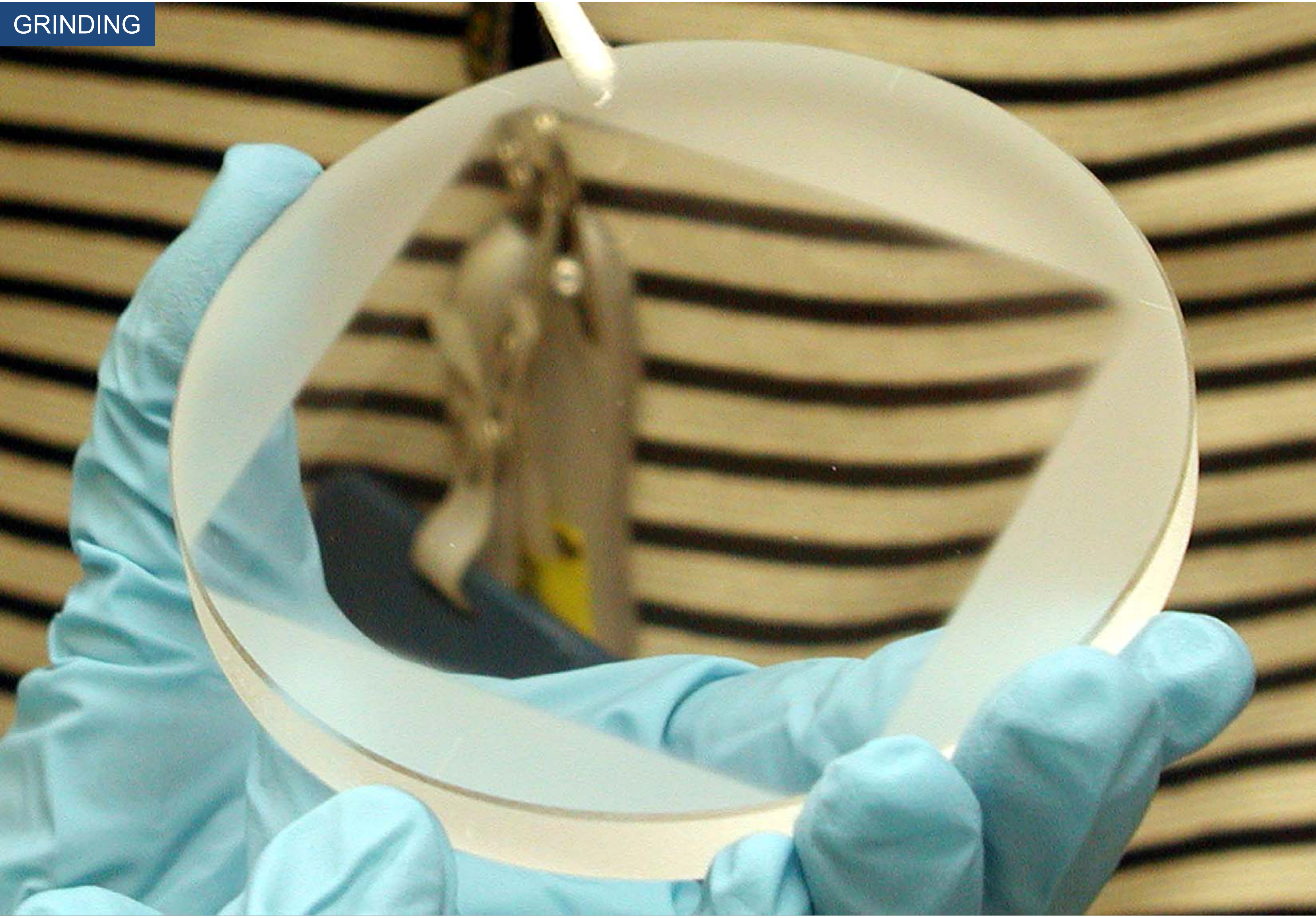

The SSD depth distribution has been measured for a series of standard grinding processes

Measured Crack Depth Distribution

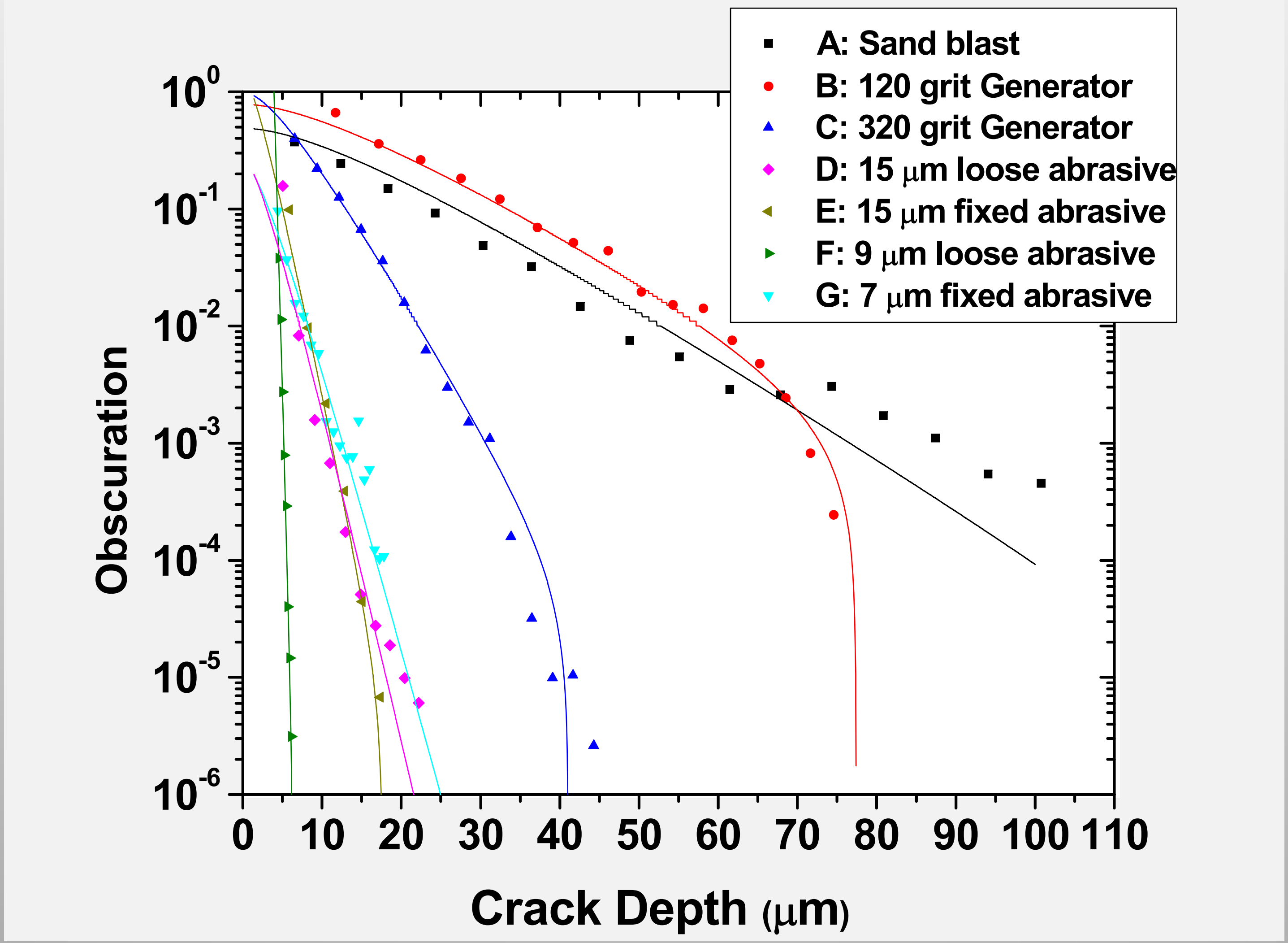

T. Suratwala, JNCS 352 (2006) 5601

Coarse Generator Grind (120 grit) (Sample B)

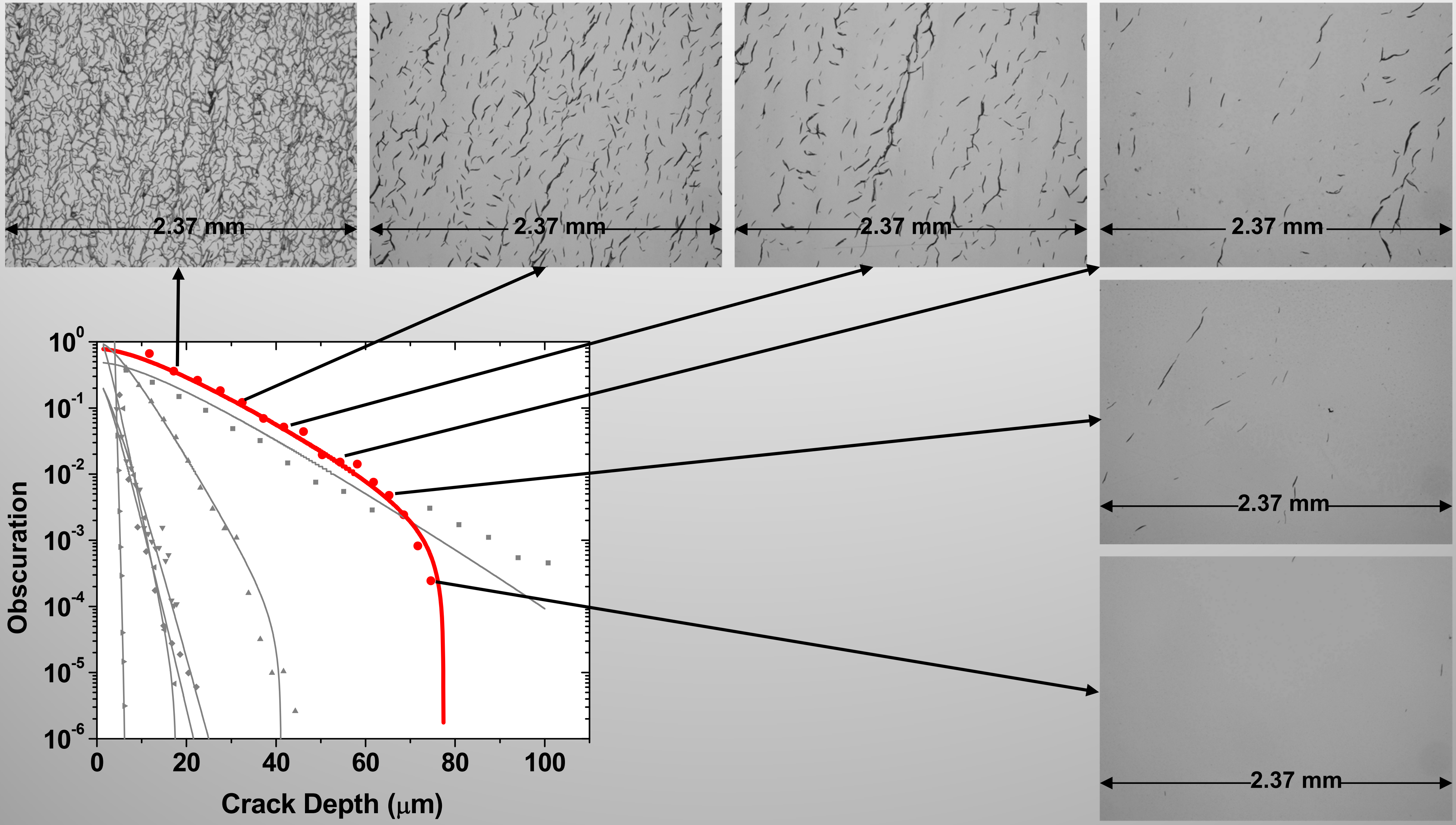

T. Suratwala, JNCS 352 (2006) 5601

Microscope images of the fractures show a unique size character for each grinding step

Sand blasted

120 Grit (125 μm)

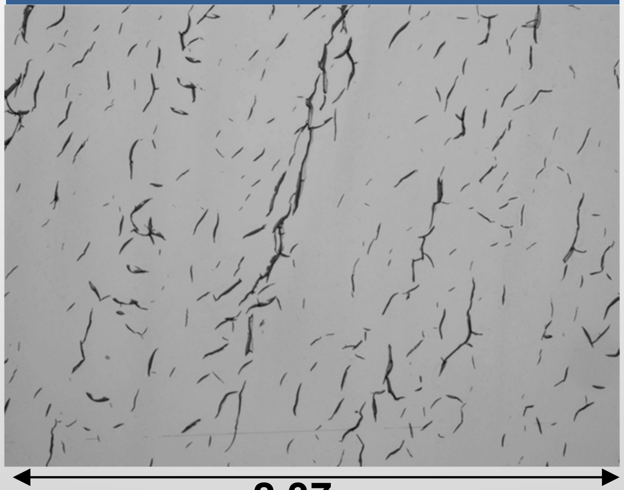

150 Grit (100 μm)

15 μm loose abrasive

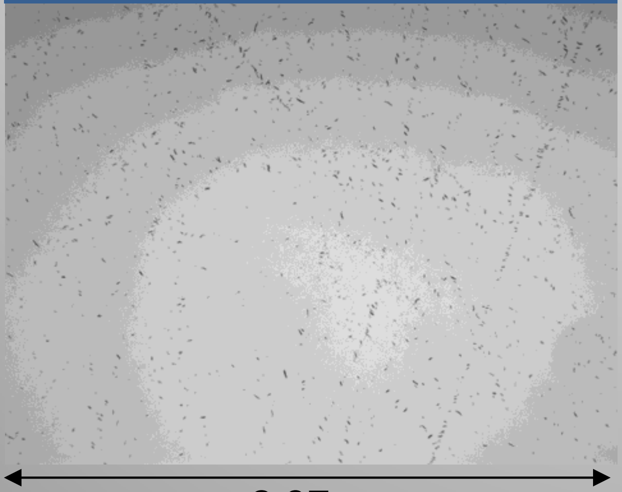

15 μm fixed abrasive

9 μm loose abrasive

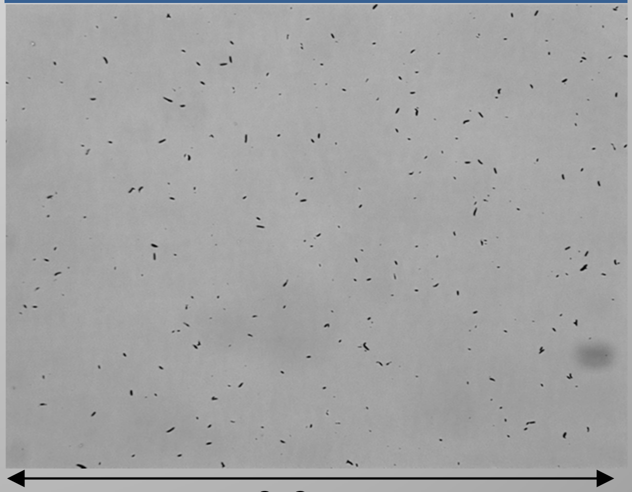

T. Suratwala, JNCS 352 (2006) 5601

Microscope images of the fractures show a unique size character for each grinding step

Sand blasted

120 Grit (125 μm)

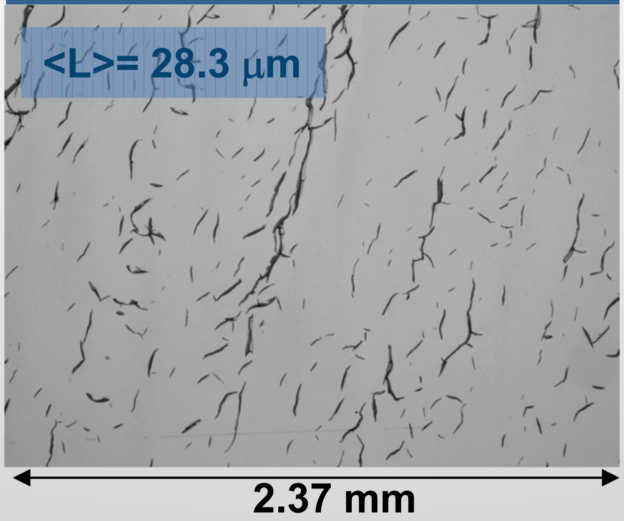

150 Grit (100 μm)

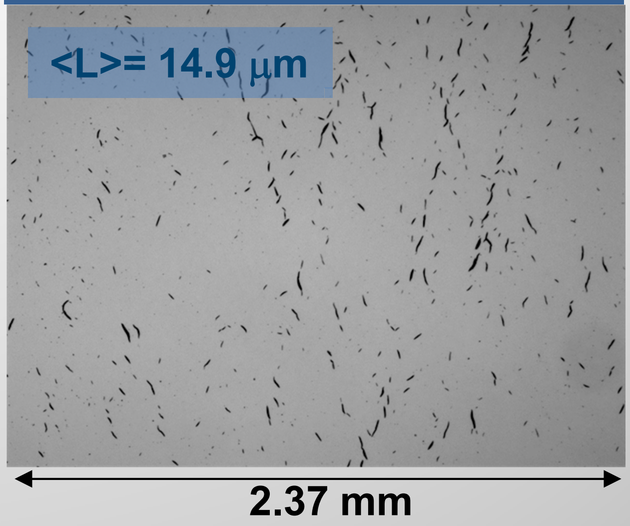

15 μm loose abrasive

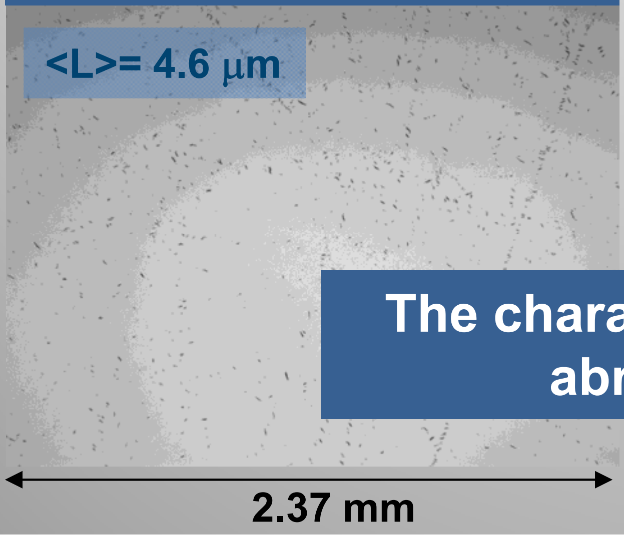

15 μm fixed abrasive

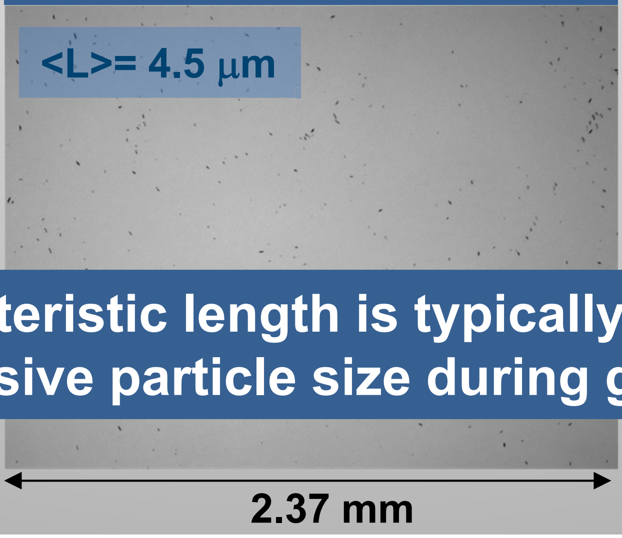

9 μm loose abrasive

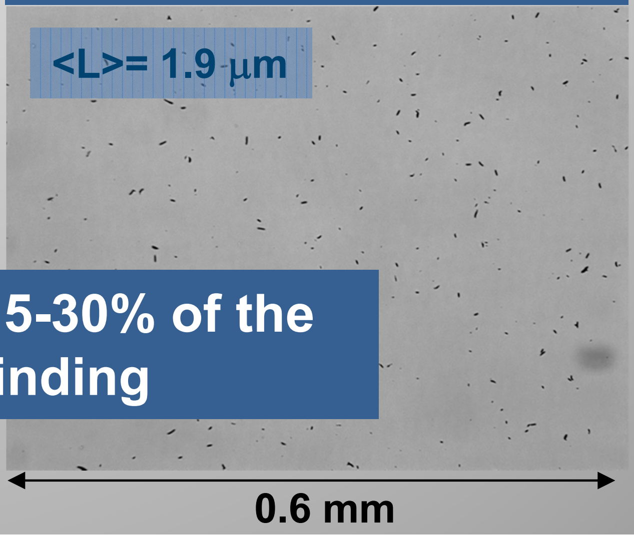

The characteristic length is typically 15-30% of the abrasive particle size during grinding

T. Suratwala, JNCS 352 (2006) 5601

A brittle fracture model has been successfully used to explain the observed distribution of crack depth and lengths

Schematic of Model*

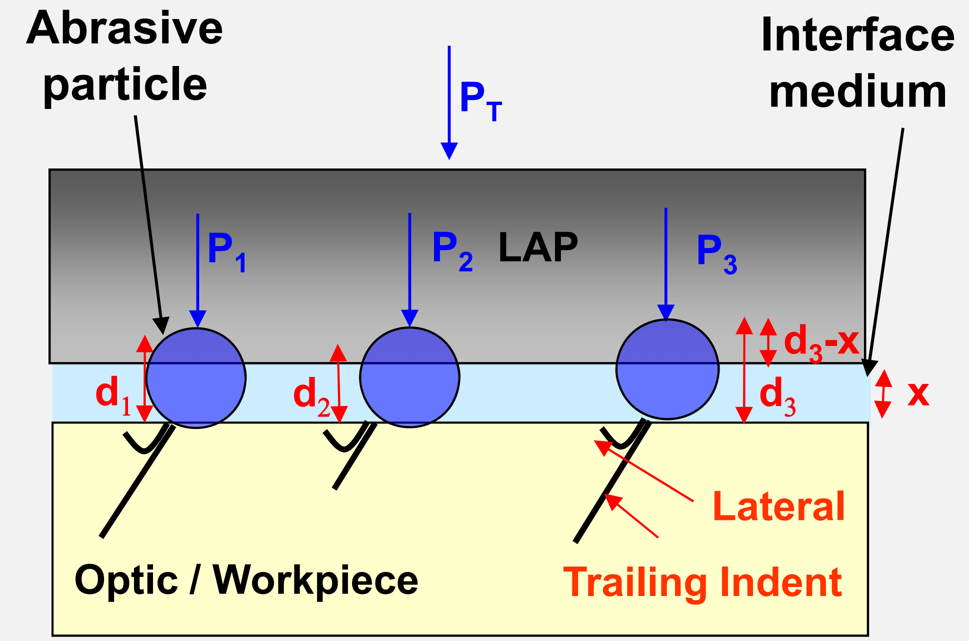

$P_T = \Sigma P_i$ $\quad$ $P_i \propto (d_i - x) \propto d_i$

Key assumption: The load on particle is proportional to its vertical dimension

*T. Suratwala, JNCS 352 (2006) 5601.
*P. Miller, SPIE 5991 (2006).

We recommend using the ’90’ rule for material removal (c_{90}=0.9<L>) for isolated SSD observed on polished parts

Measured mean crack length vs SSD depth

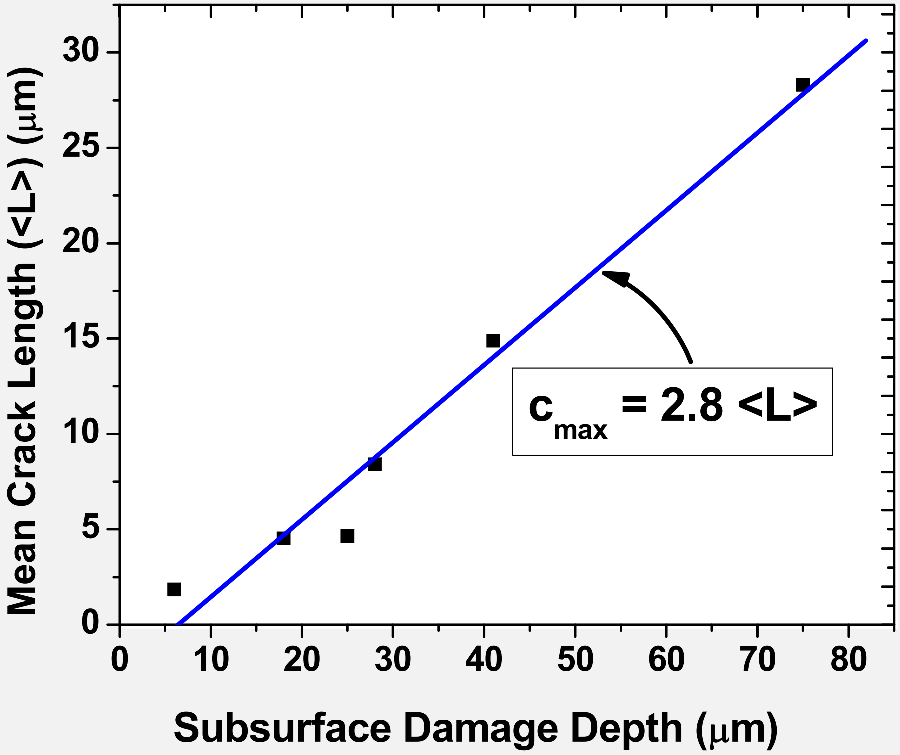

Probability of finding a crack of depth c for a given crack length

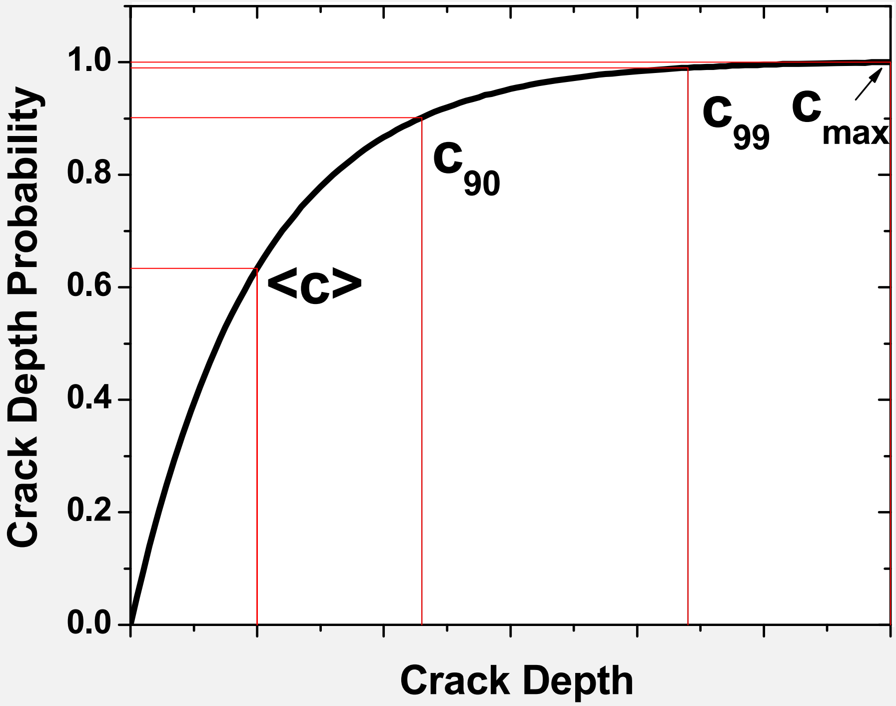

$$c_{\max} = 2.8 < L >$$

$$c_{90} = 0.9 < L >$$

T. Suratwala, JNCS 352 (2006) 5601

The addition of a small amount of 15 μm particles in a 9 μm slurry results in a significant increase in SSD

Particle size distributions of the alumina particles used

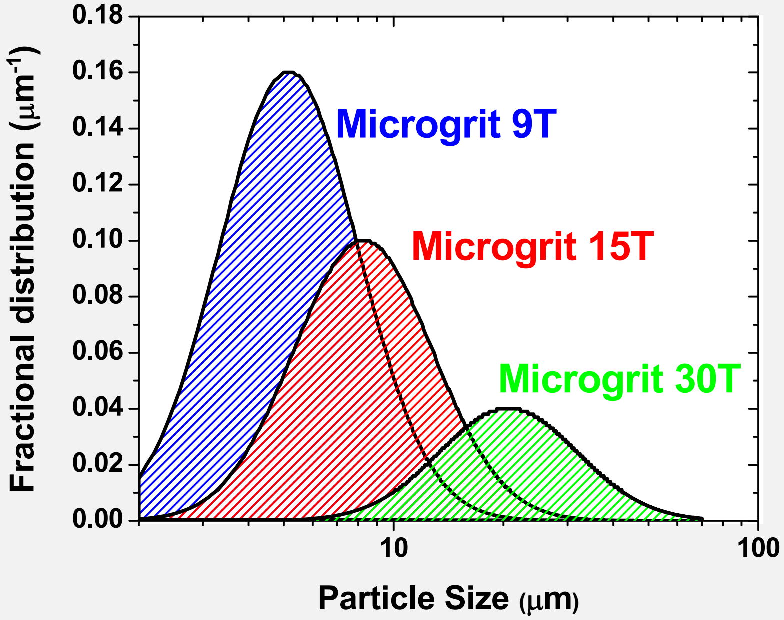

Crack depth distributions: Loose abrasive grinding with addition of rogue particles

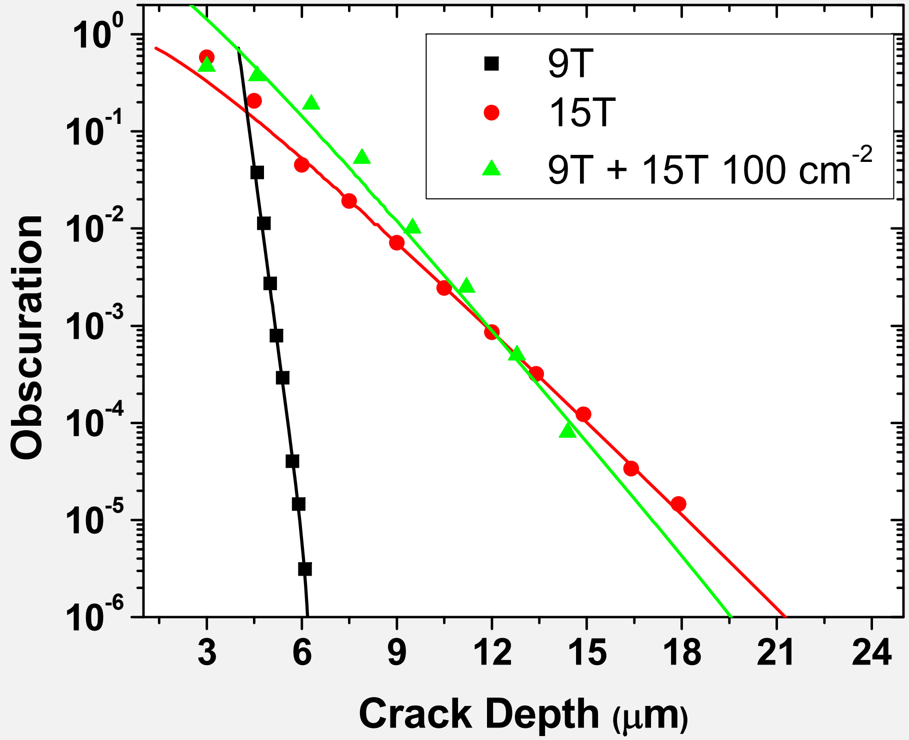

T. Suratwala, JNCS 354 (2006) 2023

The loaded particles are the largest particles in the abrasive particle distribution

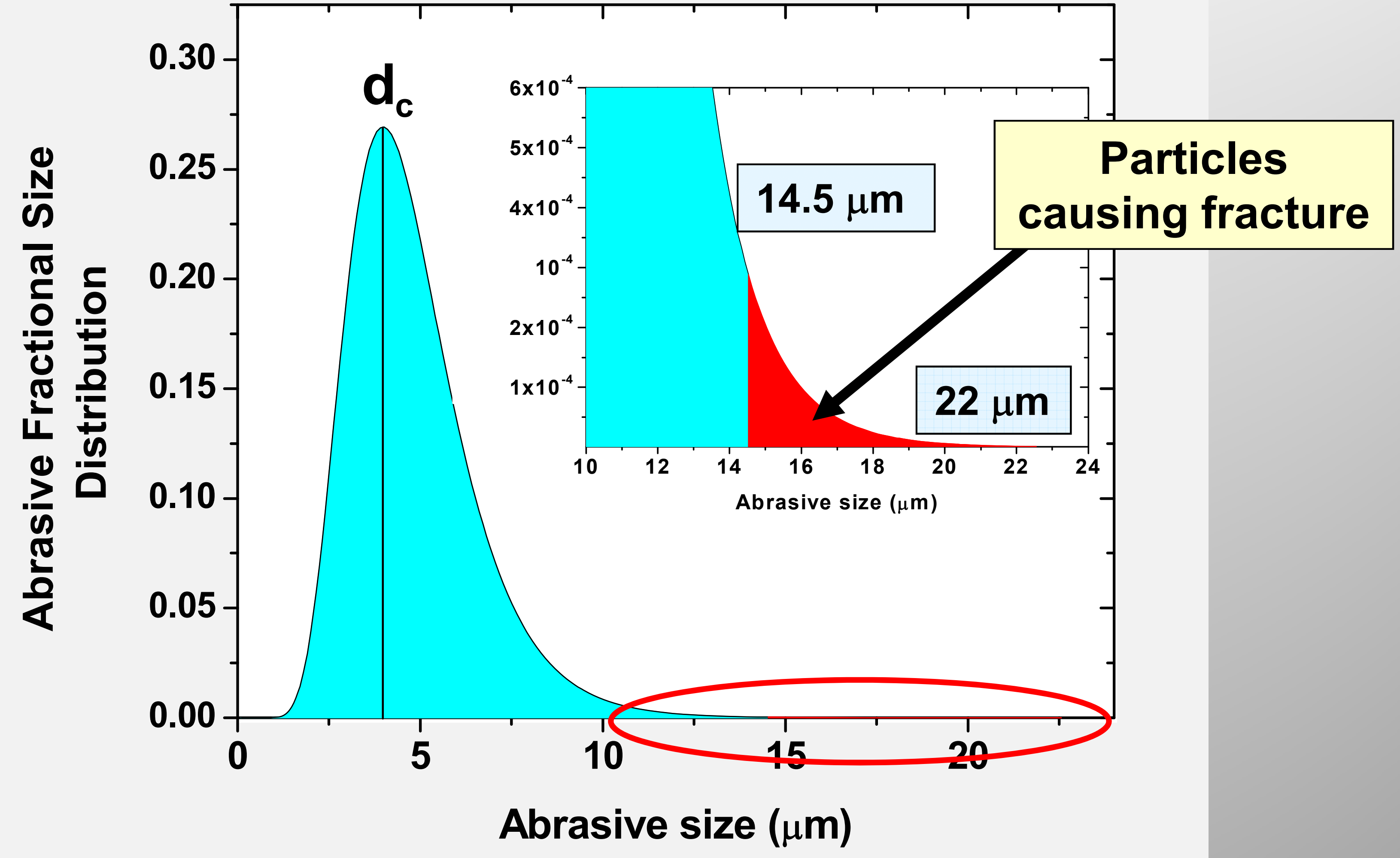

Abrasive size distribution for 9 μm loose abrasive

14.5 μm

22 μm

Particles causing fracture

T. Suratwala, JNCS 354 (2006) 2023

There are five major areas of effort that have aided in managing sub-surface fractures

GRINDING

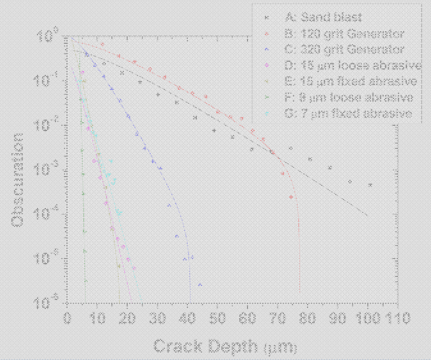

1. Developed fracture mechanics understanding of sub-surface fracture distributions

POLISHING

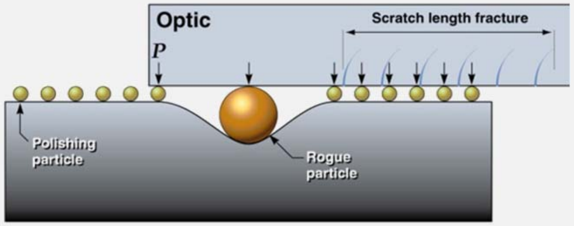

2. Identified/characterized behavior of rogue particles causing sub-surface fractures

CHEMICAL ETCHING

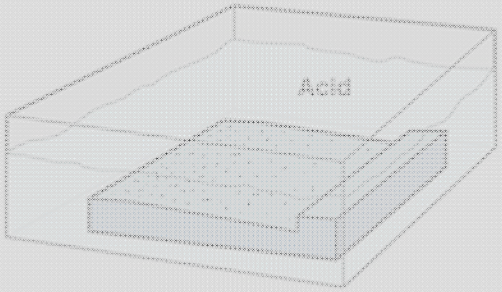

3. Established techniques using etching to reveal and remove subsurface fractures

SCRATCH FORENSICS

4. Developed quantitative rules for post-diagnosis of cause of surface fractures

LASER DAMAGE

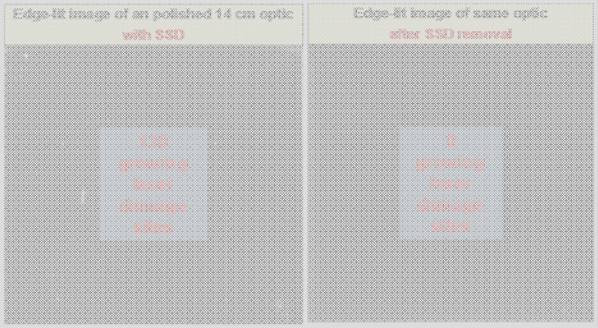

5. Showed link between sub-surface fracture removal & improved laser resistance

Rogue particles of diamond were added to a ceria slurry during polishing at various sizes & concentrations

Particle size distributions of ceria and rogue diamonds

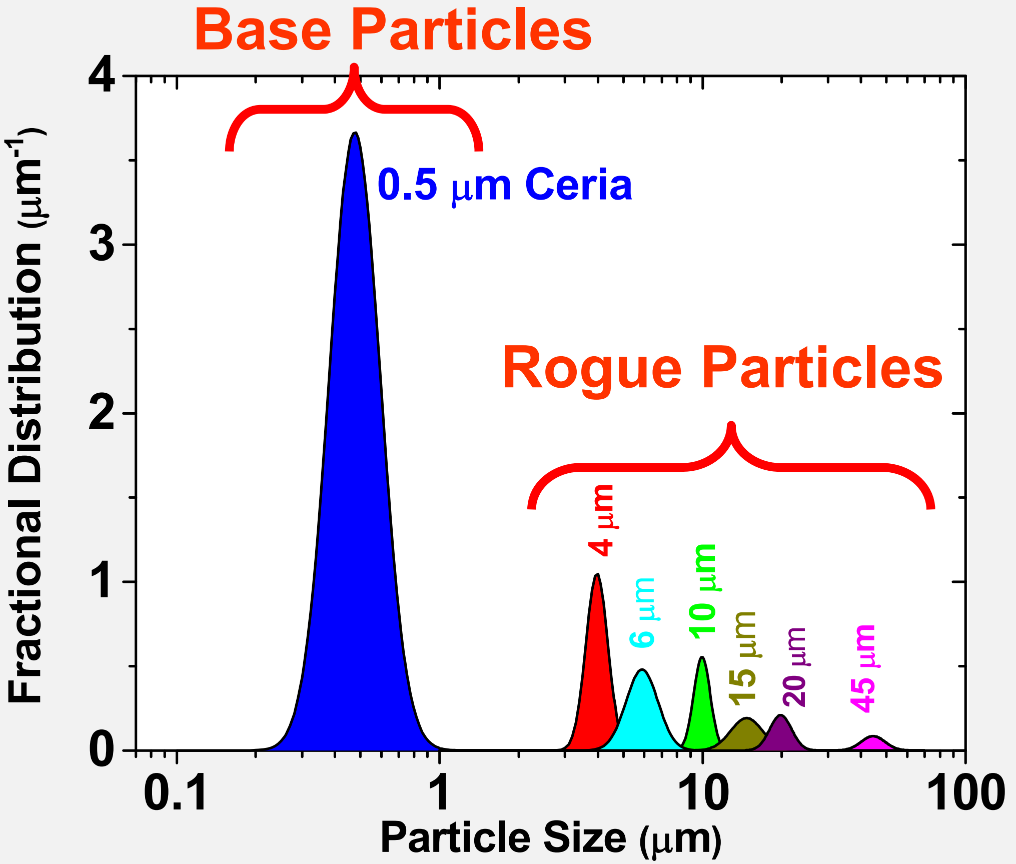

T. Suratwala, JNCS 354 (2006) 2023

Rogue particles can cause multiple types of scratches

Plastic
Abrasive Wear

Sleek

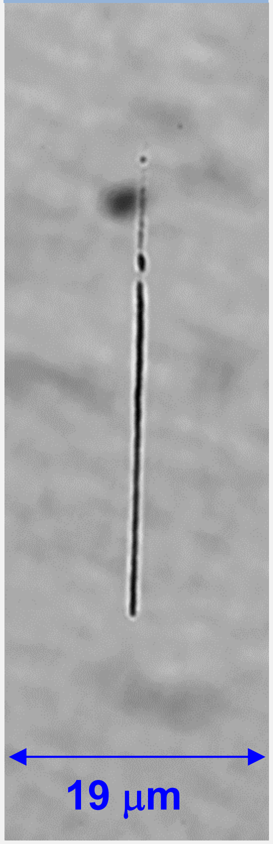

Mixed
Brittle fracture / Plastic Abrasive Wear

Sleek + lateral fracture

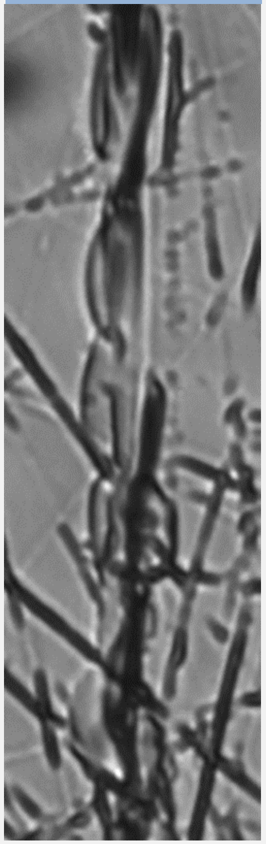

Sleek + trailing indent fracture

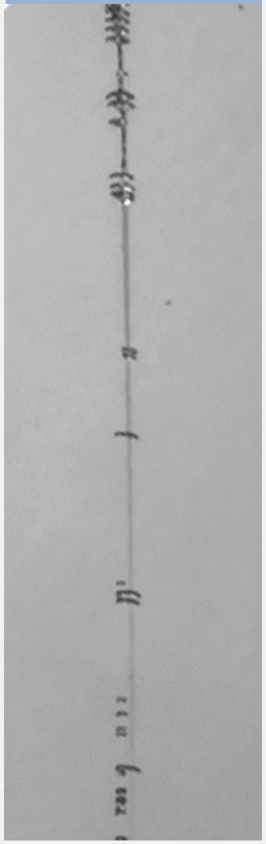

Sleek + trailing indent + lateral fracture

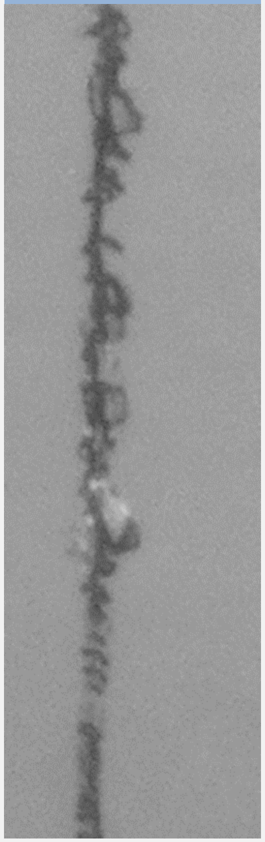

Brittle
Fracture

Trailing indent fracture

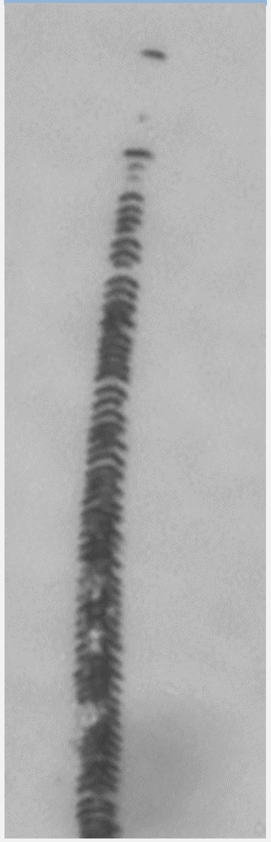

Trailing indent + lateral fracture

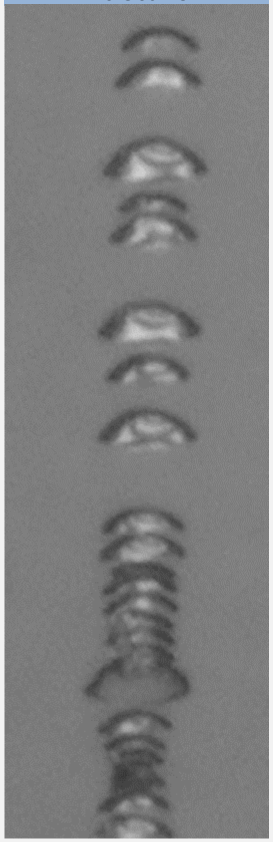

The scratch length increases with rogue particle size

Cumulative scratch length distribution

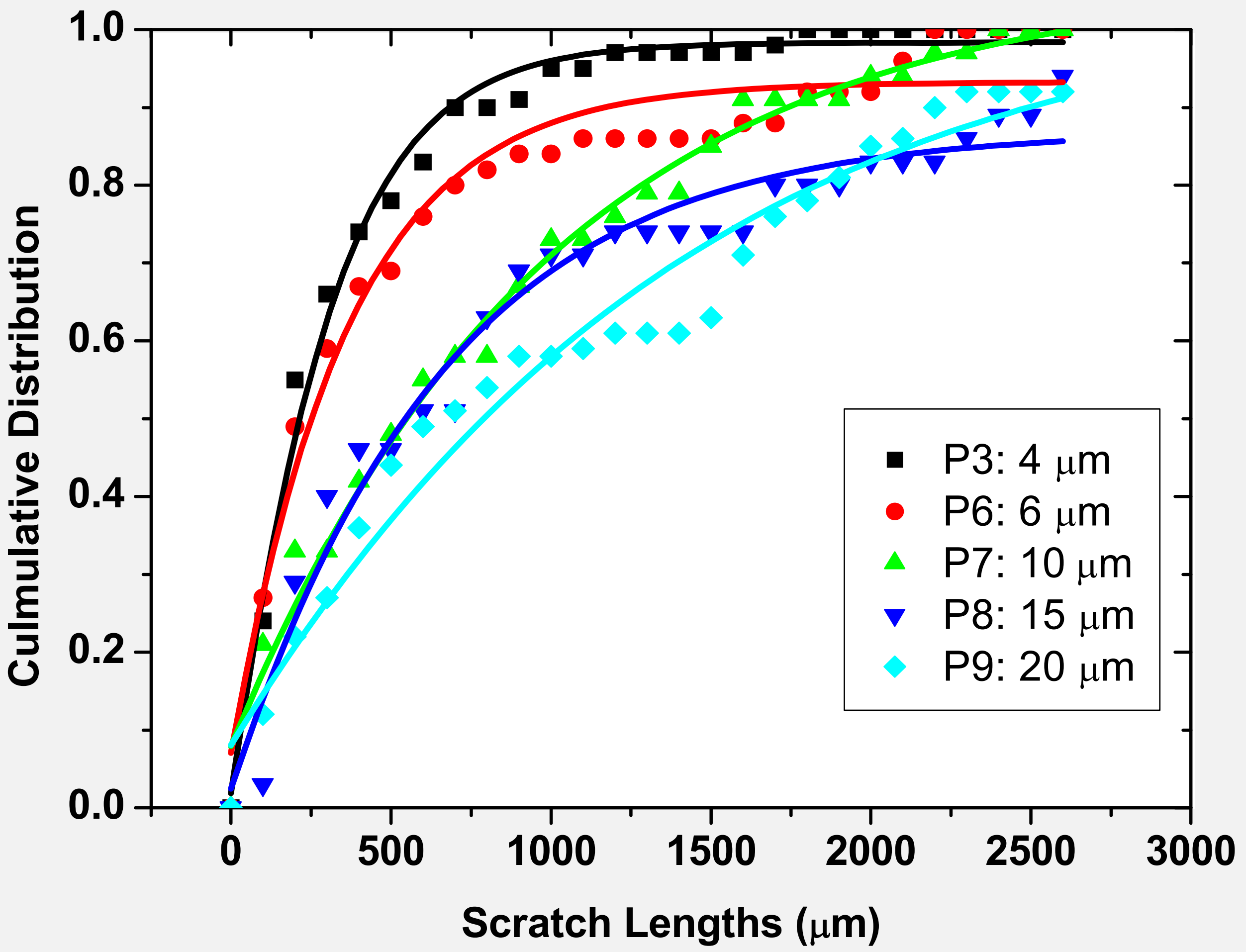

T. Suratwala, JNCS 354 (2006) 2023

The observed scratch lengths can be explained by the viscoelastic penetration of a rogue particle

$$L_{scratch} = 8.9\frac{\nu_{ave}\eta R^2}{P}$$

$t = t_0$

$P_1 =$ *Load on rogue particle*

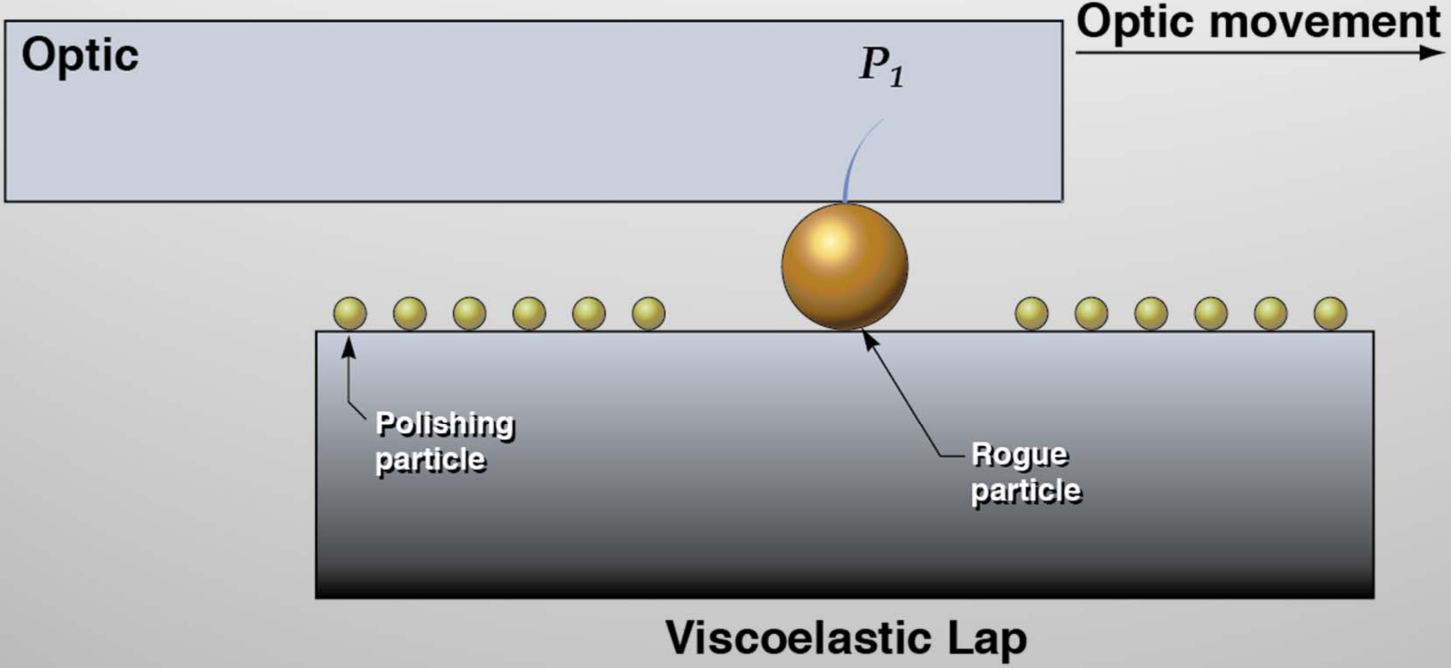

This behavior has been modeled using hard sphere penetration into a linear viscoelastic lap at large penetration

T. Suratwala, JNCS 354 (2006) 2023

The observed scratch lengths can be explained by the viscoelastic penetration of a rogue particle

$$L_{scratch} = 8.9 \frac{\nu_{ave} \eta R^2}{P}$$

$t = t_1$

$P_1 = $ Load on rogue particle

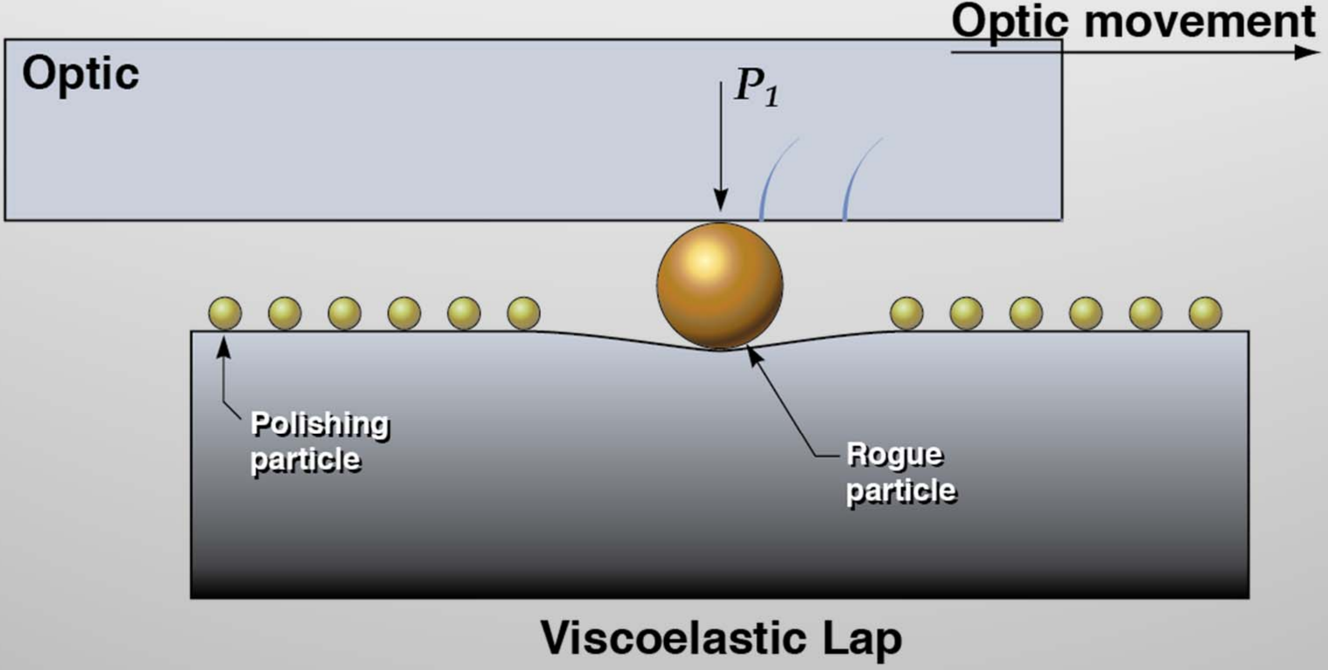

This behavior has been modeled using hard sphere penetration into a linear viscoelastic lap at large penetration

T. Suratwala, JNCS 354 (2006) 2023

The observed scratch lengths can be explained by the viscoelastic penetration of a rogue particle

$$L_{scratch} = 8.9 \frac{\nu_{ave} \eta R^2}{P}$$

$t = t_2$

$P_1 = Load\ on\ rogue\ particle$

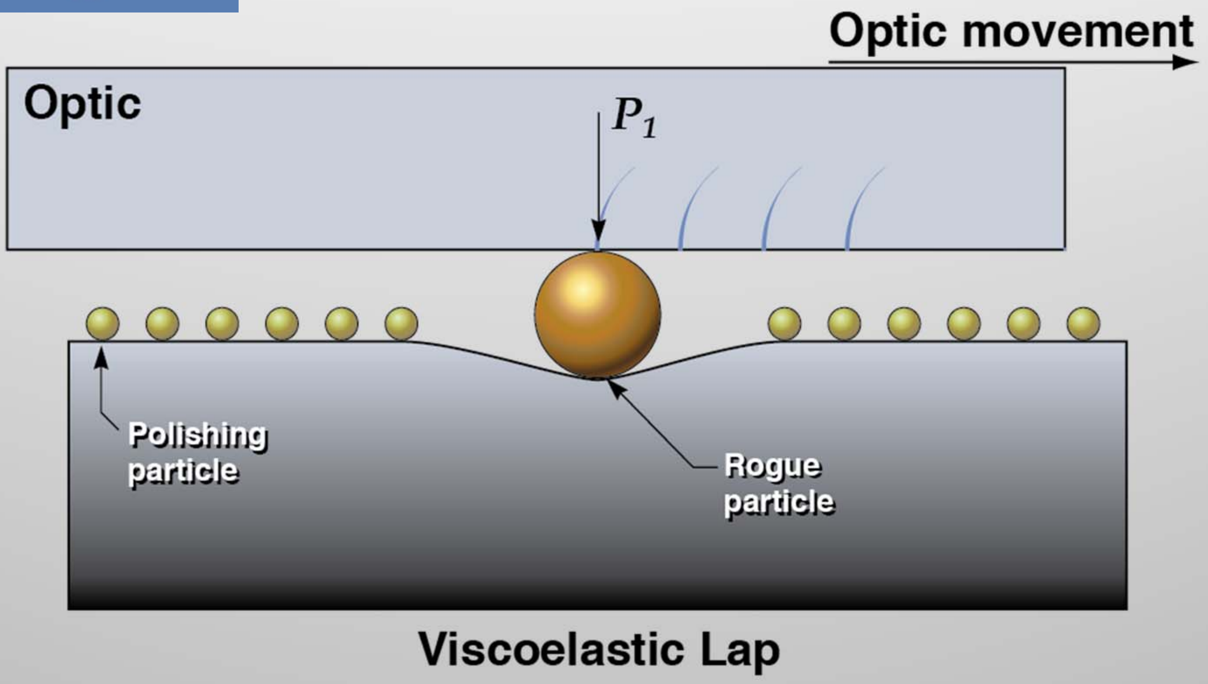

This behavior has been modeled using hard sphere penetration into a linear viscoelastic lap at large penetration

T. Suratwala, JNCS 354 (2006) 2023

The observed scratch lengths can be explained by the viscoelastic penetration of a rogue particle

$$L_{scratch} = 8.9\,\frac{\nu_{ave}\,\eta\,R^2}{P}$$

$t = t_3$

$P_1 = \text{Load on rogue particle}$

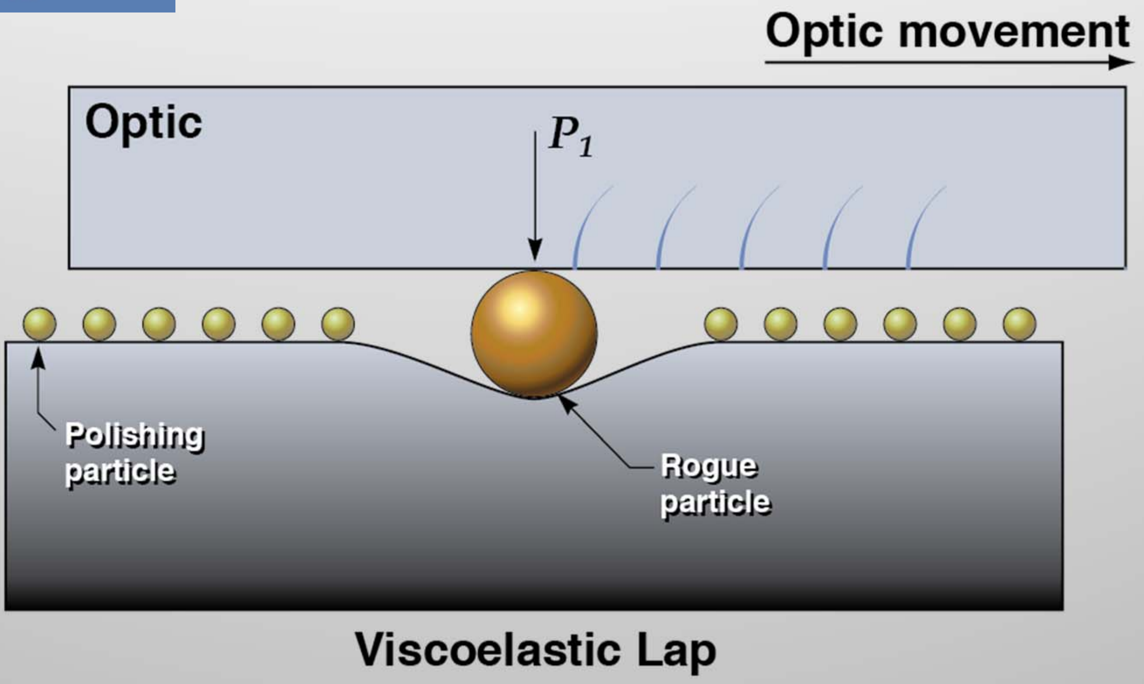

This behavior has been modeled using hard sphere penetration into a linear viscoelastic lap at large penetration

T. Suratwala, JNCS 354 (2006) 2023

The observed scratch lengths can be explained by the viscoelastic penetration of a rogue particle

$$L_{scratch} = 8.9 \frac{\nu_{ave} \eta R^2}{P}$$

$t = t_4$
P_1 = Load on rogue particle

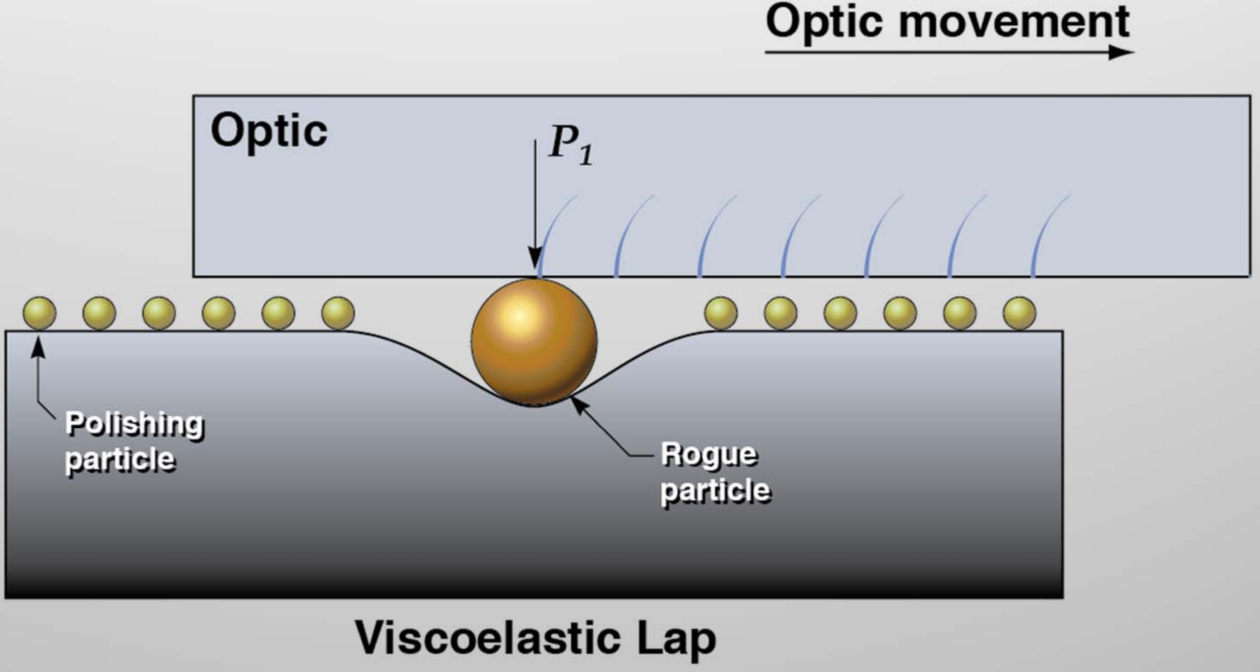

This behavior has been modeled using hard sphere penetration into a linear viscoelastic lap at large penetration

T. Suratwala, JNCS 354 (2006) 2023

The observed scratch lengths can be explained by the viscoelastic penetration of a rogue particle

$$L_{scratch} = 8.9\frac{\nu_{ave}\eta R^2}{P}$$

$t = t_5$
$P = Load\ on\ all\ particles$

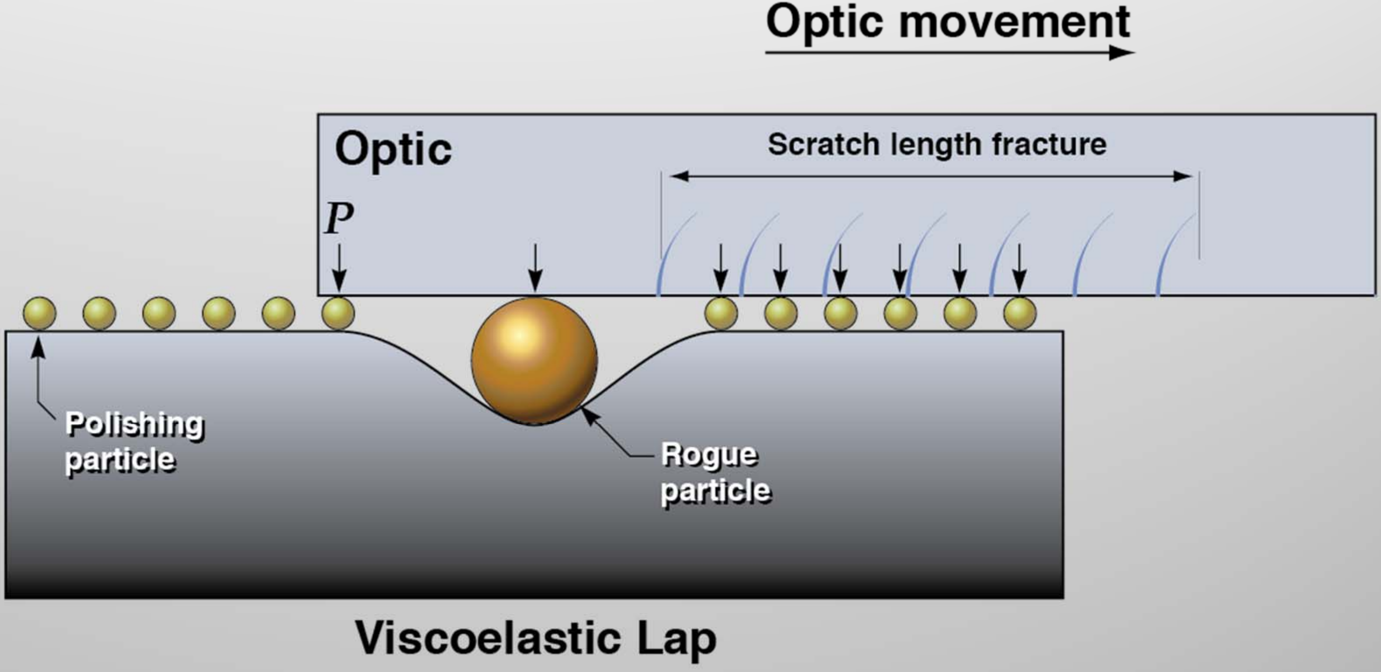

This behavior has been modeled using hard sphere penetration into a linear viscoelastic lap at large penetration

T. Suratwala, JNCS 354 (2006) 2023

The scratch length correlates with viscoelastic model wrt rogue particle size, pressure, lap viscosity, and lap temperature

Scratch length as a fn of various process parameters

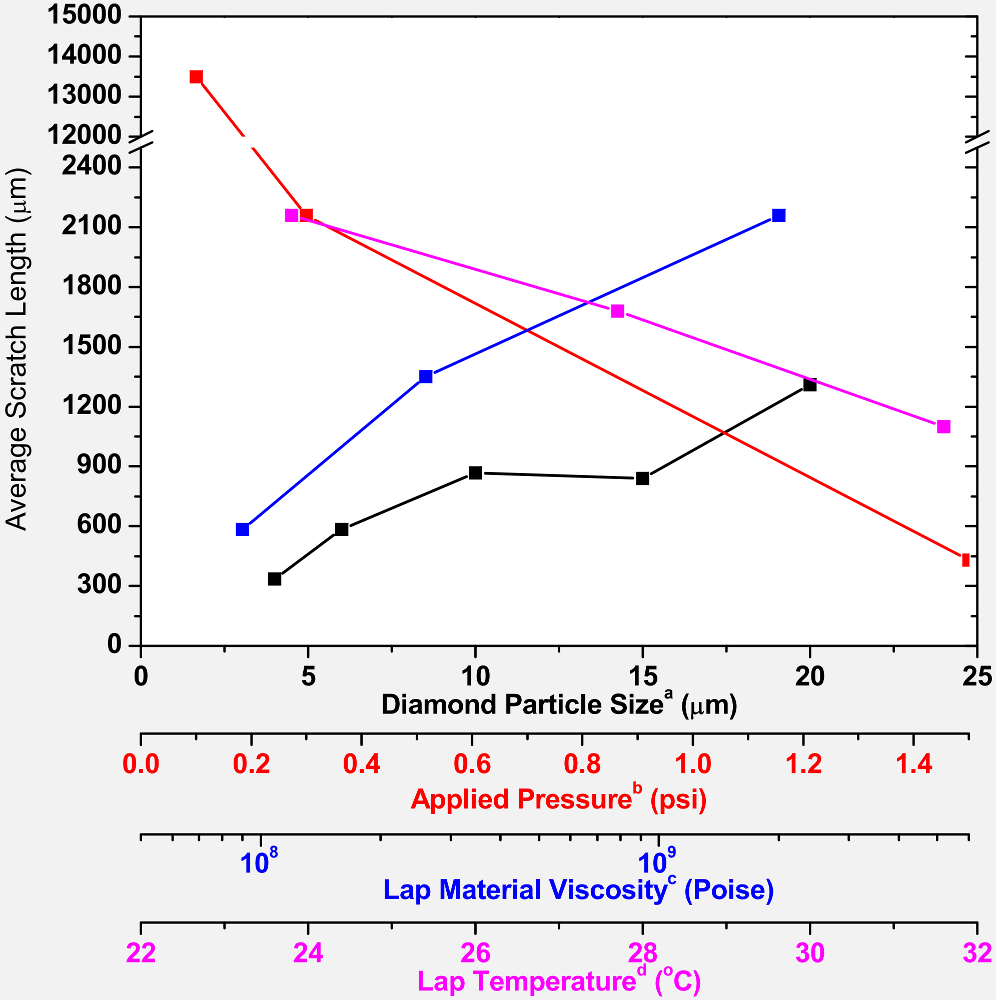

T. Suratwala, JNCS 354 (2006) 2023; T. Suratwala OPN (Sep 2008) 12

There are five major areas of effort that have aided in managing sub-surface fractures

GRINDING

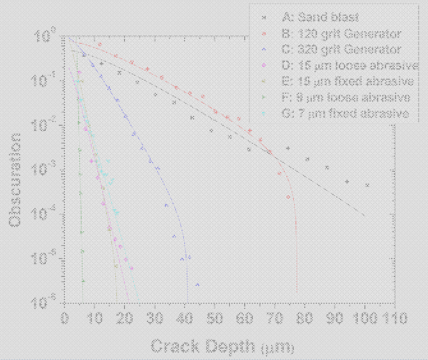

1. Developed fracture mechanics understanding of sub-surface fracture distributions

POLISHING

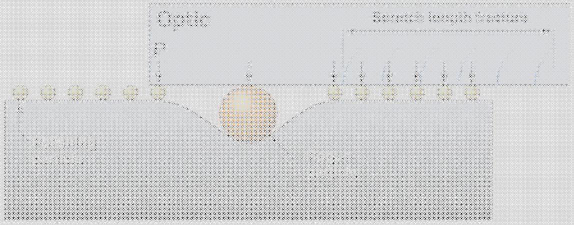

2. Identified/characterized behavior of rogue particles causing sub-surface fractures

CHEMICAL ETCHING

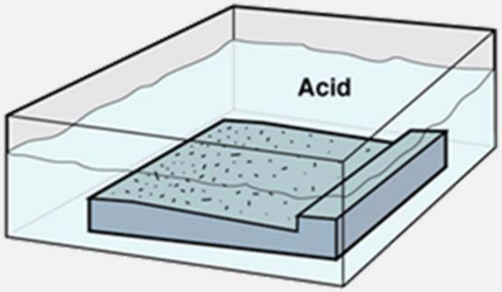

3. Established techniques using etching to reveal and remove subsurface fractures

SCRATCH FORENSICS

4. Developed quantitative rules for post-diagnosis of cause of surface fractures

LASER DAMAGE


Edge-lit image of an polished 14 cm optic with SSD

Edge-lit image of same optic after SSD removal

5. Showed link between sub-surface fracture removal & improved laser resistance

$HF:NH_4F$ etching of fused silica glass allows for removing the Bielby layer and visually observing surface cracks

Cross section view of cracks *before* etching

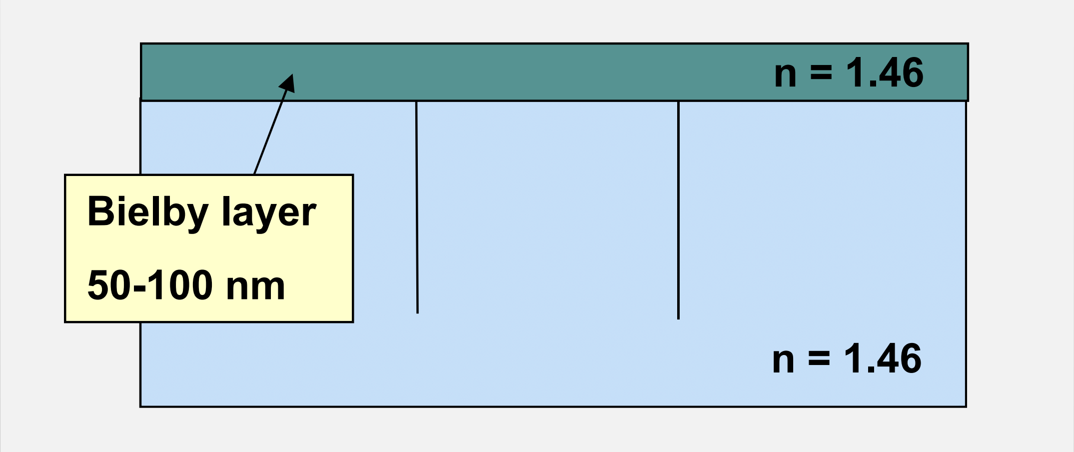

Sleek on fused silica optic (before etch)

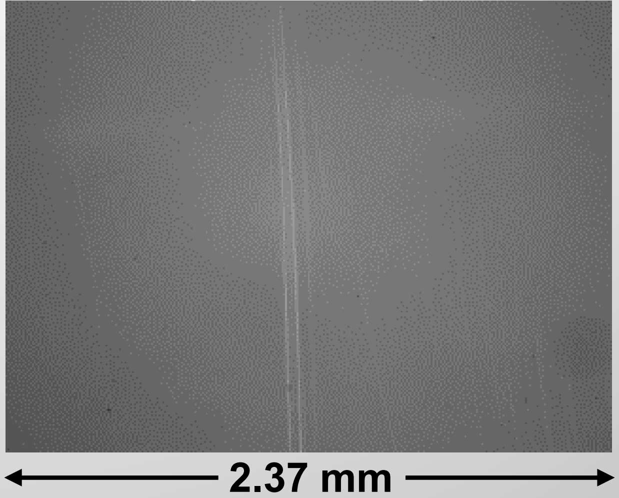

Cross section view of cracks *after* etching

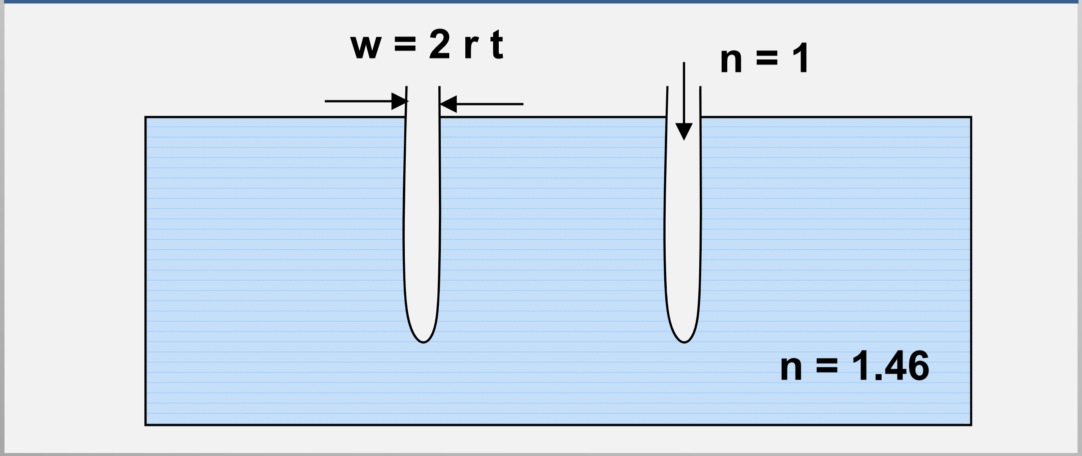

Sleek on fused silica optic (after etch)

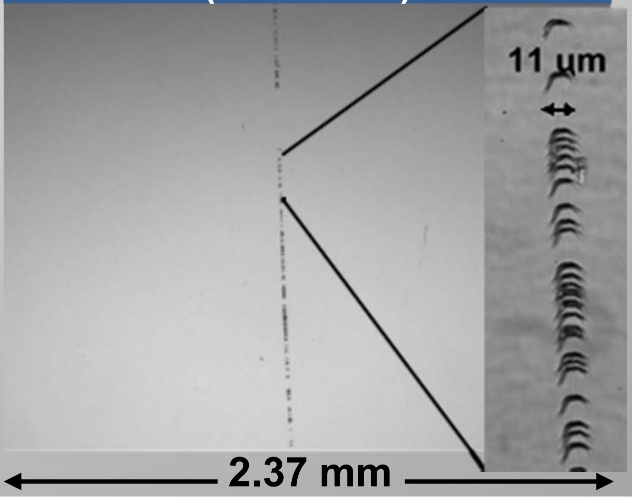

L. Wong, JNCS 355 (2009) 797

HF Etching exposes sub-surface fractures allowing detection

- **Polished Optic (14 cm x 14 cm) viewed off axis by side lighting**

Before etching

After etching

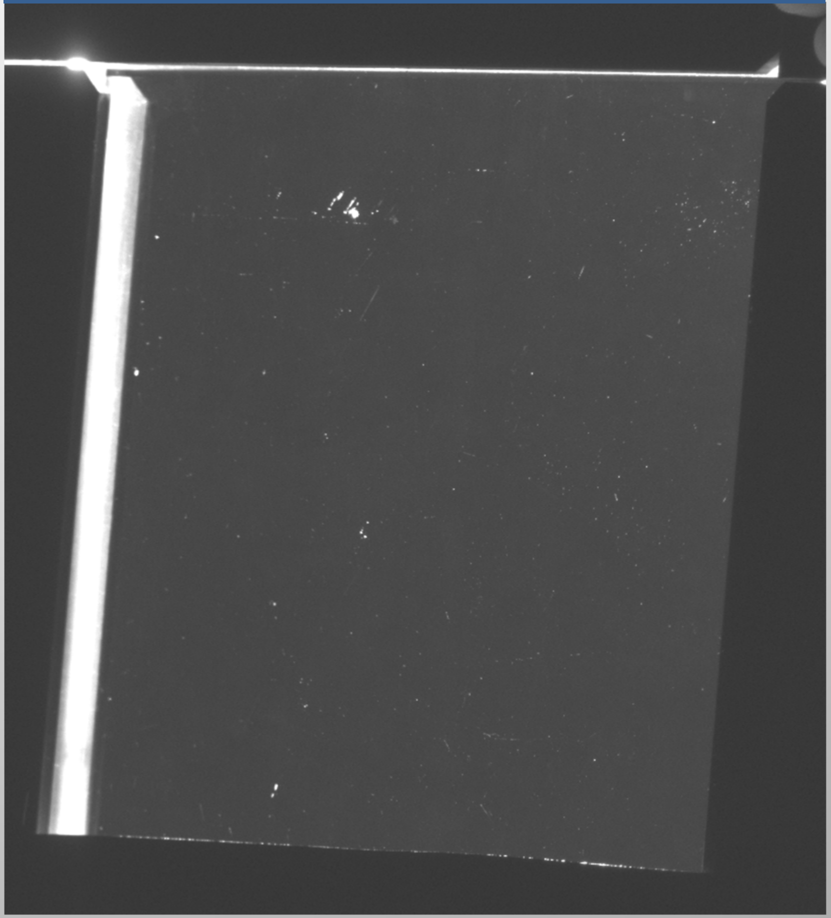

Preston reported this behavior in 1921

L. Wong, JNCS 355 (2009) 797

HF etching can be used after grinding to remove subsurface fracture because it annihilates neighboring cracks

Etching a scratch

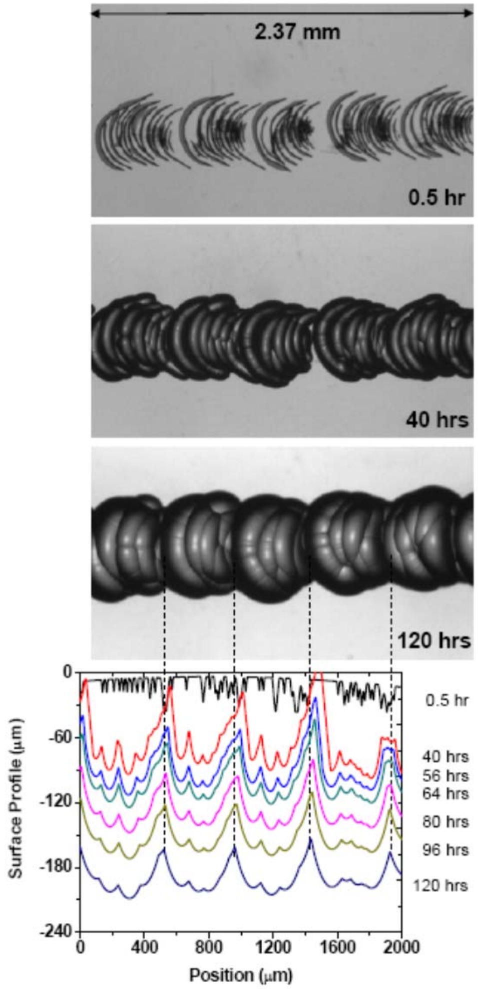

Etching ground surface

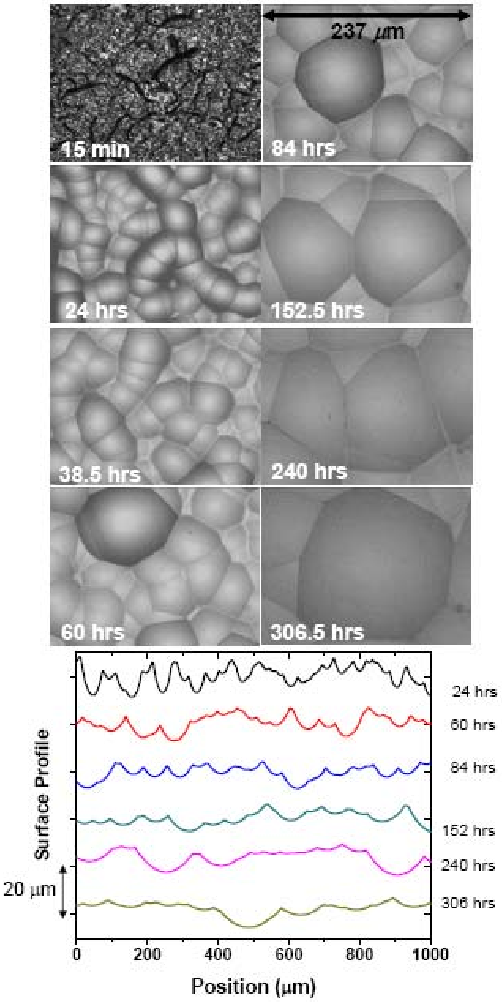

Simple Geometric Model

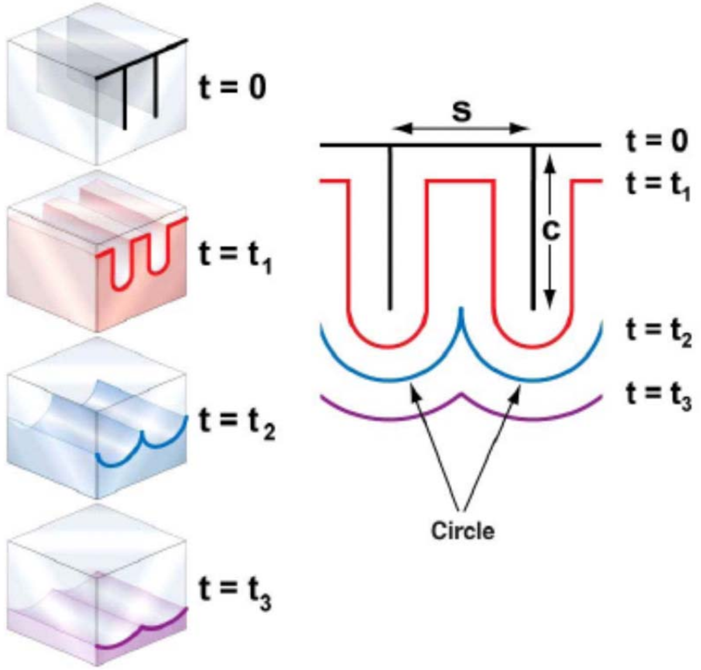

L. Wong, JNCS 355 (2009) 797

There are five major areas of effort that have aided in managing sub-surface fractures

GRINDING

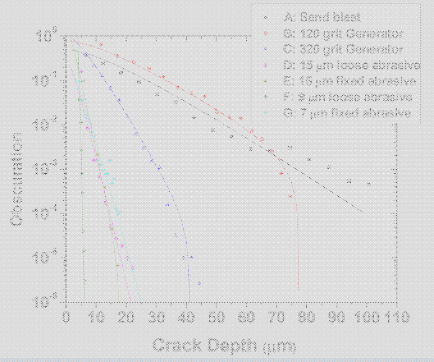

1. Developed fracture mechanics understanding of sub-surface fracture distributions

POLISHING

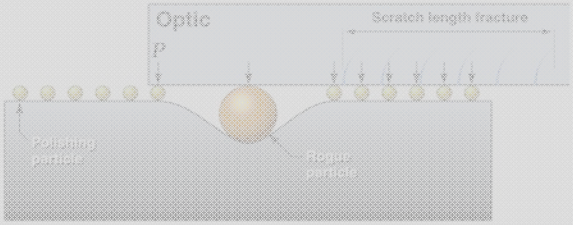

2. Identified/characterized behavior of rogue particles causing sub-surface fractures

CHEMICAL ETCHING

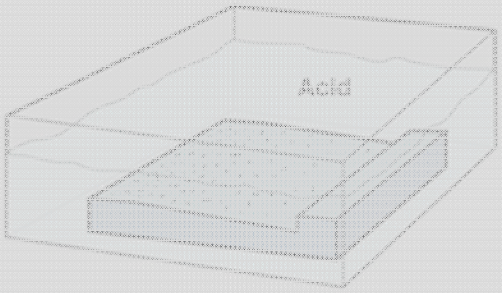

3. Established techniques using etching to reveal and remove subsurface fractures

SCRATCH FORENSICS

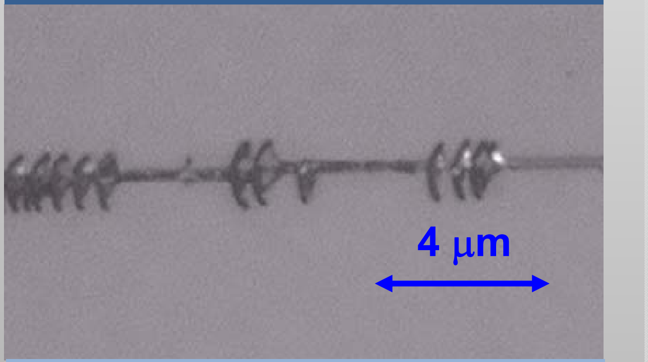

4. Developed quantitative rules for post-diagnosis of cause of surface fractures

LASER DAMAGE

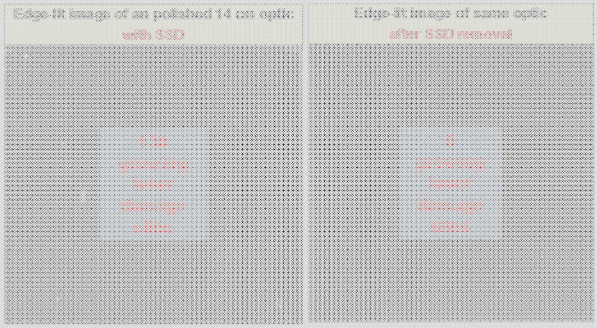

5. Showed link between sub-surface fracture removal & improved laser resistance

Our studies have provided new rules that Opticians use to diagnose the cause of or to mitigate scratches

Property of scratch	What can it tell you?	Rule / Example
1. Scratch width or trailing indent length (L)	- Size of rogue particle (d) - Size distribution of Rogue Particles - Process step - Depth of fracture (c_{90} or c_{max})	For grinding $0.15\ d \le L \le 0.3\ d$ For polishing $0.3\ d \le L \le 0.5\ d$ $c_{90} = 0.9 \langle L \rangle \quad c_{max} = 2.8 \langle L \rangle$
2. Number density	- Rogue particle concentration	
3. Scratch length ($L_{scratch}$)	- Lap properties and rogue particle size	$L_{scratch} = 8.9 \frac{v_{ave} \eta R^2}{P}$
4. Scratch type (plastic, brittle, mixed)	- Load during fracture - Sharpness of particle	$P \approx 0.001 - 0.1\ N$ Plastic only $P \approx 0.1 - 5\ N$ Plastic & Brittle $P > 5\ N$ Plastic & rubble
5. Orientation and pattern of trailing indent	- Particle movement direction - Particle rotation - Stick slip behavior	
6. Curvature or scratch pattern	- Pathway of indenting particle - Shape of tool - Handling vs polishing	
7. Location on optic	- Material removal and surface figure	

Sample	<L>
A: Sandblast	27.1 μm
B: 120 grit	28.3 μm
C: 320 grit	14.9 μm
D: 15 μm loose	4.6 μm
E: 15 μm fixed	4.5 μm
F: 9 μm loose	1.9 μm
G: 7 μm fixed	8.4 μm

T. Suratwala, JNCS 354 (2006) 2023; T. Suratwala OPN (Sep 2008) 12

Example of scratch forensics

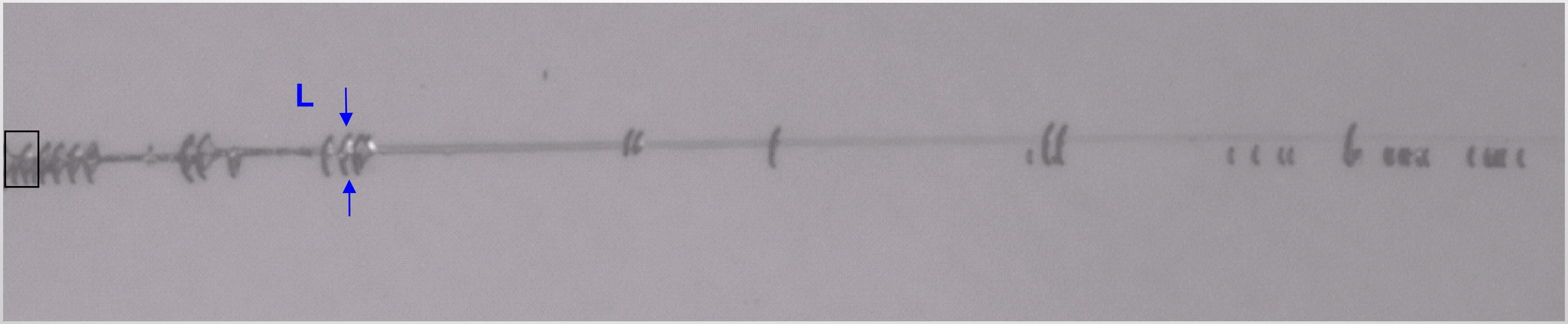

T. Suratwala OPN (Sep 2008) 12

Example of scratch forensics

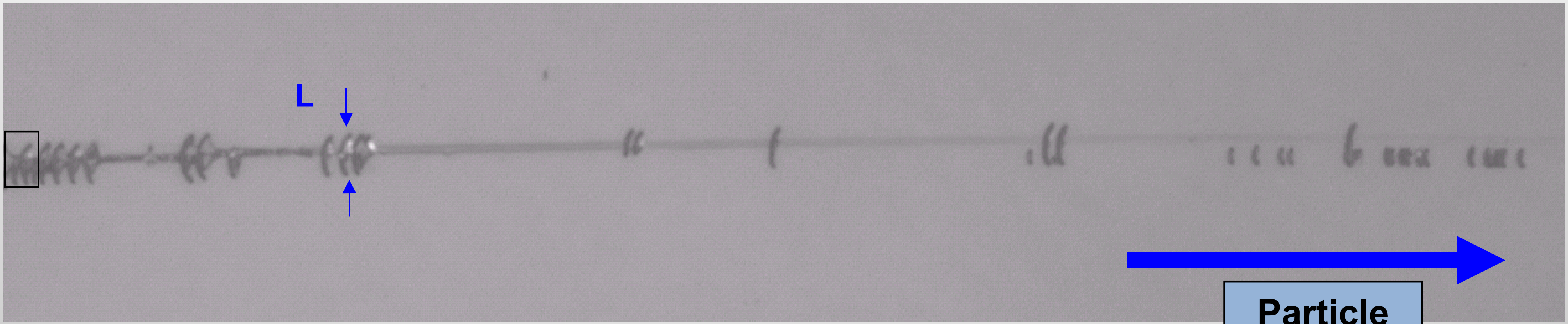

Particle Sliding Direction

Scratch Type = Plastic + Brittle: trailing indent

Trailing Indent length: L= 1.9 μm

Rogue Particle ~ 3.8 – 5.7 μm

c_{90}= 1.8 μm

Scratch Length ~130 μm

Scratch time ~0.16 msec

T. Suratwala OPN (Sep 2008) 12

Strategy for reducing the scratch density on optical surfaces

1. Measure the SSD at each step
2. Define proper removal rate at each step such that all the SSD from previous step is removed
3. Can use etching as a means to remove SSD just after grinding
4. Ensure handling and cleaning at each step does not let rogue particles make contact with surface
5. Remove all rogue particles in polishers; Use scratch forensics to determine source
6. Use etched scratch dig inspections between steps and at end of process

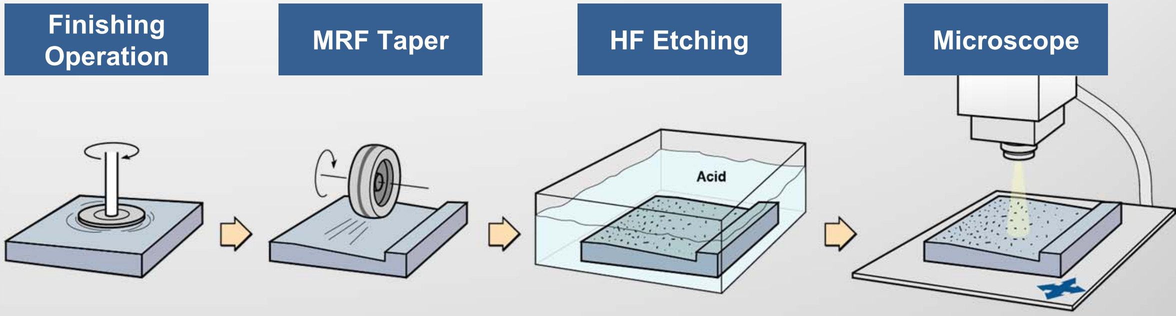
Finishing Operation

MRF Taper

HF Etching

Microscope

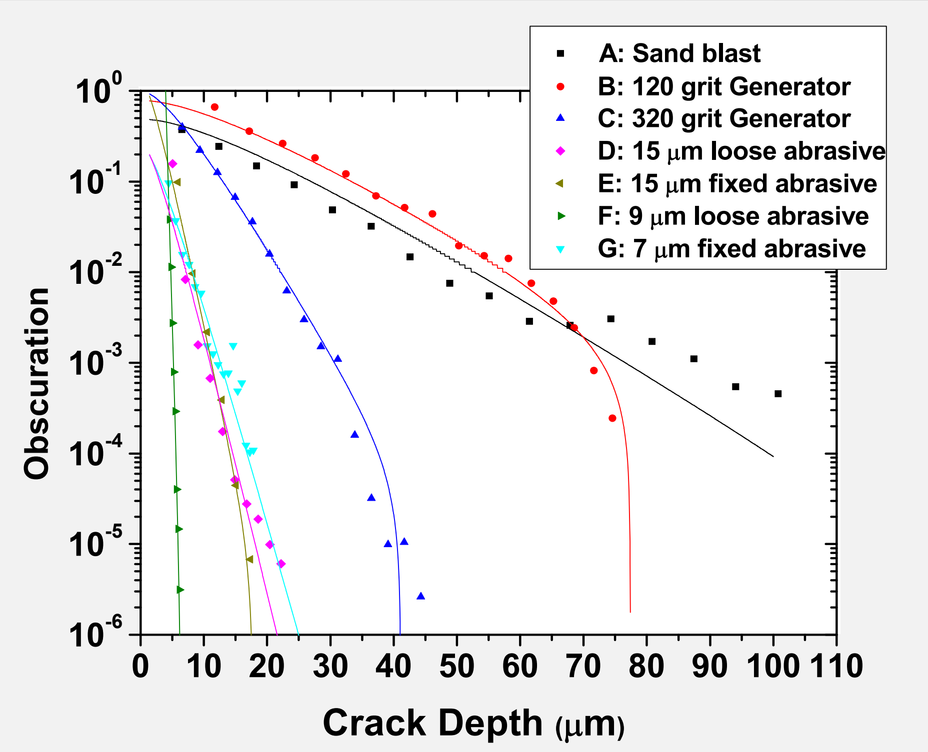

Strategy for reducing the scratch density on optical surfaces

1. Measure the SSD at each step
2. Define proper removal rate at each step such that all the SSD from previous step is removed
3. Can use etching as a means to remove SSD just after grinding
4. Ensure handling and cleaning at each step does not let rogue particles make contact with surface
5. Remove all rogue particles in polishers; Use scratch forensics to determine source
6. Use etched scratch dig inspections between steps and at end of process

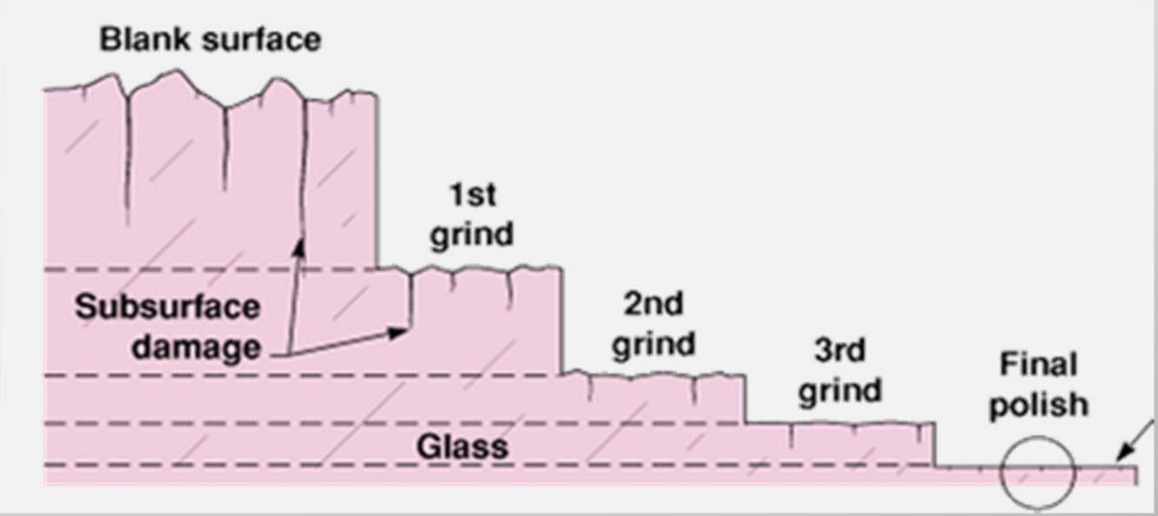

Strategy for reducing the scratch density on optical surfaces

1. Measure the SSD at each step
2. Define proper removal rate at each step such that all the SSD from previous step is removed
3. Can use etching as a means to remove SSD just after grinding
4. Ensure handling and cleaning at each step does not let rogue particles make contact with surface
5. Remove all rogue particles in polishers; Use scratch forensics to determine source
6. Use etched scratch dig inspections between steps and at end of process

Schematic

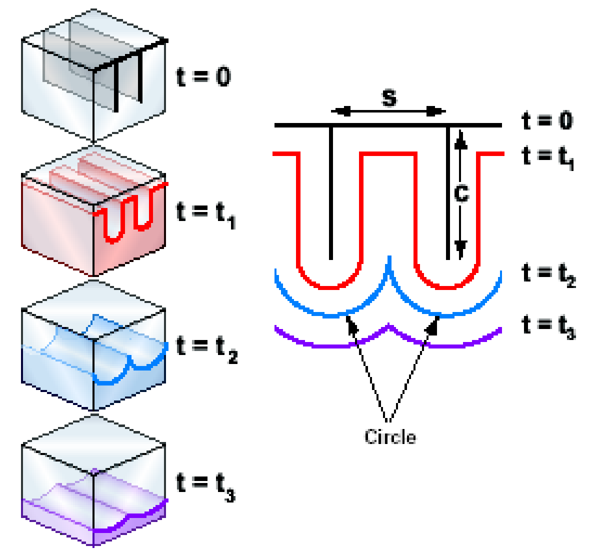

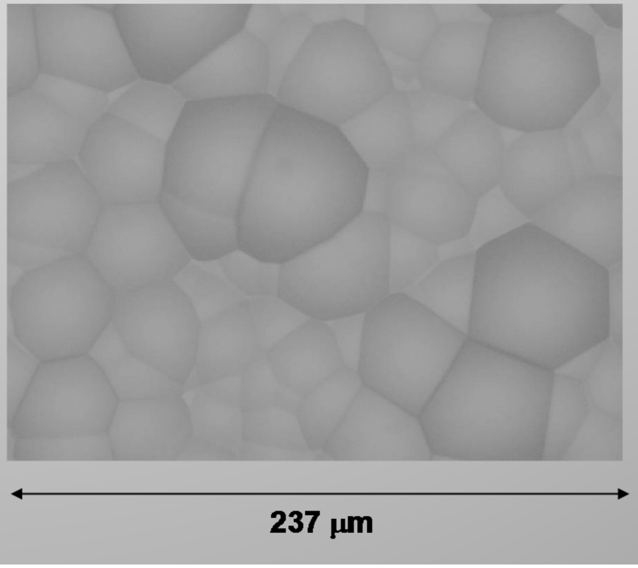

Strategy for reducing the scratch density on optical surfaces

1. Measure the SSD at each step
2. Define proper removal rate at each step such that all the SSD from previous step is removed
3. Can use etching as a means to remove SSD just after grinding
4. Ensure handling and cleaning at each step does not let rogue particles make contact with surface
5. Remove all rogue particles in polishers; Use scratch forensics to determine source
6. Use etched scratch dig inspections between steps and at end of process

Crack *depth* distributions:
Loose abrasive grinding with addition of rogue particles

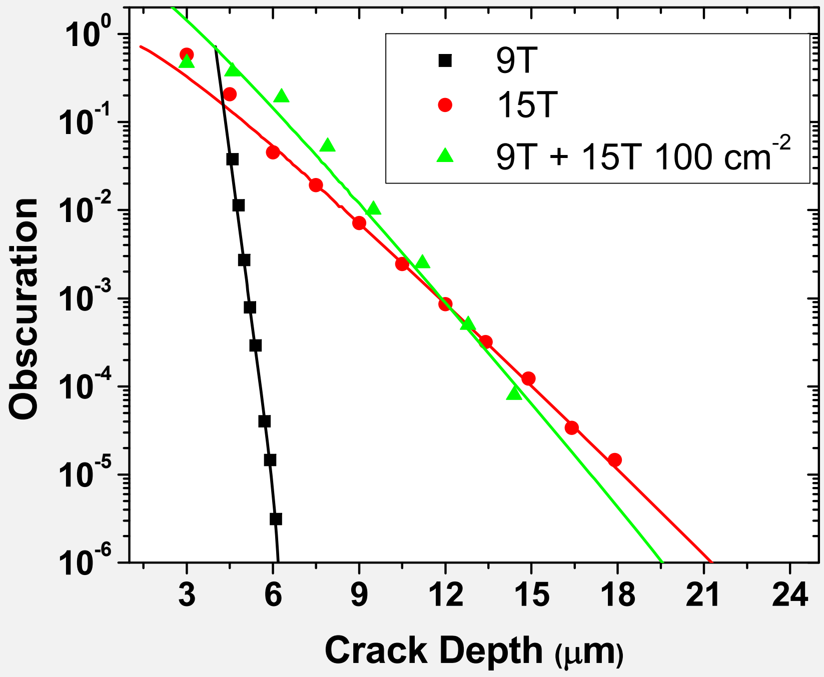

Rogue particle sources

1) In slurry from foreign particle or agglomerates
2) Dried slurry on components falling in
3) Contamination from polisher exterior

Strategy for reducing the scratch density on optical surfaces

1. Measure the SSD at each step
2. Define proper removal rate at each step such that all the SSD from previous step is removed
3. Can use etching as a means to remove SSD just after grinding
4. Ensure handling and cleaning at each step does not let rogue particles make contact with surface
5. Remove all rogue particles in polishers; Use scratch forensics to determine source
6. **Use etched scratch dig inspections between steps and at end of process**

Etching provides a means of revealing subsurface damage masked by hydrated silica

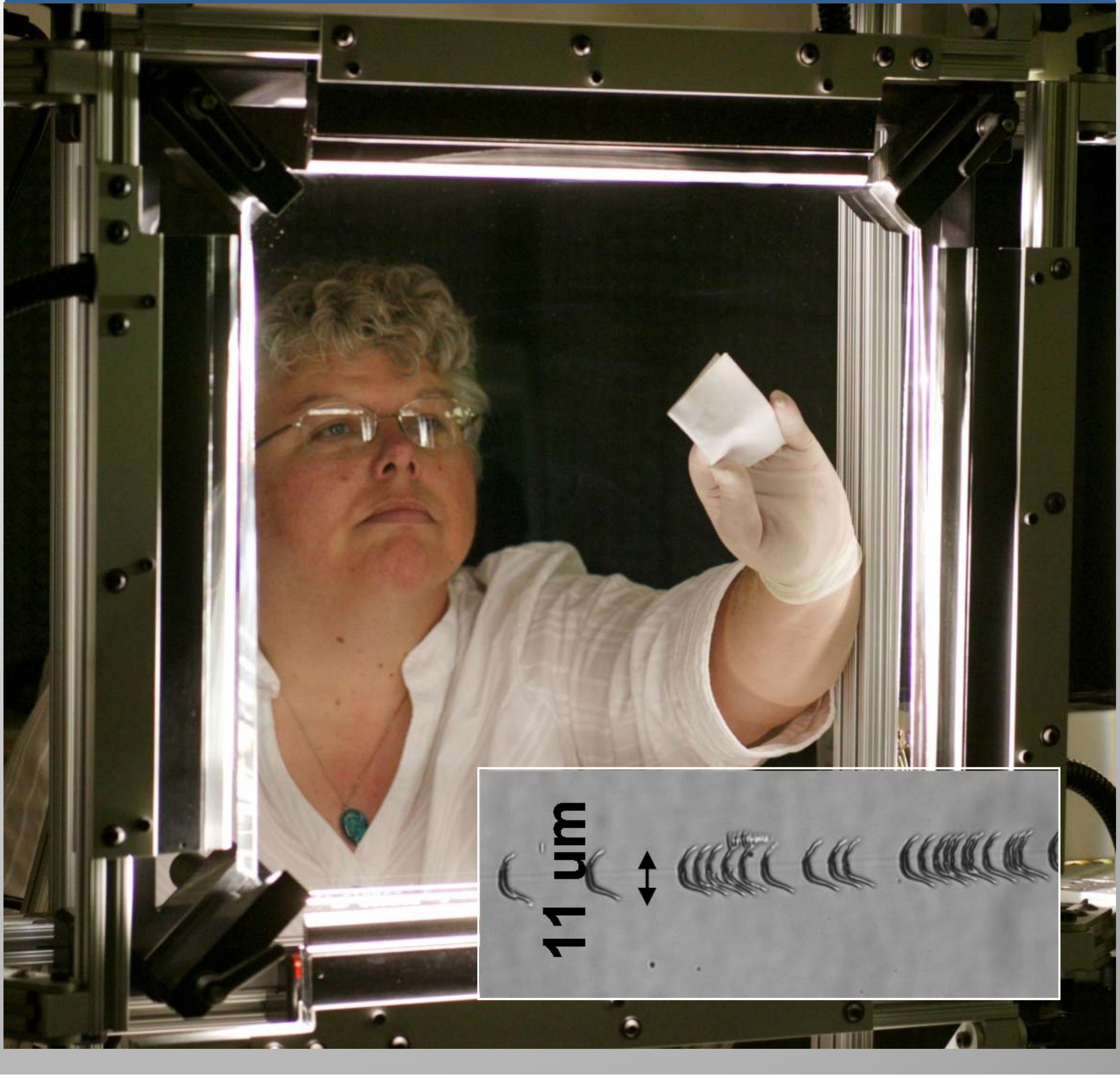

There are five major areas of effort that have aided in managing sub-surface fractures

GRINDING

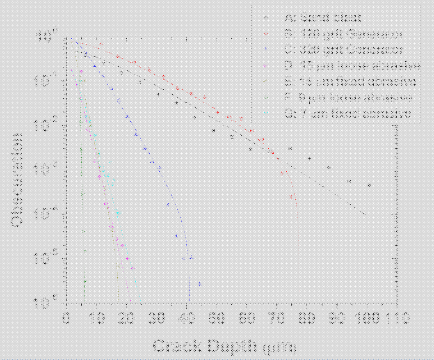

1. Developed fracture mechanics understanding of sub-surface fracture distributions

POLISHING

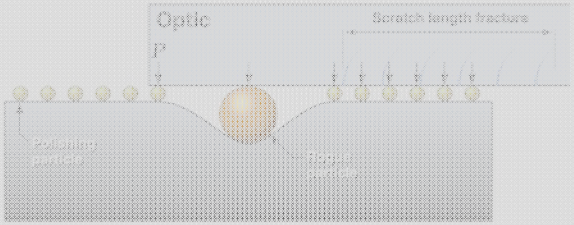

2. Identified/characterized behavior of rogue particles causing sub-surface fractures

CHEMICAL ETCHING

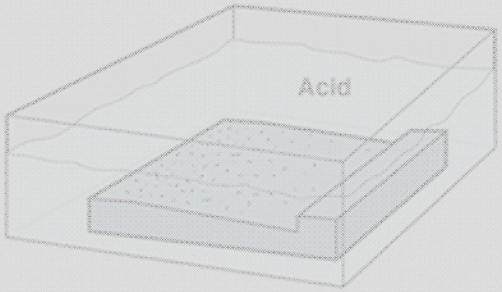

3. Established techniques using etching to reveal and remove subsurface fractures

SCRATCH FORENSICS

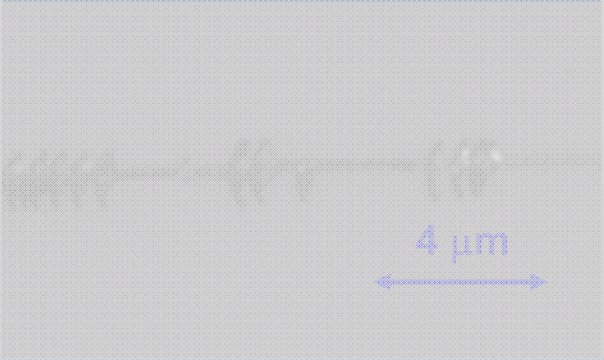

4. Developed quantitative rules for post-diagnosis of cause of surface fractures

LASER DAMAGE

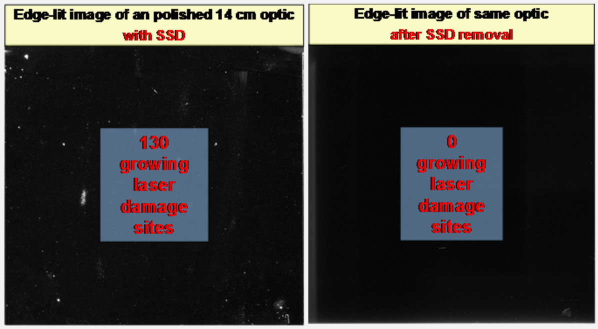

5. Showed link between sub-surface fracture removal & improved laser resistance

SSD-free test optics have been fabricated such it does not laser damage, supporting the "absorber-in-a-crack" theory

Edge-lit image of an polished 14 cm optic with SSD

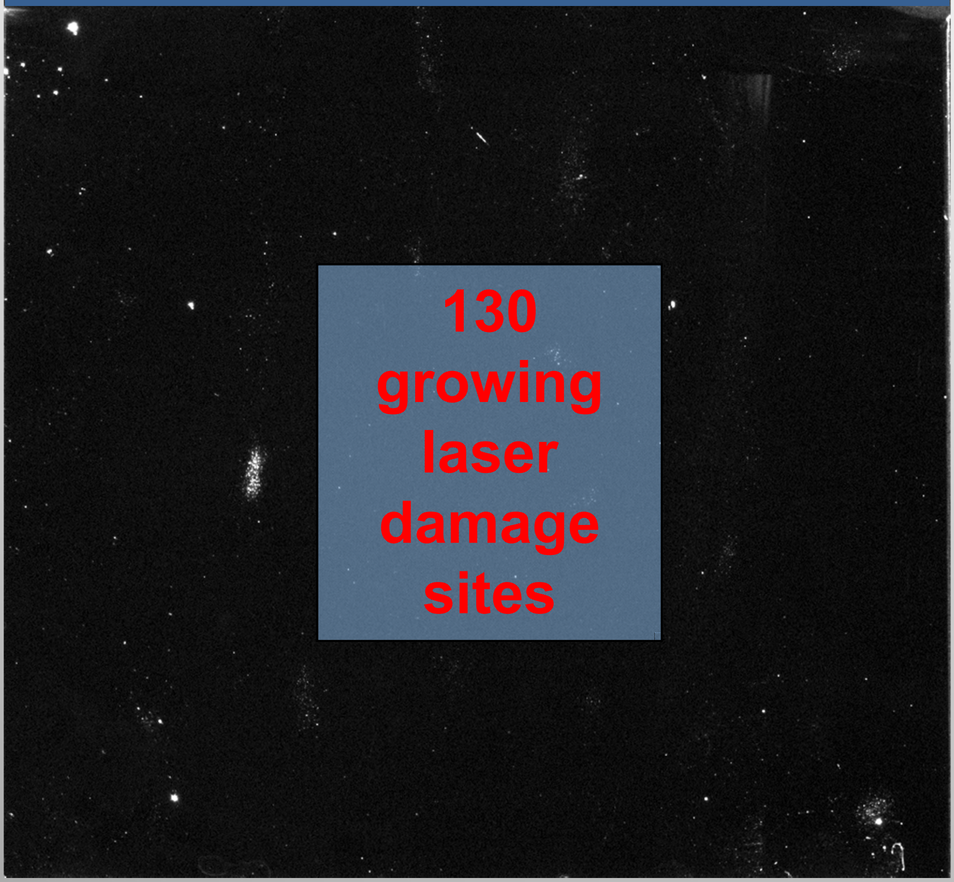

130 growing laser damage sites

Edge-lit image of same optic after SSD removal

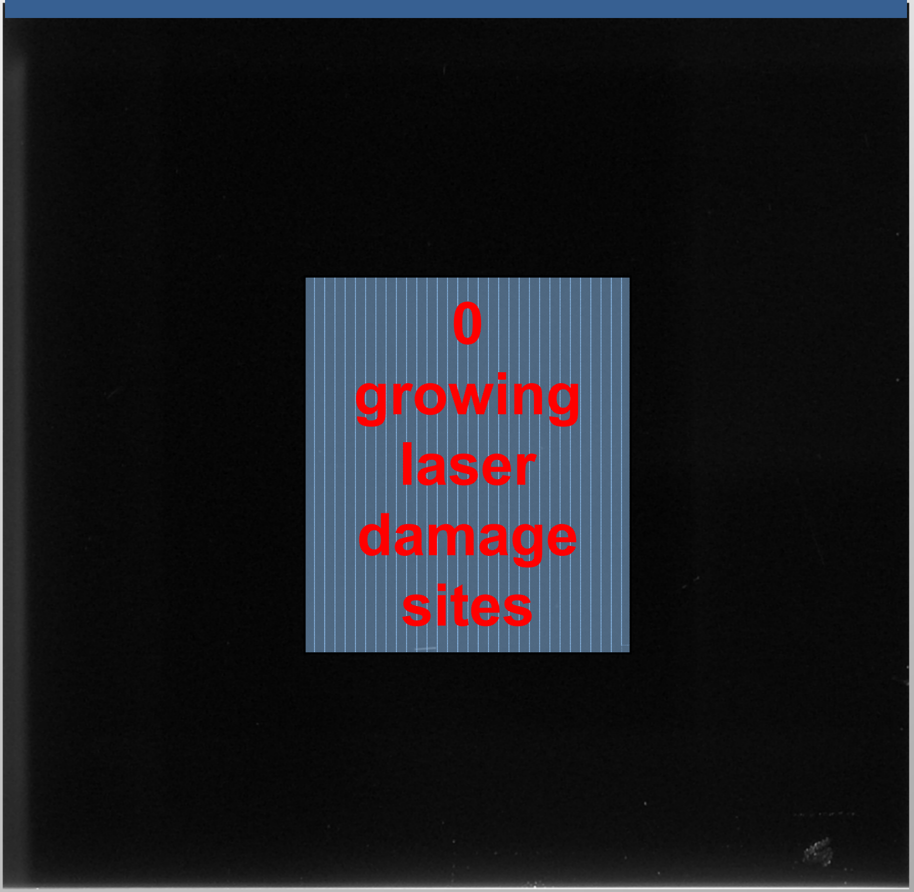

0 growing laser damage sites

Laser testing on a 14 cm x 14 cm test optic to 14 J/cm^2 (351 nm, 3 ns equiv) resulted in the elimination of growing laser initiation site upon SSD removal

AMP process system

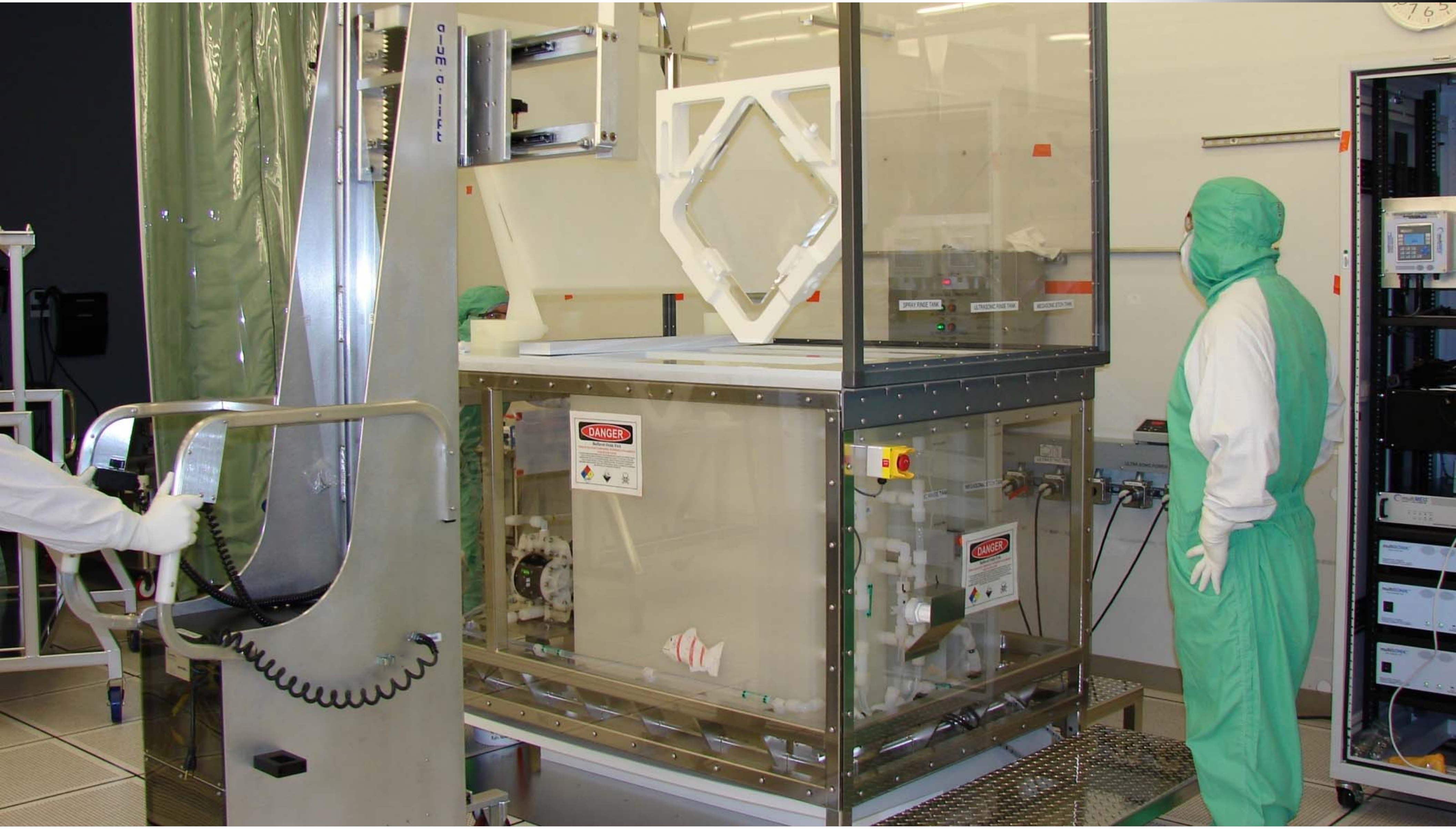

T. Suratwala JACS 94(2) (2010) 416; P. Miller US Patent 0079931 (2011)

AMP process significantly reduces laser damage initiation per unit scratch length

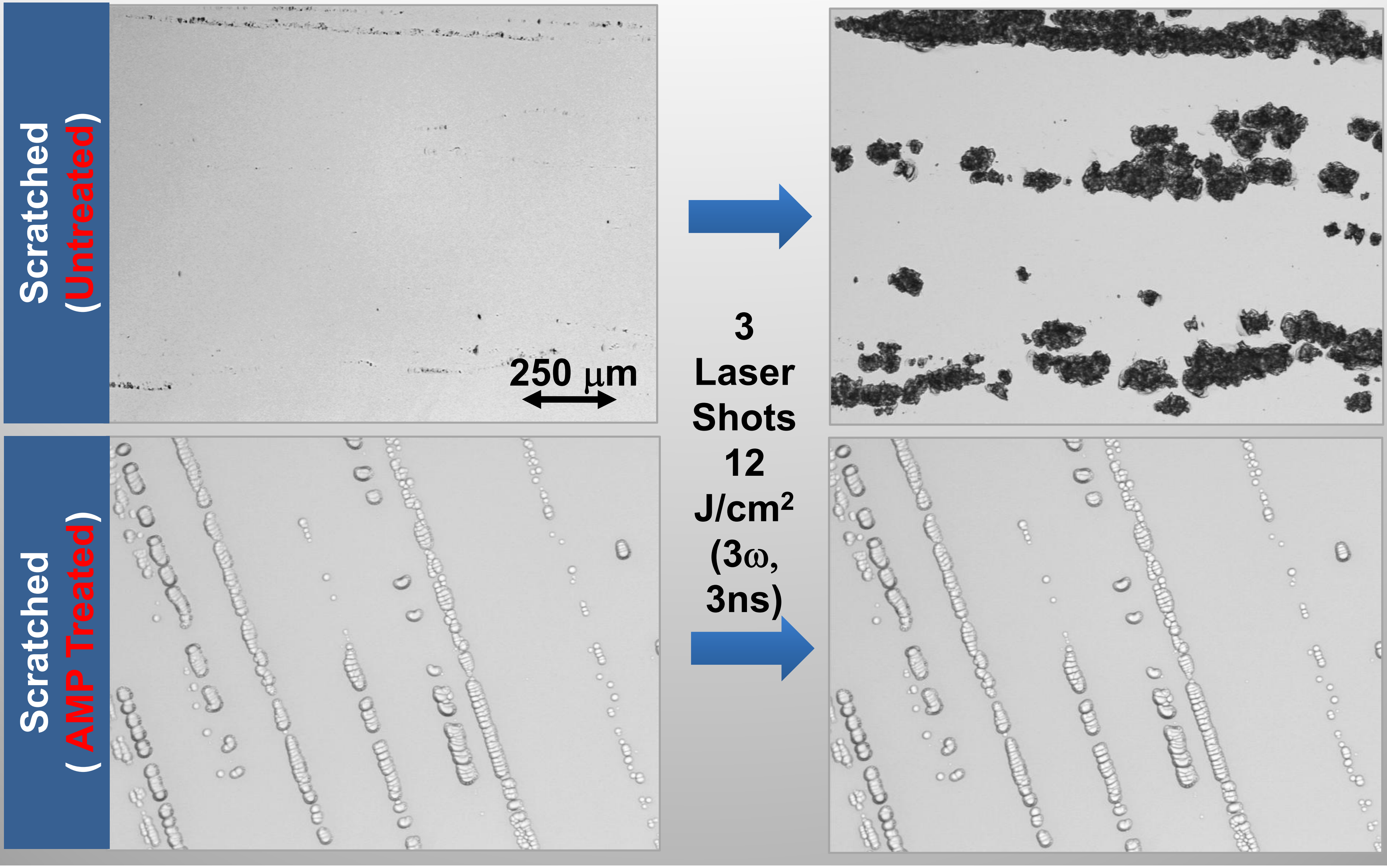

3 Laser Shots 12 J/cm^2 (3ω, 3ns)

T. Suratwala JACS 94(2) (2010) 416; P. Miller US Patent 0079931 (2011)

The materials science behind grinding & polishing

1. Sub-surface Damage (scratch/dig)
2. **Roughness**
3. Surface Figure

To understand surface roughness, one need to understand the complex microscopic & chemical interactions during polishing

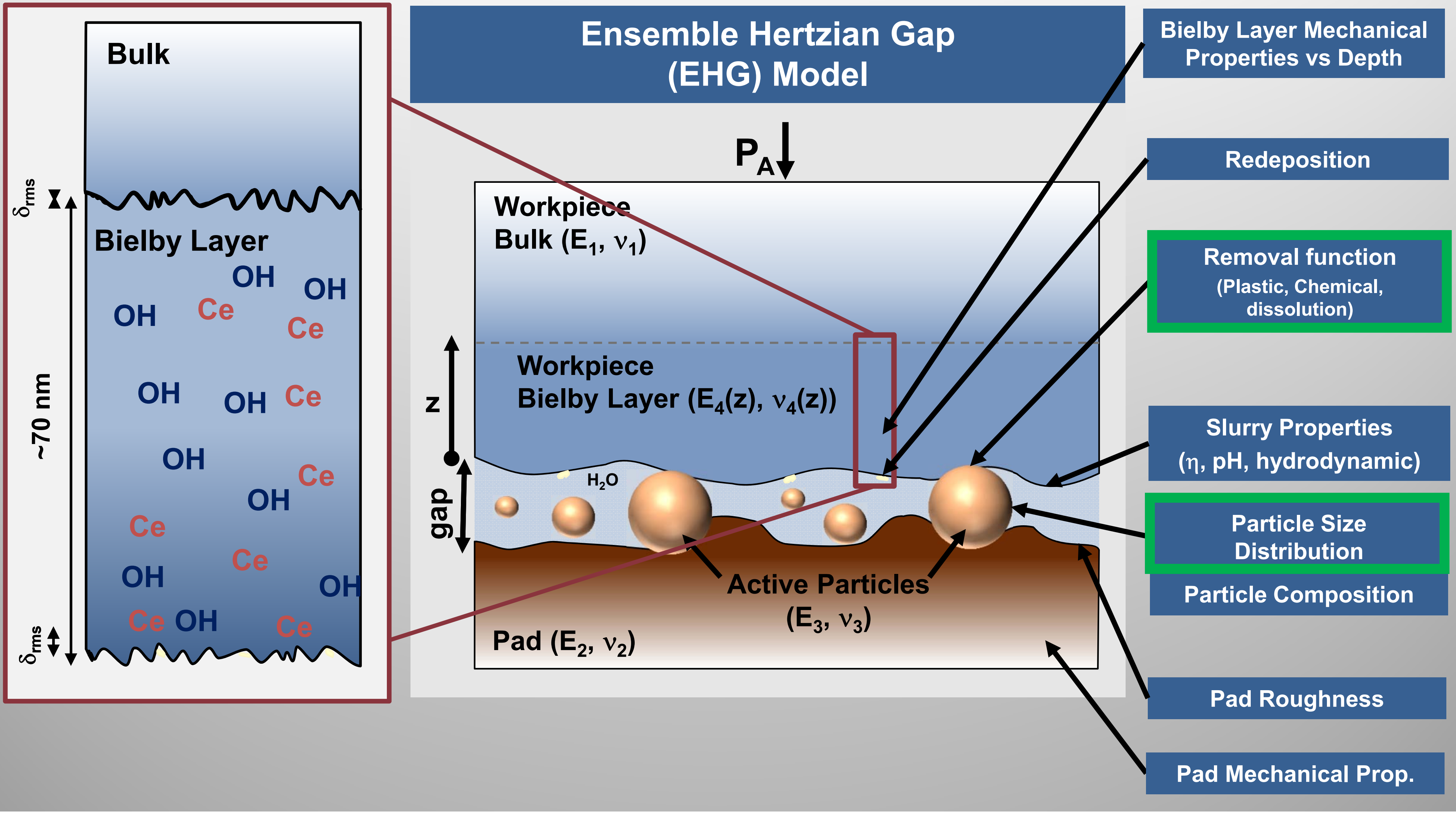

Ensemble Hertzian Gap (EHG) Model

Bielby Layer Mechanical Properties vs Depth

Redeposition

Removal function
(Plastic, Chemical, dissolution)

Slurry Properties
(η, pH, hydrodynamic)

Particle Size Distribution

Particle Composition

Pad Roughness

Pad Mechanical Prop.

The tail end of the slurry's PSD* strongly correlates with workpiece roughness

Measured PSD* of ceria slurries

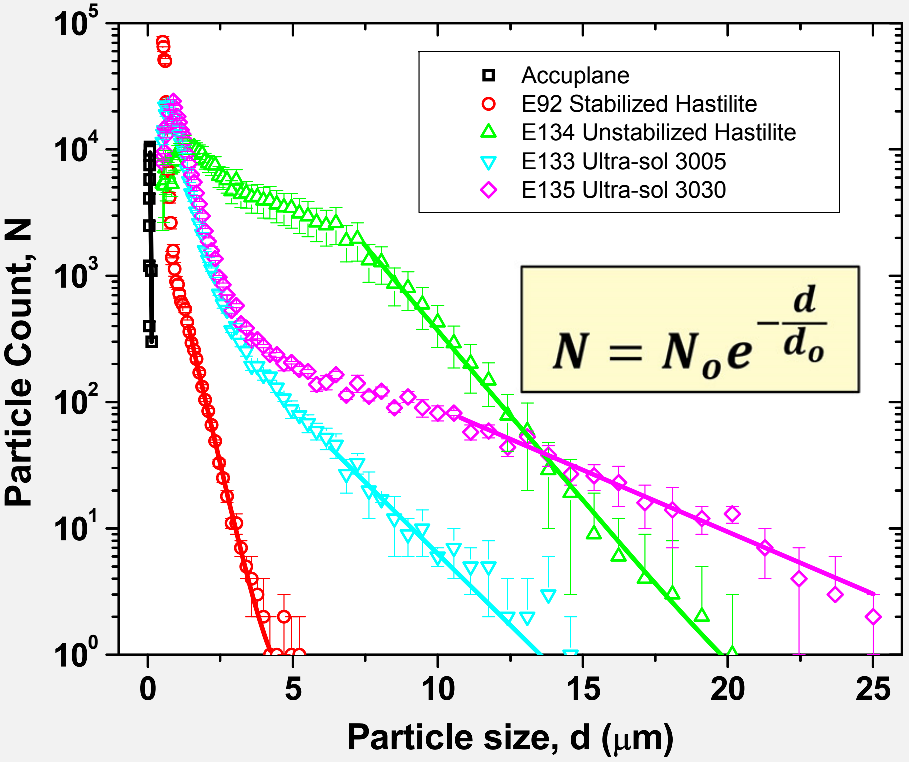

$$N = N_o e^{-\frac{d}{d_o}}$$

The tail end of each slurry follows a single exponential distribution

***Particle size distribution**

AFM images of fused silica workpieces after polishing with different ceria slurries

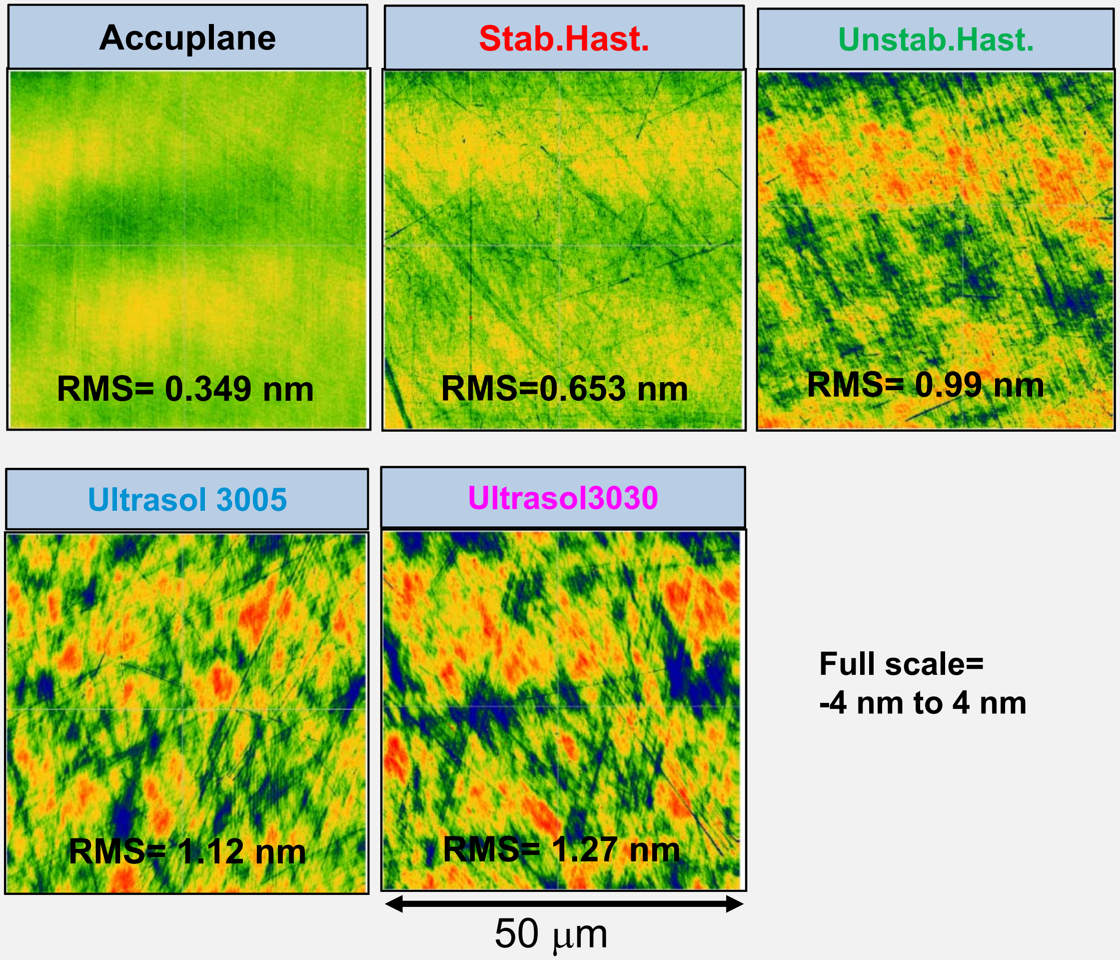

Full scale=
-4 nm to 4 nm

Suratwala et. al., *J. Am. Cer. Soc.* 97(1) 2014

The tail end of the slurry's PSD* strongly correlates with workpiece roughness

Measured PSD* of ceria slurries

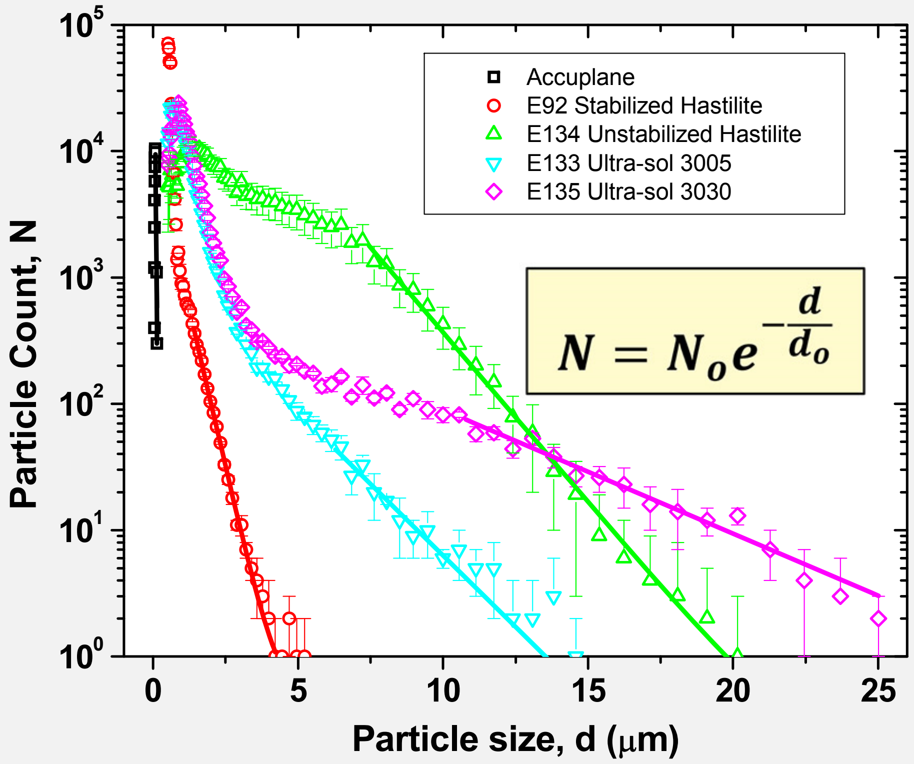

The tail end of each slurry follows a single exponential distribution

*Particle size distribution

Exponent constant in PSD of slurry vs RMS roughness of polished surface

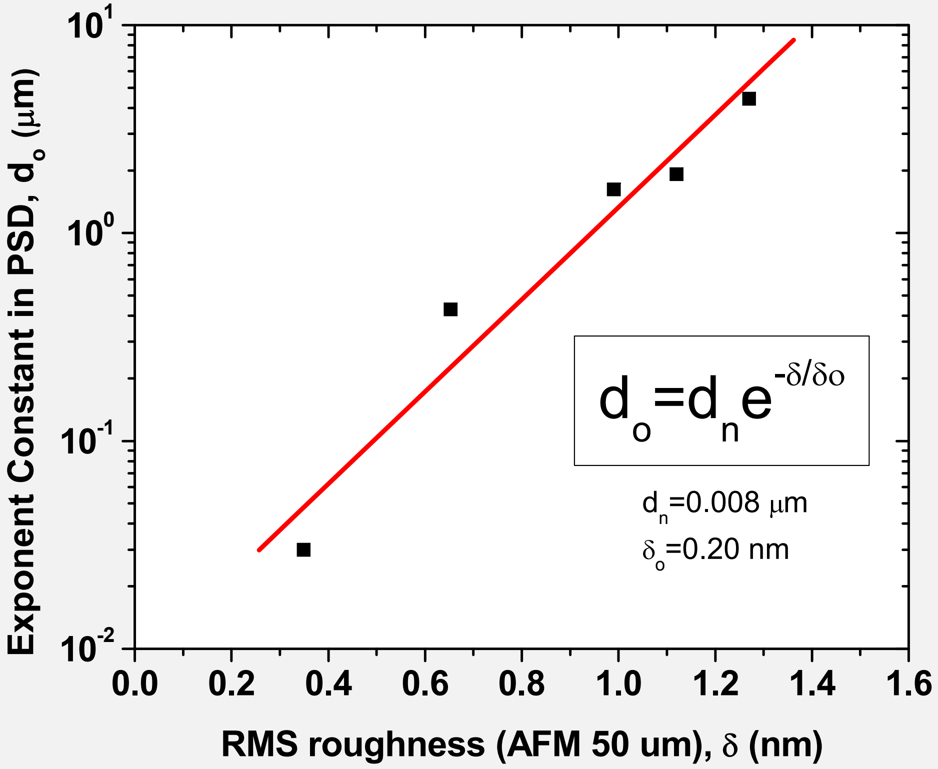

The slope of the slurry's PSD quantitatively scales with the rms roughness

Suratwala et. al., *J. Am. Cer. Soc.* 97(1) 2014

Novel chemical slurry stabilization and engineered filtration has resulted in improve slurry PSD

Chemical Stabilization

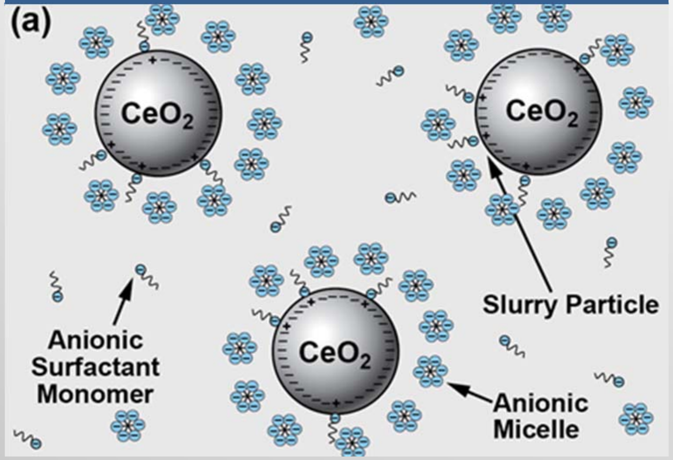

Engineered Filtration

Improved Particle Size Distributions

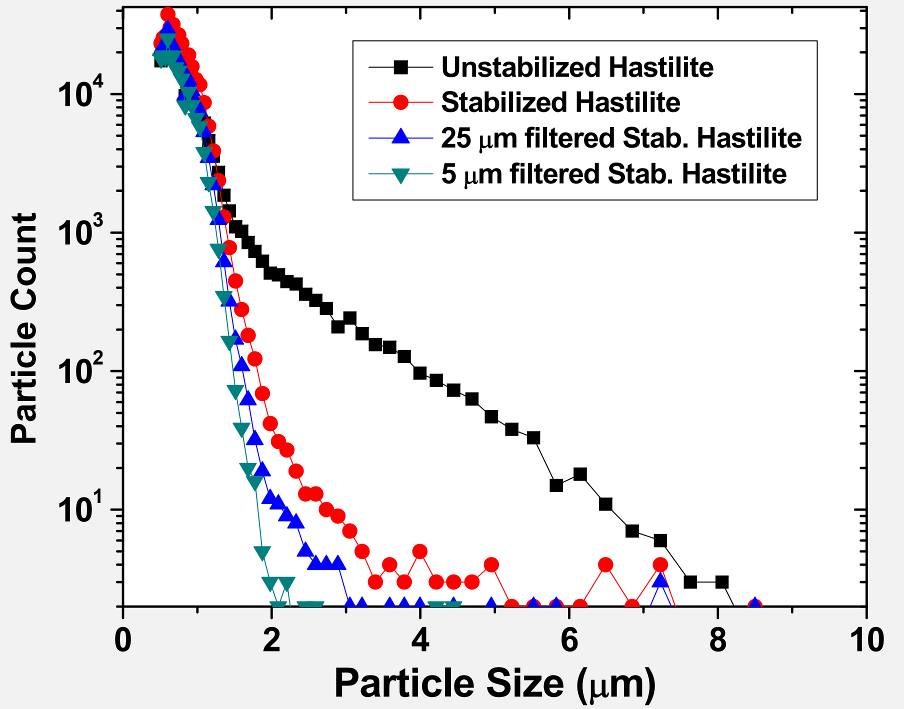

- Surfactant dramatically reduces agglomeration without reducing removal rate
- Appropriate filtration further improves PSD

US Patent Application WO 2012129244 A1 (September 27, 2012)
R. Dylla-Spears, Colloids & Surfaces A 447 (2014) 32
T. Suratwala, JACS 97 (2014) 81

Single pass ceria particle sliding experiments suggest 'plastic' - type removal can occur during polishing

AFM Image (2 μm x 2 μm) of fused silica surface

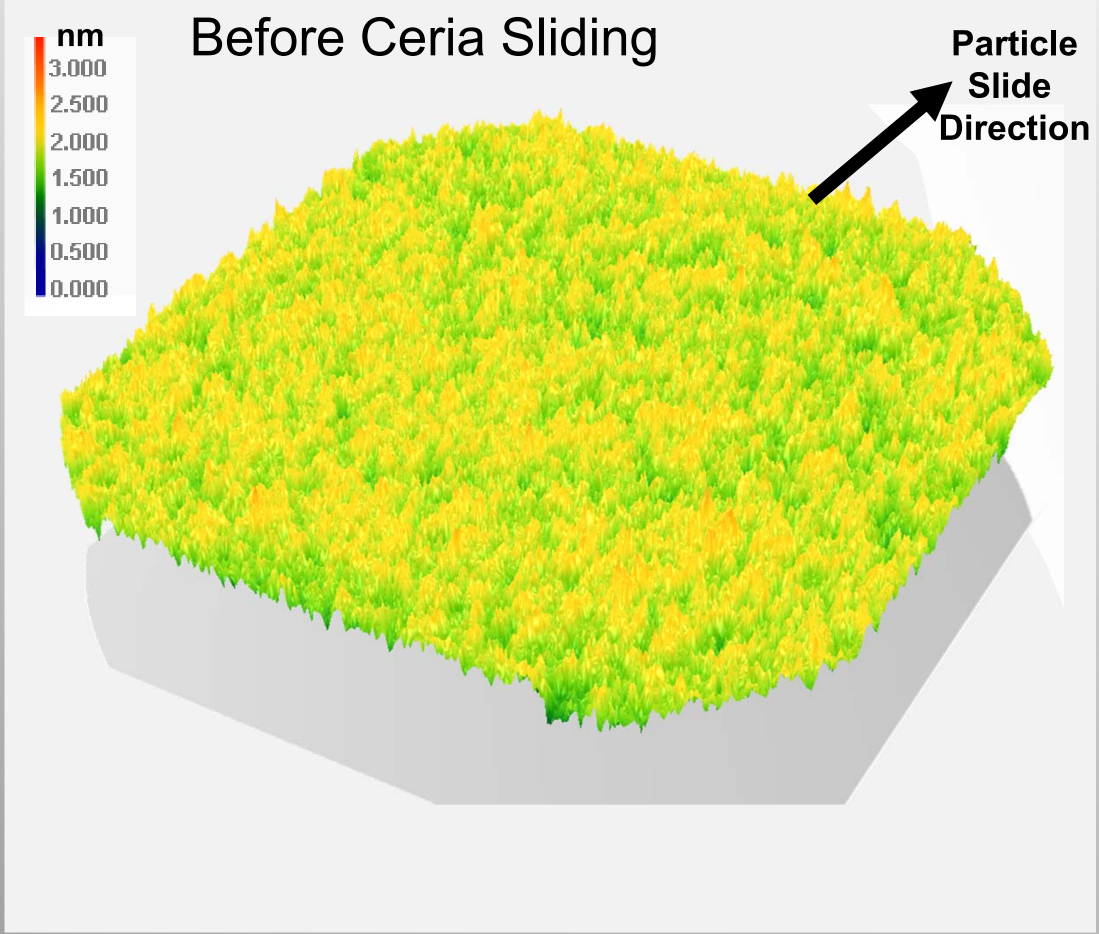

Sample 4: using Stabilized Hastilite

Suratwala et. al., *J. Am. Cer. Soc.* 97(1) 2014

Single pass ceria particle sliding experiments suggest ‘plastic’ - type removal can occur during polishing

AFM Image (2 μm x 2 μm) of fused silica surface

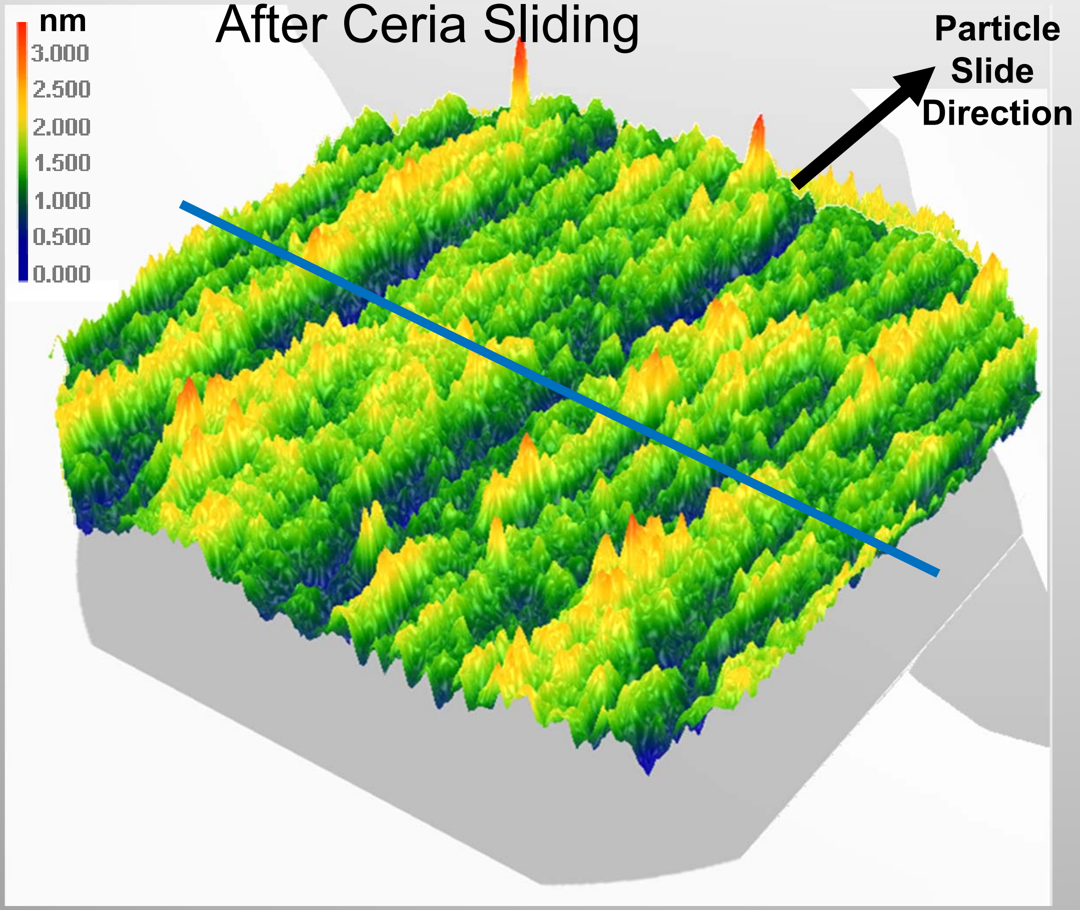

Sample 4: using Stabilized Hastilite

Lineout of AFM Perp. to slide particle slide direction

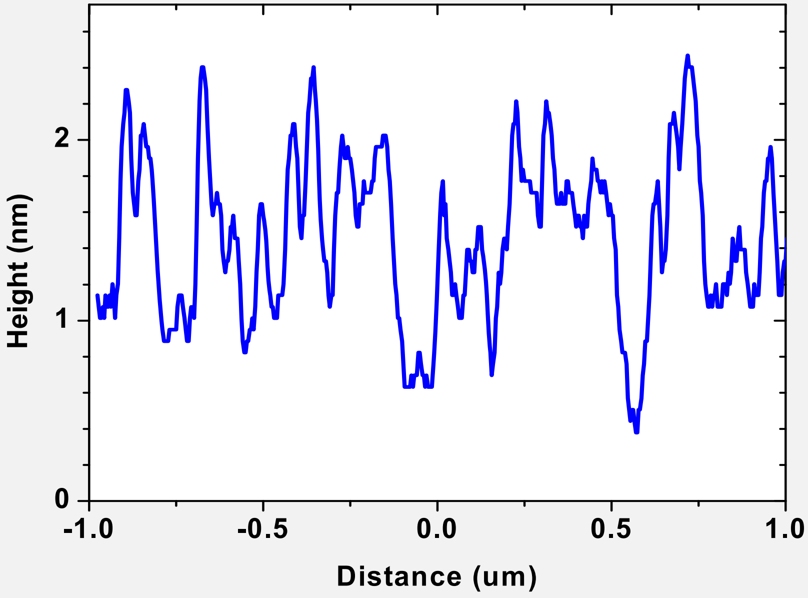

- **Single pass of ceria particle removes ~1 nm of material (~7 Si-O units)**

Suratwala et. al., *J. Am. Cer. Soc.* 97(1) 2014

Ensemble Hertzian Gap (EHG) model is used to determine the gap, fraction of particles loaded, & the load per particle

EHG Model Setup

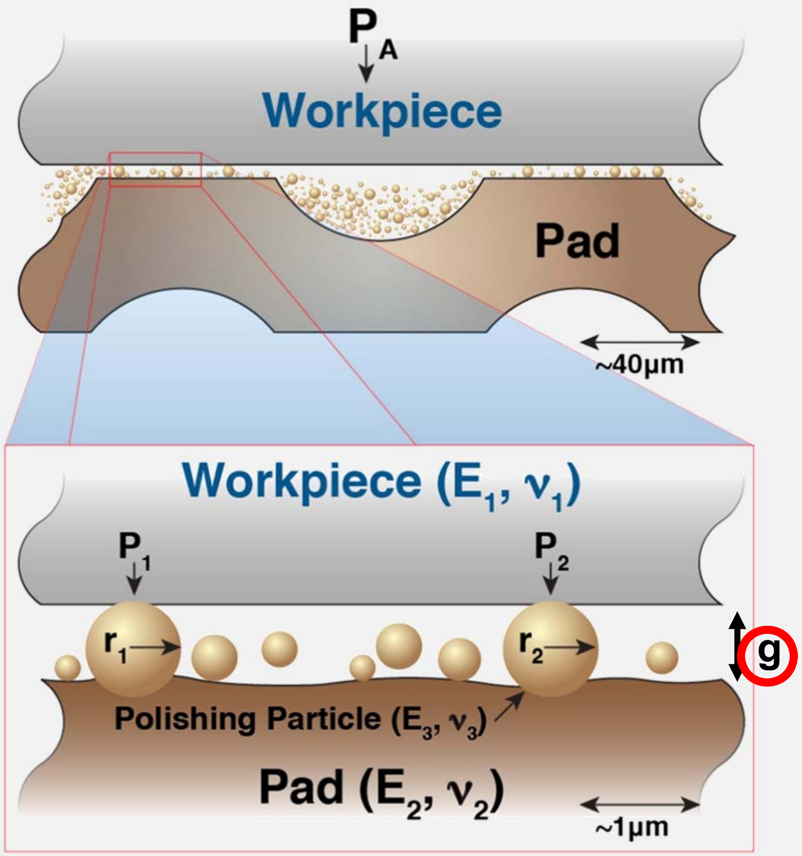

Suratwala et. al., *J. Am. Cer. Soc.* 97(1) 2014

Governing Relationships

Load Balance

$$P_A = N_b 2\pi r_o^2 \int_{\frac{g}{2}}^{\infty} F(r)\,P(r,g)\,dr$$

Number density of particles in gap

$$N_b = f_A N_p = f_A \frac{\int F(r)\,dr}{\int F(r)\,2\pi r\,dr}$$

Load on each particle (Hertzian Contact)

$$P(r,g) = \frac{4}{3} E_{eff} \sqrt{r(2r-g)^3}$$

g = gap at interface

f_A= fraction of pad area making contact with workpiece

N_p= # of particles/area

In this formalism, only need to solve for g

Using the EHG model, the calculated fraction of “active” particles is very small

Full PSD for stabilized and unstabilized Hastilite Polishing Slurry

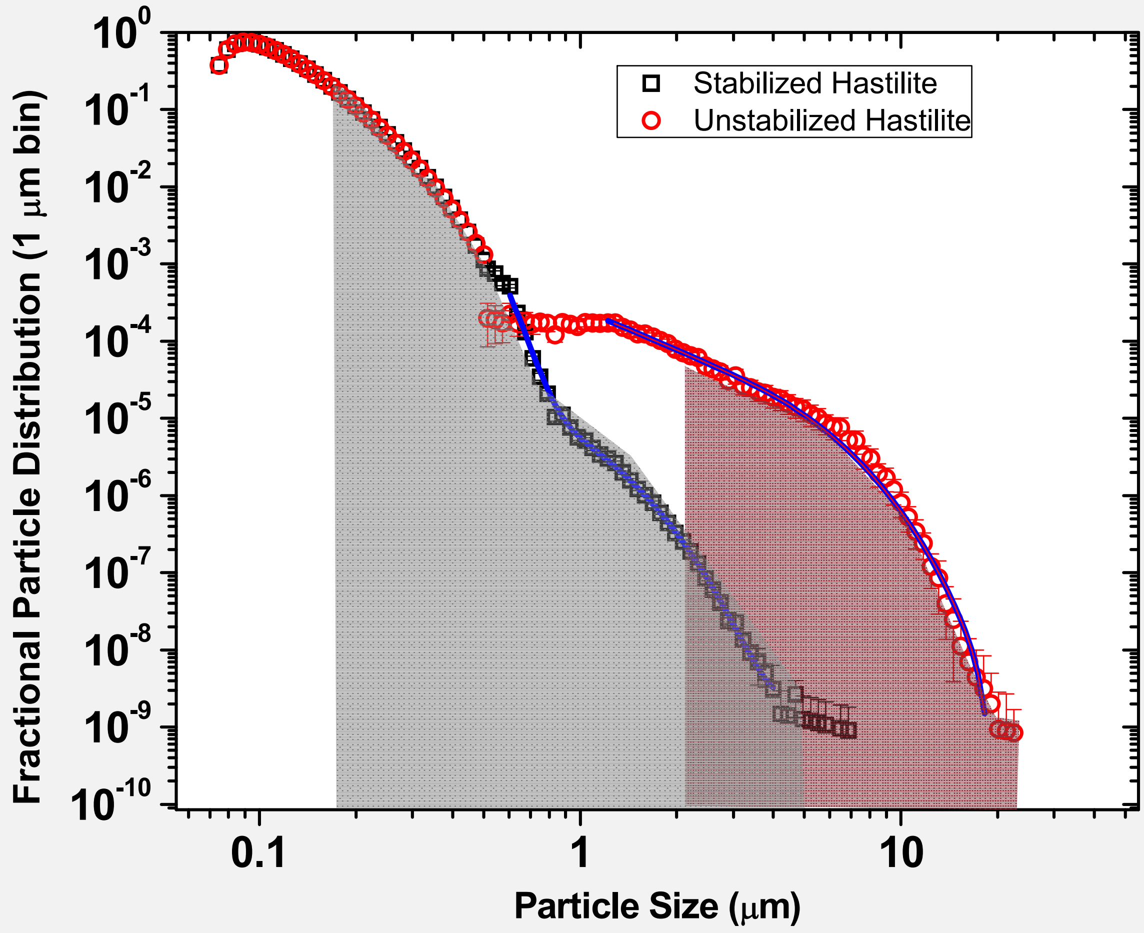

- Shaded region represents active (i.e., loaded) particles (using $f_A=1.5\text{x}10^{-4}$)
- Stabilized Hastilite uses much smaller particles during polishing compared to Unstabilized Hastilite

Slurry	Gap	Fraction of active particles
Stabilized Hastilite	0.07 μm	0.224
Unstabilized Hastilite	0.42 μm	0.0005

Suratwala et. al., *J. Am. Cer. Soc.* 97(1) 2014

Using the EHG model, polished surfaces using different PSDs have been simulated over multiple spatial scale lengths

<u>Unstabilized</u> Hastilite PO Polished Surface

Measured

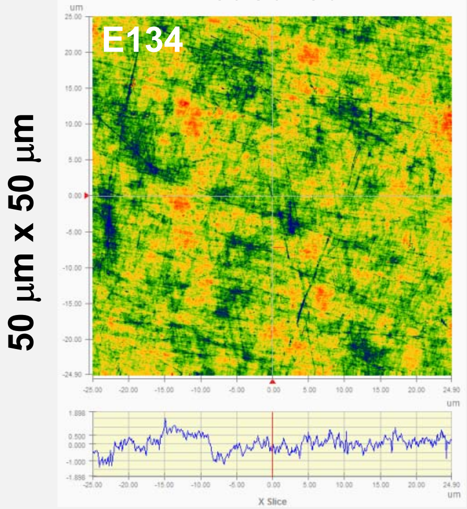

<u>Stabilized</u> Hastilite PO Polished Surface

Measured

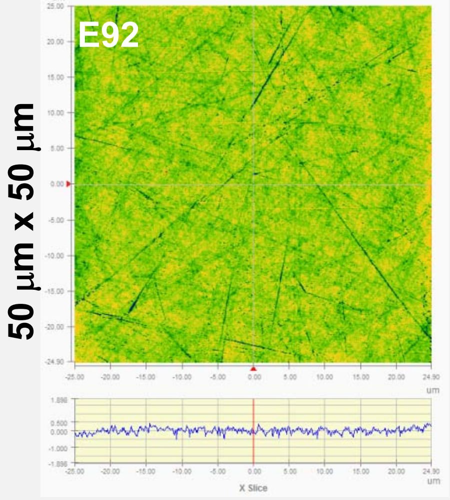

Suratwala et. al., *J. Am. Cer. Soc.* 97(1) 2014

Using the EHG model, polished surfaces using different PSDs have been simulated over multiple spatial scale lengths

<u>Unstabilized</u> Hastilite PO Polished Surface

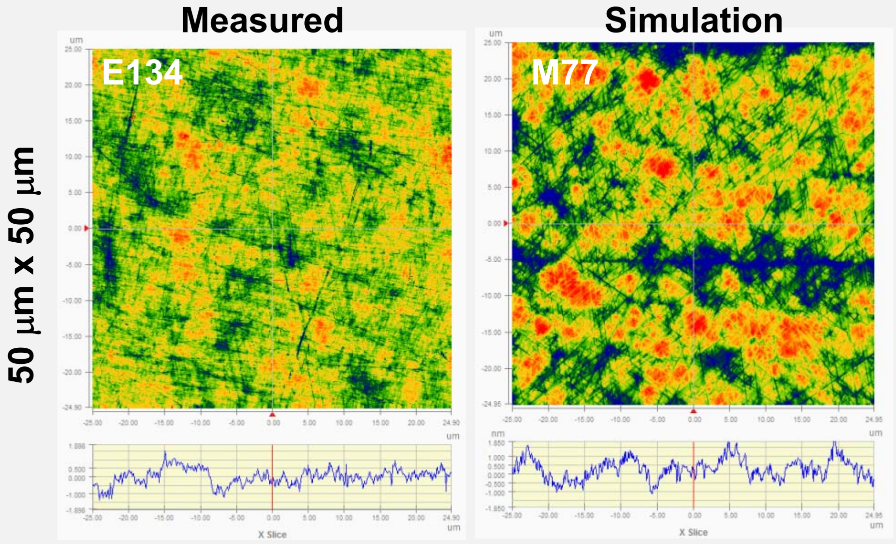
Measured

Simulation

<u>Stabilized</u> Hastilite PO Polished Surface

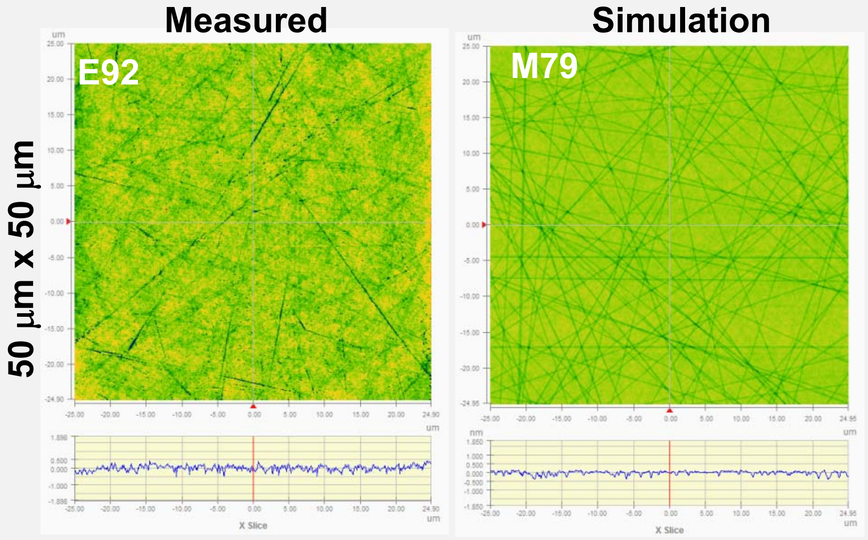
Measured

Simulation

Suratwala et. al., *J. Am. Cer. Soc.* 97(1) 2014

Using the EHG model, polished surfaces using different PSDs have been simulated over multiple spatial scale lengths

Unstabilized Hastilite PO Polished Surface

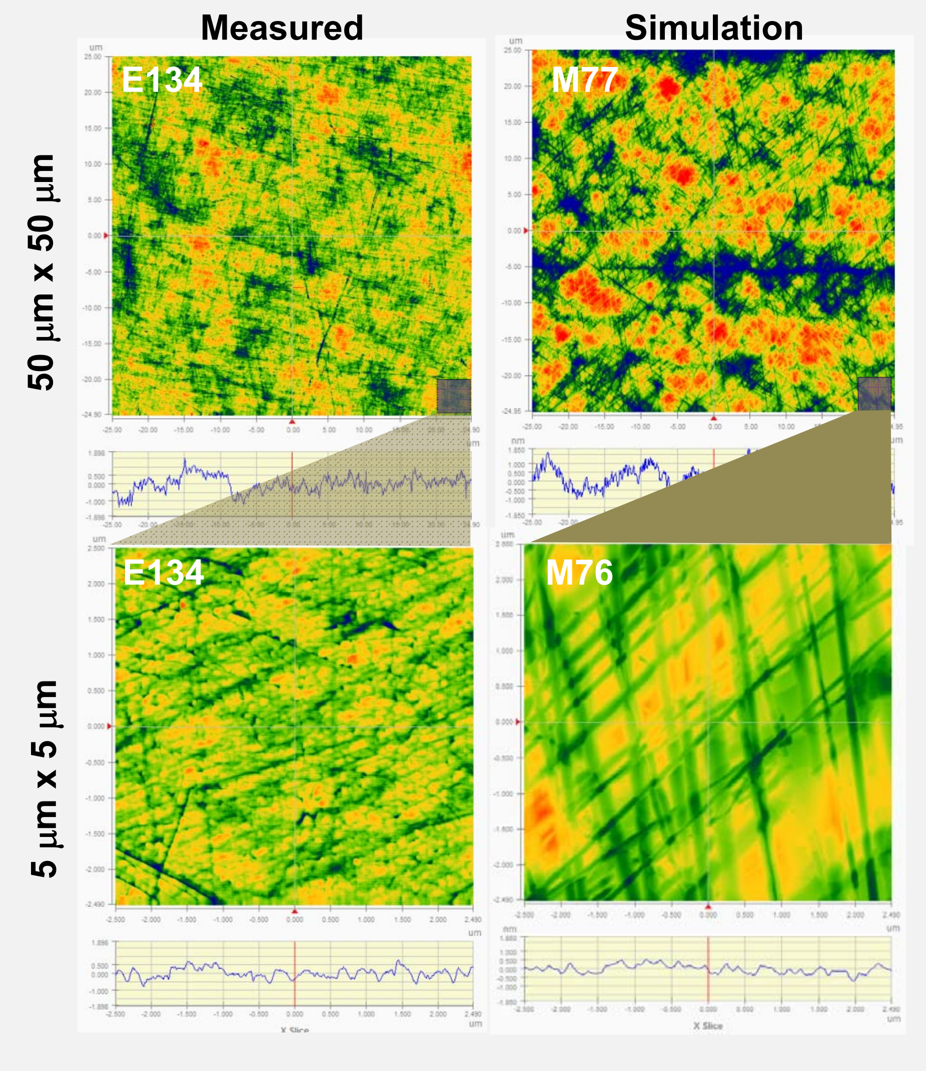

Stabilized Hastilite PO Polished Surface

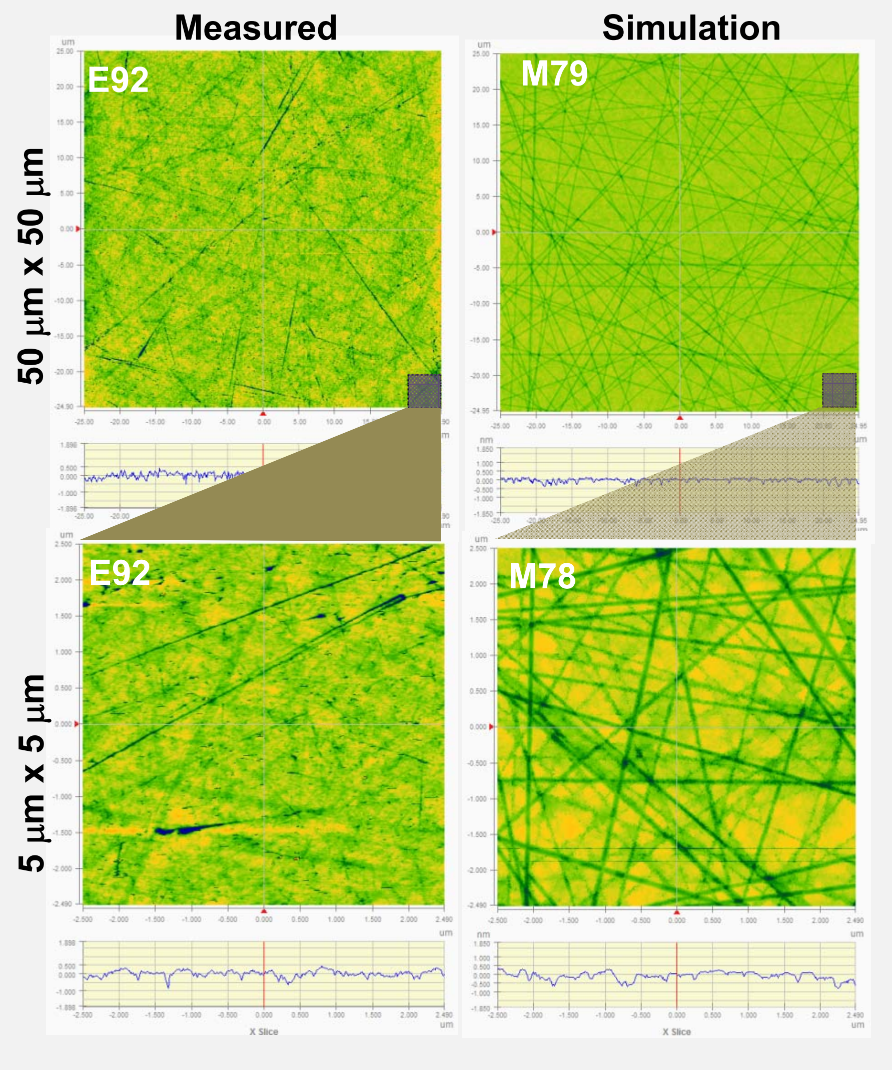

Suratwala et. al., *J. Am. Cer. Soc.* 97(1) 2014

The materials science behind grinding & polishing

1. Sub-surface Damage (scratch/dig)
2. Roughness
3. Surface Figure

The surface figure of an optic is typically measured by interferometry

Fizeau Interferometer

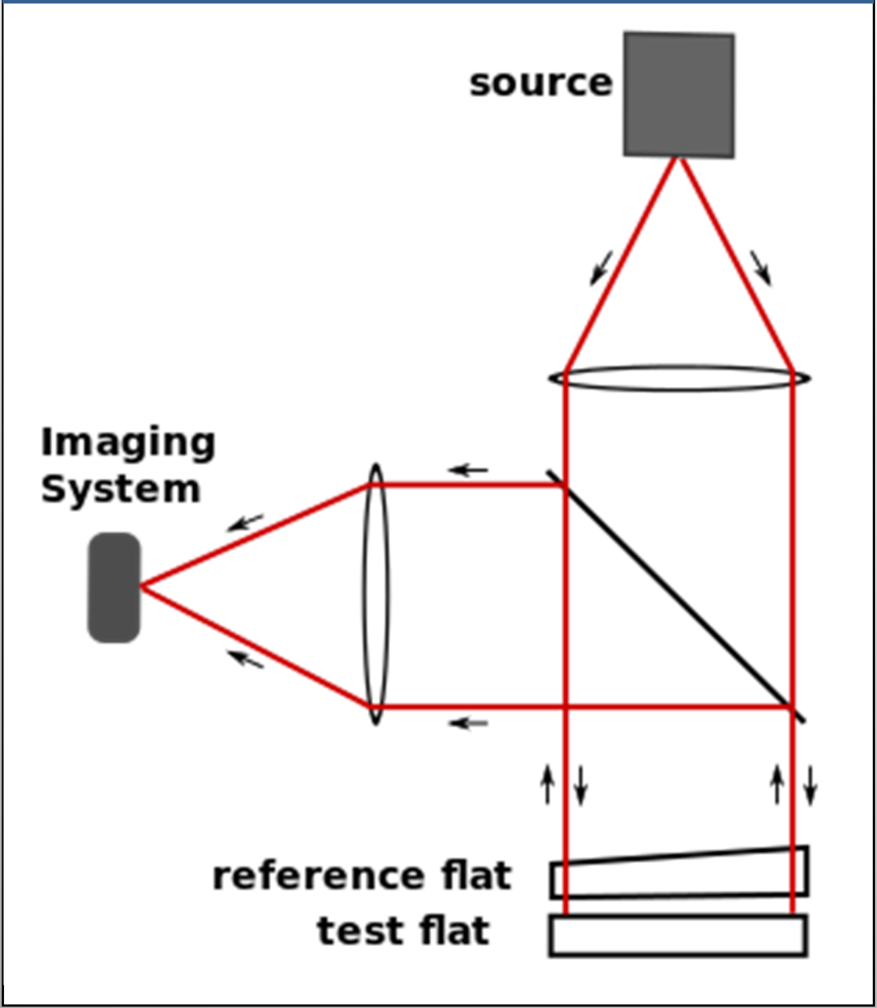

Measured Surface Figure

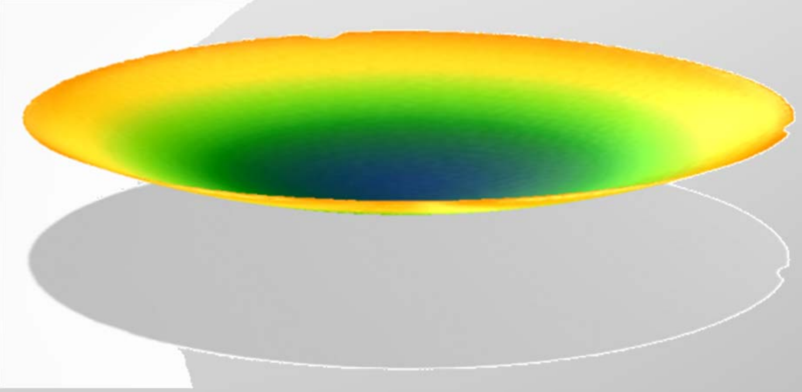

Material removal on a workpiece is governed by a large number of phenomena

$$\frac{dh}{dt}(x,y,t) = \underbrace{k_p}\,\underbrace{\mu(x,y,t)}\,\underbrace{v_r(x,y,t)}\,\underbrace{\sigma(x,y,z,t)}$$

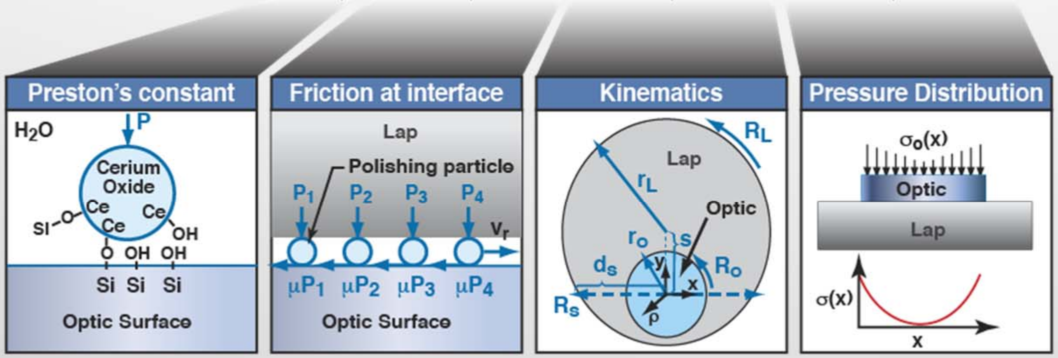

IJAGS 3(1) 14-28 (2012); J. Am. Ceram. Soc., 97 [6] 1720–1727 (2014);
J. Am. Ceram. Soc., 93 [5] 1326–1340 (2010)

Material removal on a workpiece is governed by a large number of phenomena

$$\frac{dh}{dt}(x,y,t)=k_p\,\mu(x,y,t)\,v_r(x,y,t)\,\sigma(x,y,z,t)$$

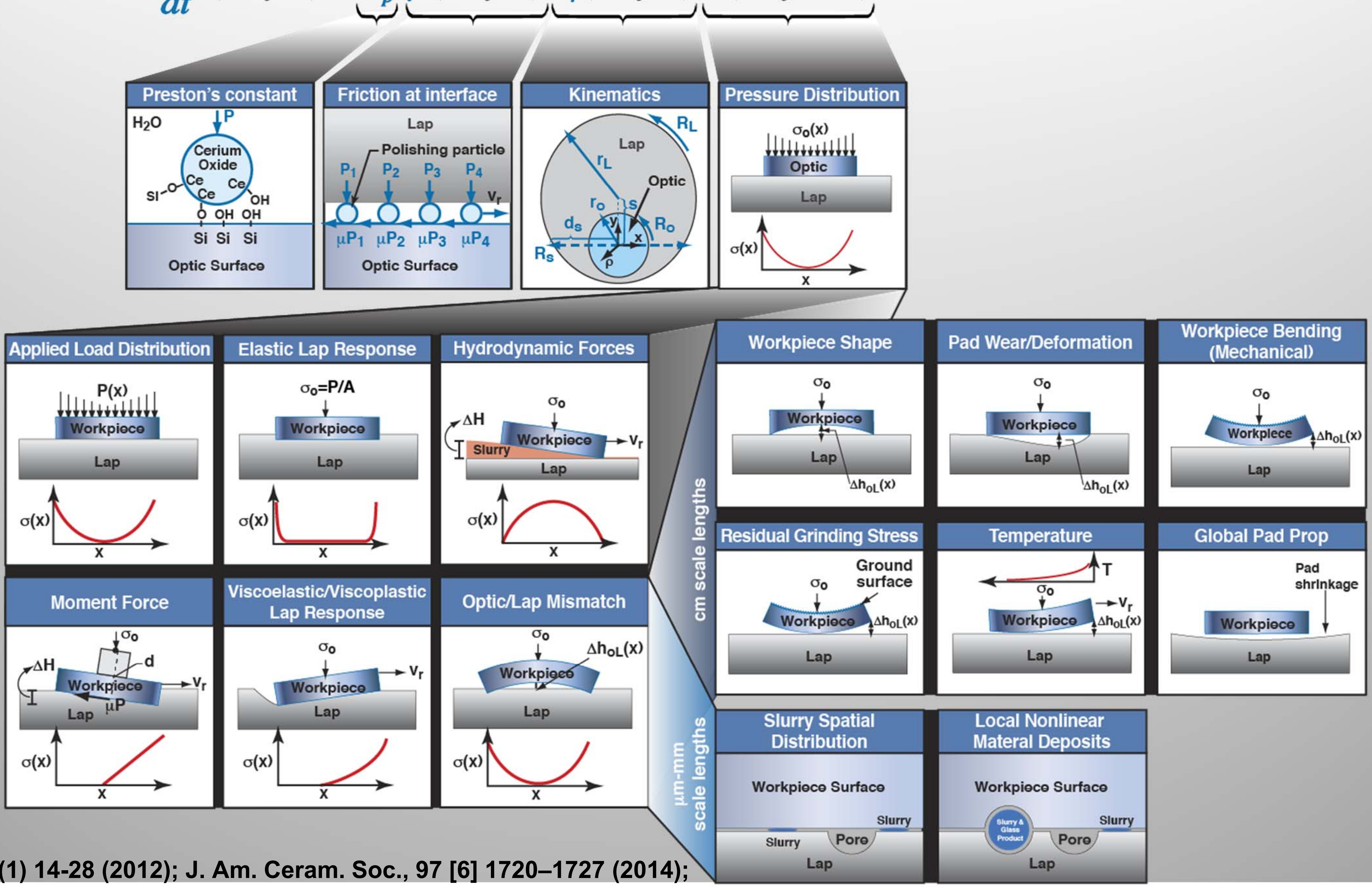

IJAGS 3(1) 14-28 (2012); J. Am. Ceram. Soc., 97 [6] 1720–1727 (2014);
J. Am. Ceram. Soc., 93 [5] 1326–1340 (2010)

The optic/lap can have different modes of contact which strongly influences the amount of material removal

Contact Mode

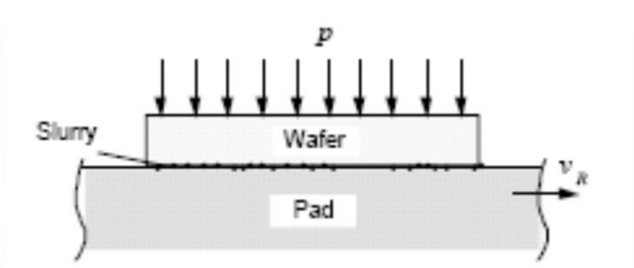

- Friction μ>0.1
- Optic/pad mechanically make contact
- High pressure/low velocity
- Real contact area < nominal contact area
- Plastic deformation of optic/ pad occurs
- Fluid film is discontinuous

Mixed Mode

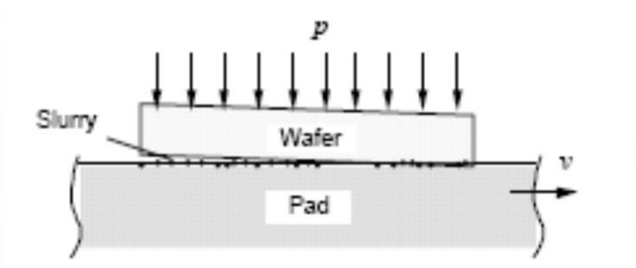

- Friction μ~0.01 to 0.1
- Transition mode during pressure or velocity changes
- Contact is made between lap asperities and optic

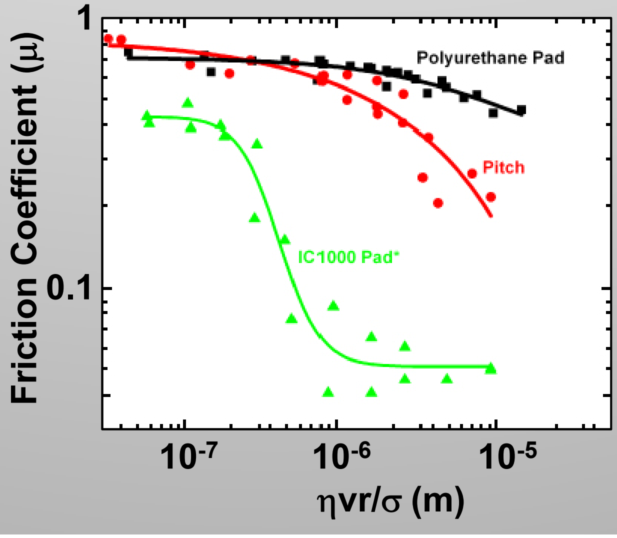

Hydroplaning Mode

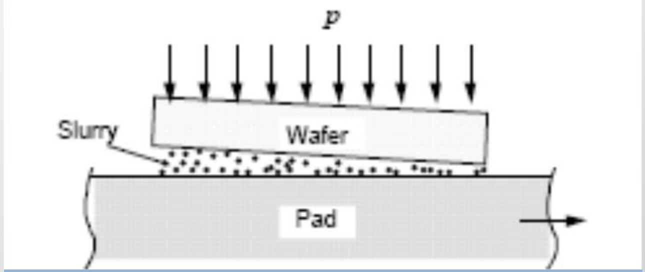

- Friction μ~0.001 to 0.01 (due to shear of viscous fluid)
- Optic glides on fluid film without directly touching pad
- Low pressure/high velocity
- Pressure build-ups in fluid to support normal load of optic
- Pressure gradient is sensitive to wedge angle

J. Lai, Thesis (2001);
J. Am. Ceram. Soc., 93 [5] 1326–1340 (2010)

A geometric model is used to estimate the figure during conventional grinding/polishing

Schematic of geometric model

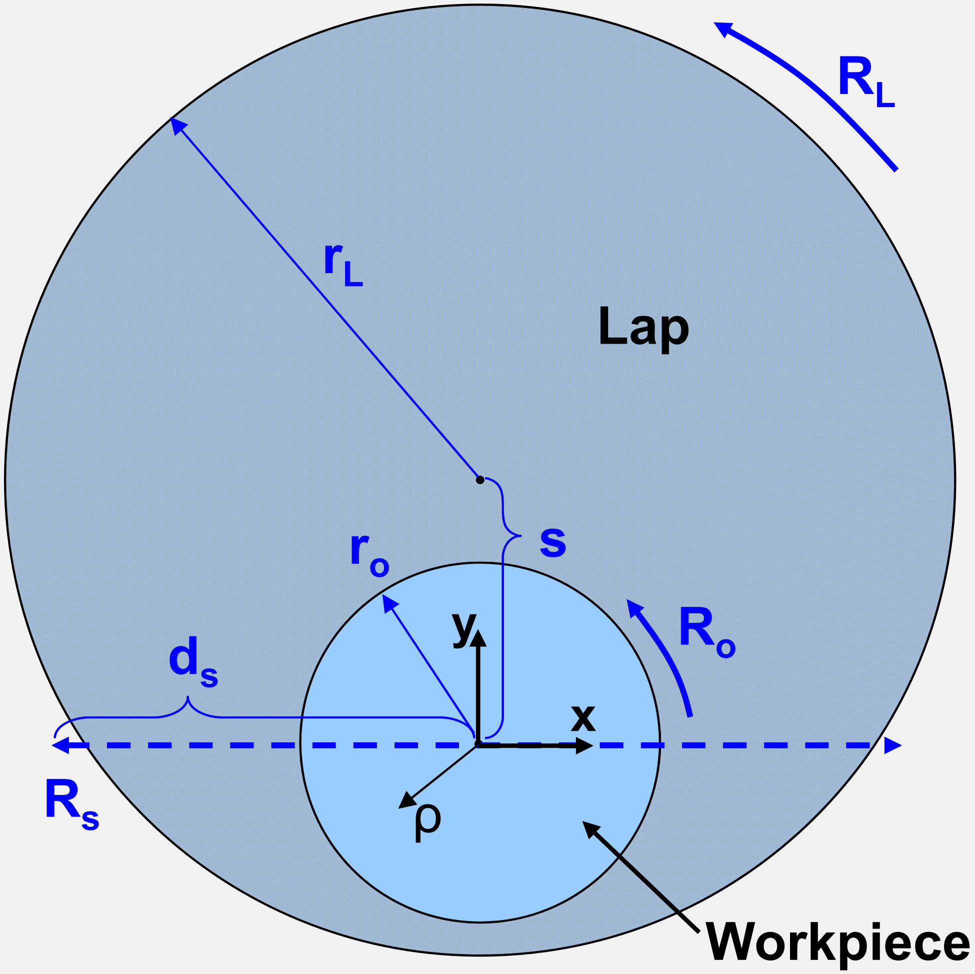

The velocity vector at each point on the optic is the velocity relative to the optic rotation minus the velocity relative to the lap rotation

$$\vec{V} = \left(\vec{R}_{optic} \times \vec{\rho}\right) - \left(\vec{R}_{Lap} \times \left(\vec{\rho} - \vec{S}\right)\right) + \vec{V}_s$$

where the vectors are:

$$\vec{R}_{optic} = \begin{pmatrix} 0 \\ 0 \\ R_{optic} \end{pmatrix} \qquad \vec{R}_{Lap} = \begin{pmatrix} 0 \\ 0 \\ R_{Lap} \end{pmatrix}$$

$$\vec{S} = \begin{pmatrix} d_s \sin\left(\frac{\pi v_s t}{d_s}\right) \\ s \\ 0 \end{pmatrix} \qquad \vec{V}_s = \begin{pmatrix} v_s \cos\left(\frac{\pi v_s t}{2 d_s}\right) \\ 0 \\ 0 \end{pmatrix}$$

$$\vec{\rho} = \begin{pmatrix} \sqrt{x^2 + y^2}\, \sin\left(a\tan(x/y) + 2\pi R_{optic} t\right) \\ \sqrt{x^2 + y^2}\, \cos\left(a\tan(x/y) + 2\pi R_{optic} t\right) \\ 0 \end{pmatrix}$$

J. Am. Ceram. Soc., 93 [5] 1326–1340 (2010)

For a translating workpiece on a viscoelastic lap, stress is highest at leading edge and lowest at end

Schematic of moving workpiece on a viscoelastic lap

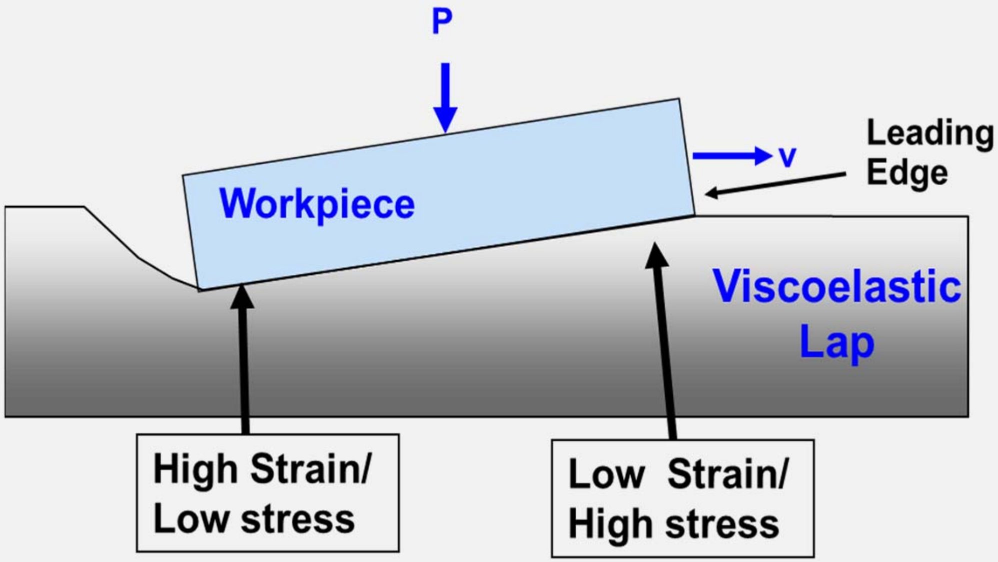

Effect of moment on workpiece tilt

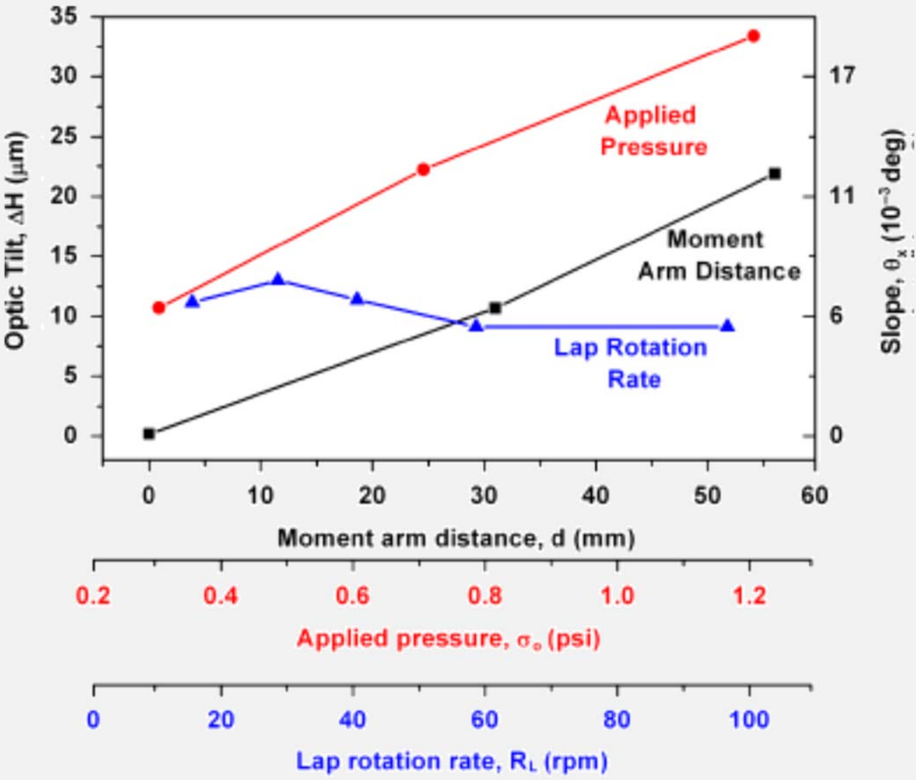

J. Am. Ceram. Soc., 93 [5] 1326–1340 (2010)

Calculated instantaneous stress distribution is qualitatively similar to measured data

Leading edge

Calculated instantaneous Stress profile

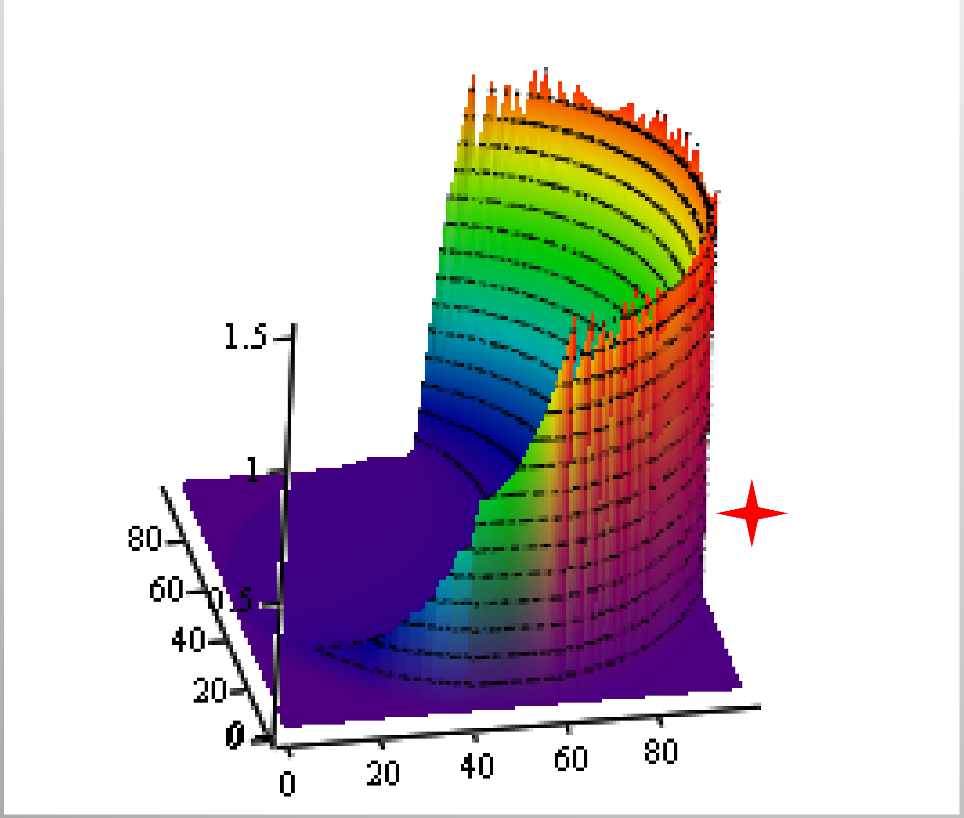

Measured removal on optic when it is not rotated (Exp B)

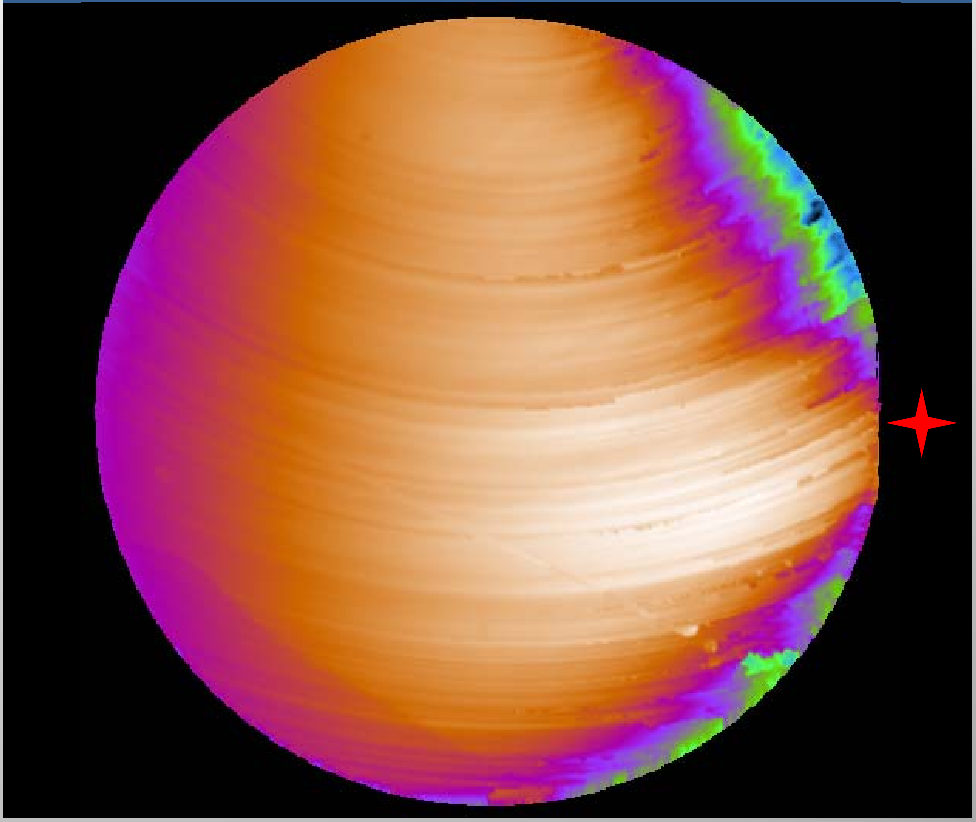

High removal was observed at leading edge consistent with viscoelastic mechanism for causing pressure distribution

J. Am. Ceram. Soc., 93 [5] 1326–1340 (2010)

The pressure distribution across the workpiece can be predicted using the rigid punch indentation model for contact mode

Rigid Flat Punch Model

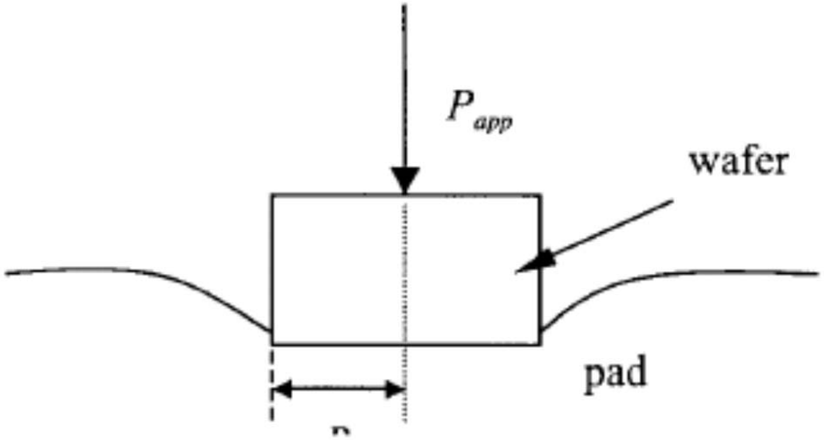

Calculated pressure/load distribution

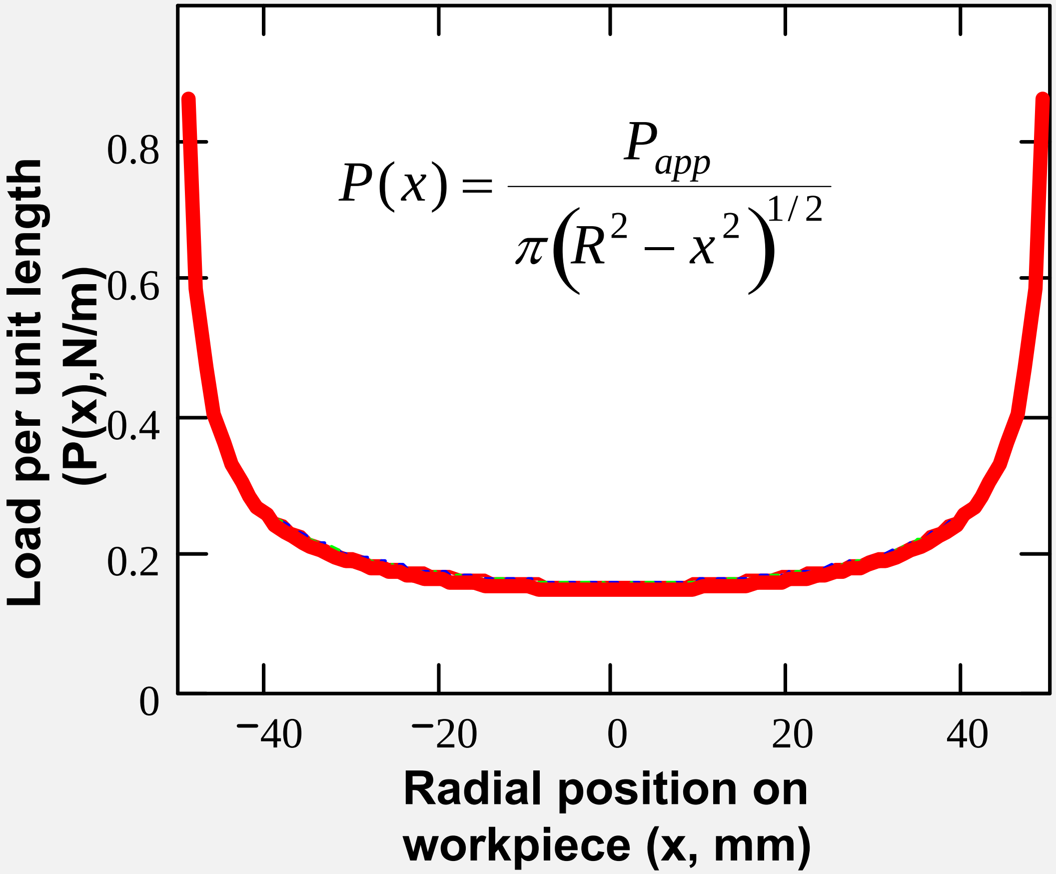

$$P(x) = \frac{P_{app}}{\pi\left(R^2 - x^2\right)^{1/2}}$$

Papp= 25 N; f=0.1; ν=0.1

Our code SurF incorporates these phenomena & does a good job at predicting surface

Experiment **Simulation**

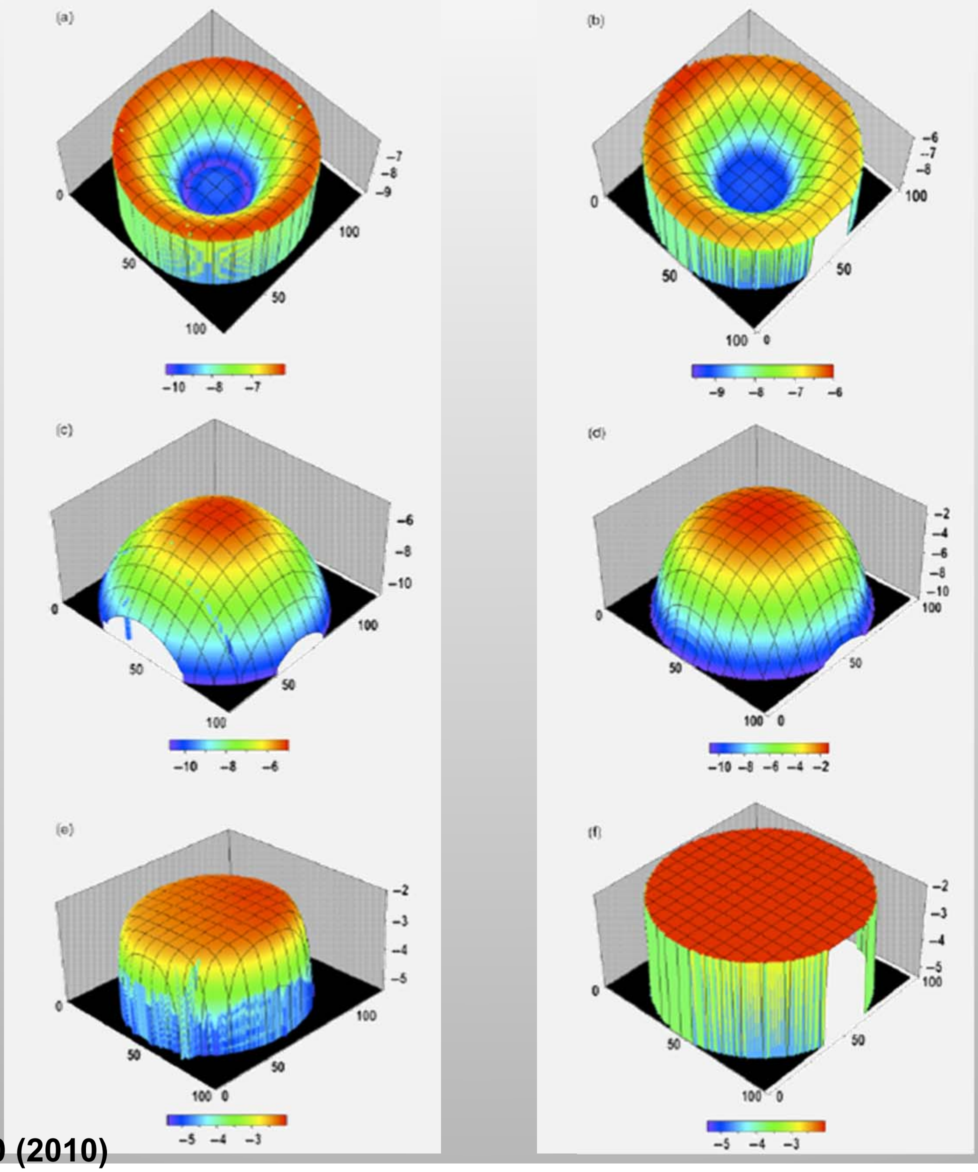

J. Am. Ceram. Soc., 93 [5] 1326–1340 (2010)

Workpiece polishing can cause non-uniform wear of the lap

Shape of lap after polishing workpiece

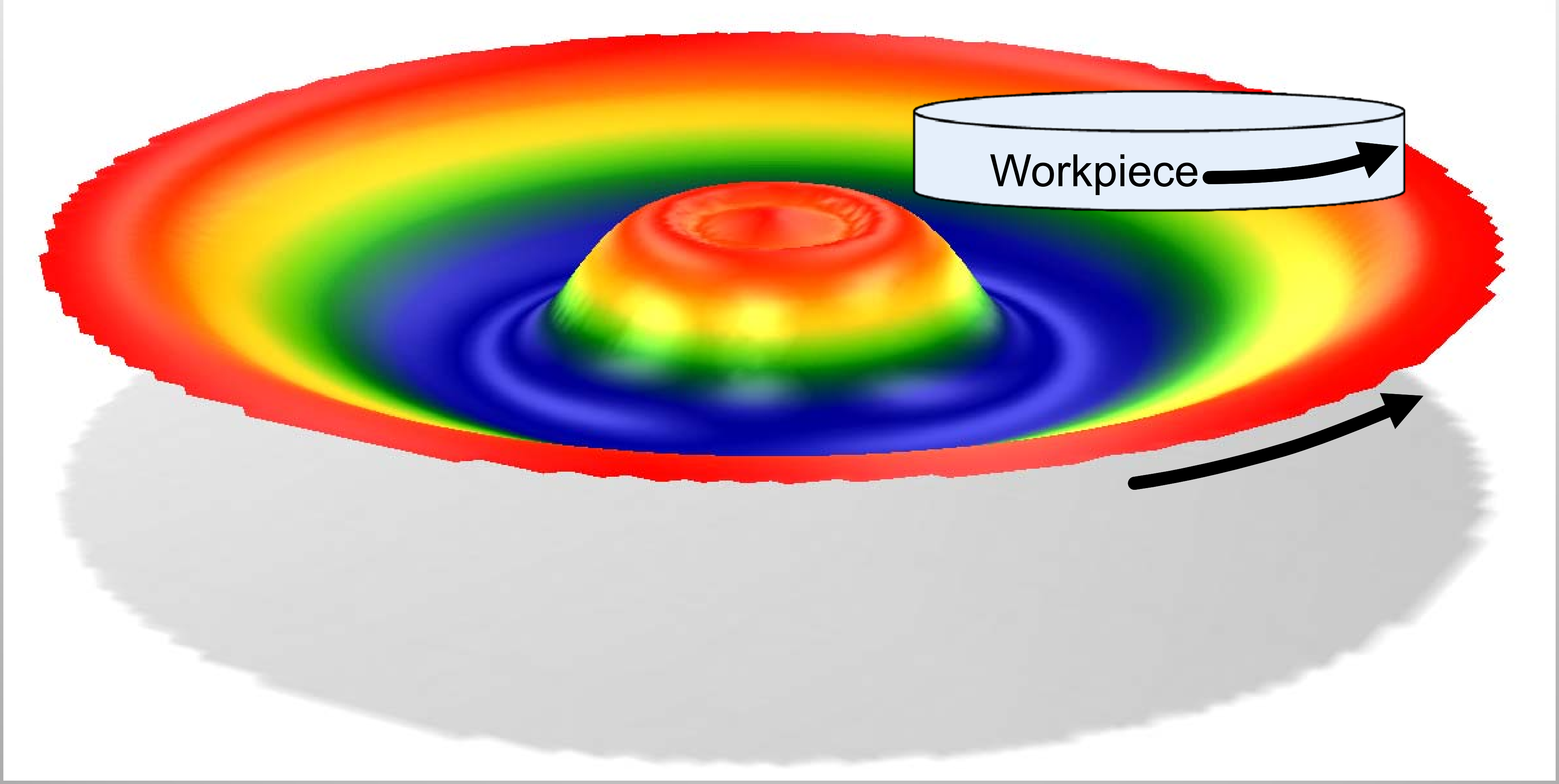

T. Suratwala et. al., IJAGS 3(1) 14-28 (2012).

A novel septum has been designed to counteract non-uniform wear on the pad

Pad wear vs lap radius due to workpiece and engineered septum

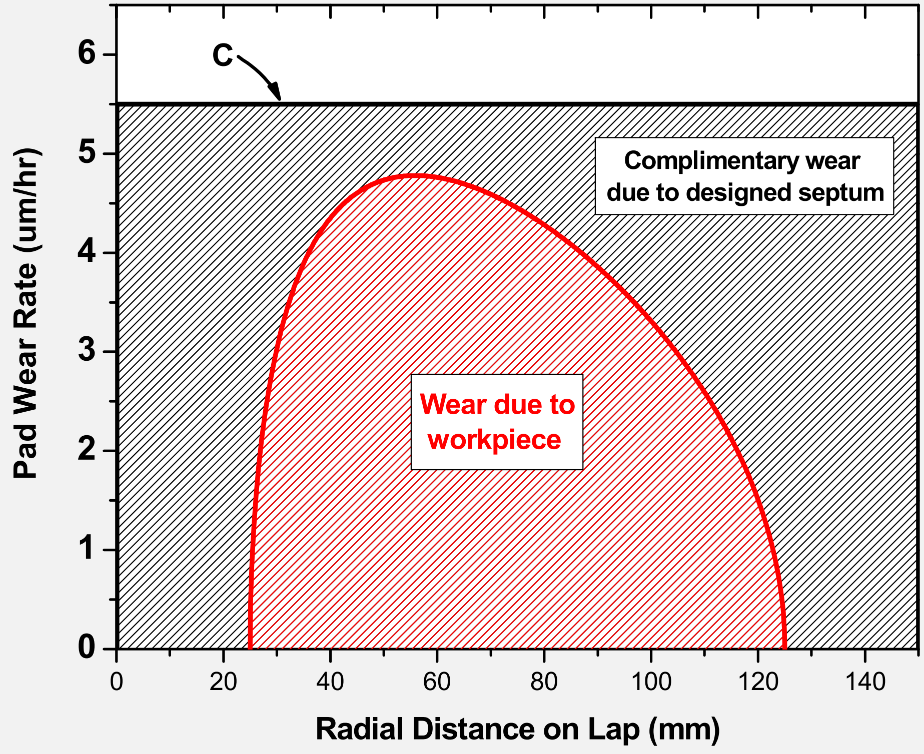

Determined shape of Septum

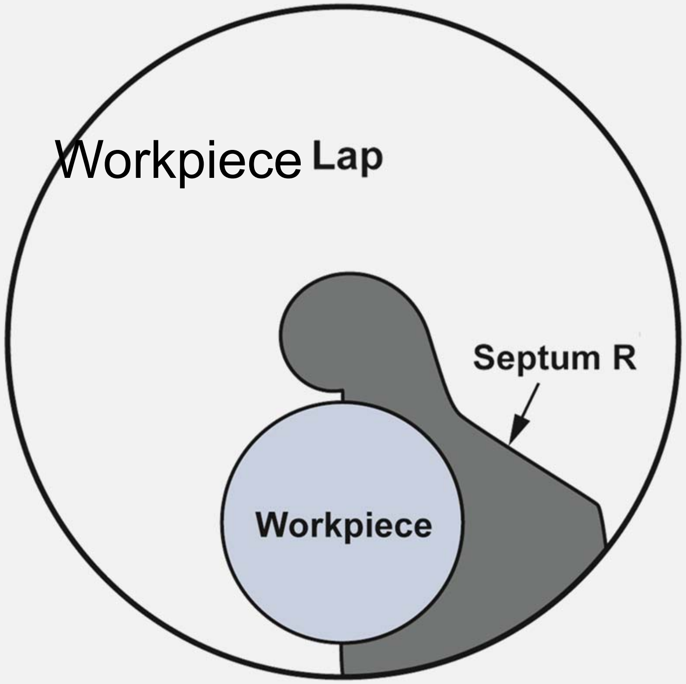

T. Suratwala et. al., IJAGS 3(1) 14-28 (2012).

Temperature variations across workpiece can be minimized using rotated workpiece and septum

Temperature on non-rotated workpiece

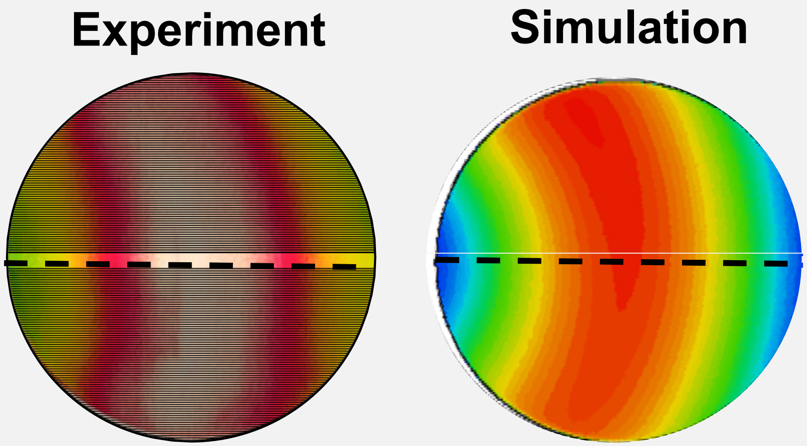
Experiment

Simulation

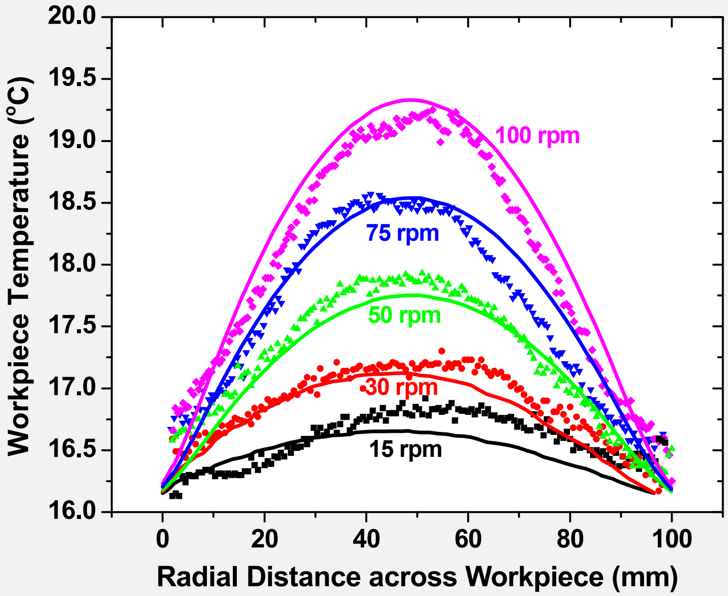

Temperature variations vs polishing configuration

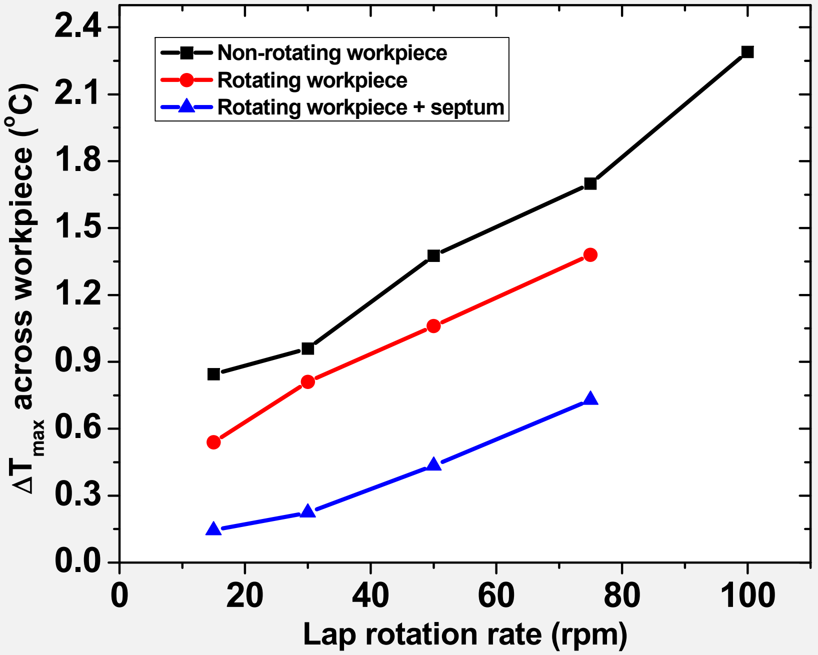

T. Suratwala et al *JACS* 97(6) (2014) 1720.

Pitch (Stiff) Button Blocking (PBB) and Foam (Compliant) Button Blocking (FBB) allows different workpiece response during polishing for High AR workpieces

Pitch Button Blocking (PBB)

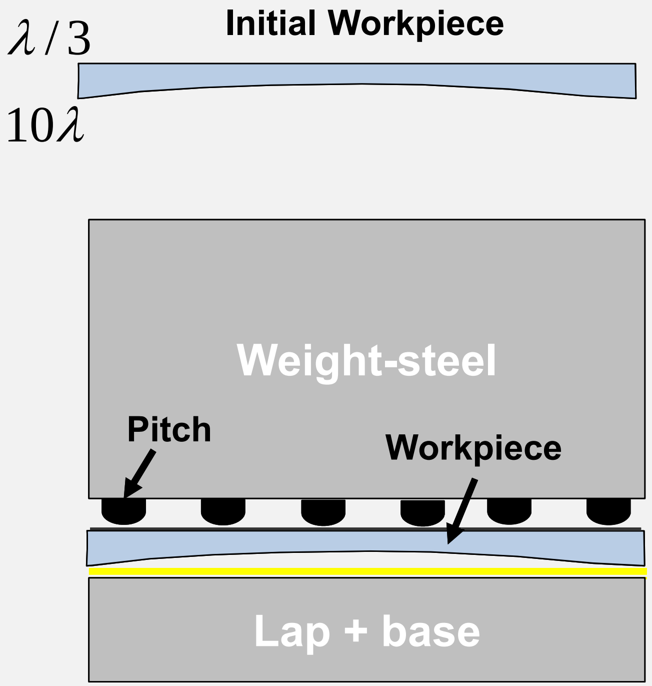

- Workpiece does <u>not</u> <u>conform</u> to lap upon loading
- Allows for surface figure to match lap figure

Foam Button Blocking (FBB)

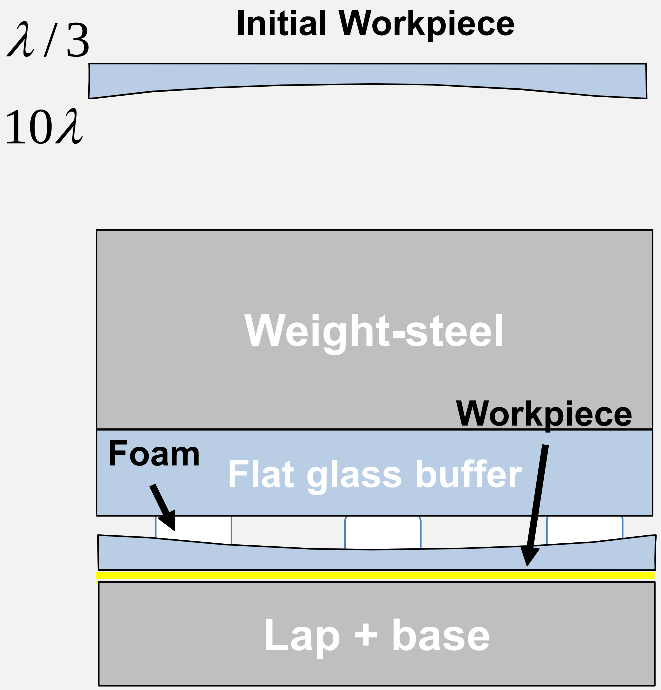

- Workpiece conforms to lap deform upon loading
- Allows for uniform removal on workpiece

Without stiff blocking, thin workpiece deflects during polishing

Thick Workpiece (26 x 26 x 4 cm^3)
FBB (Exp 1034)

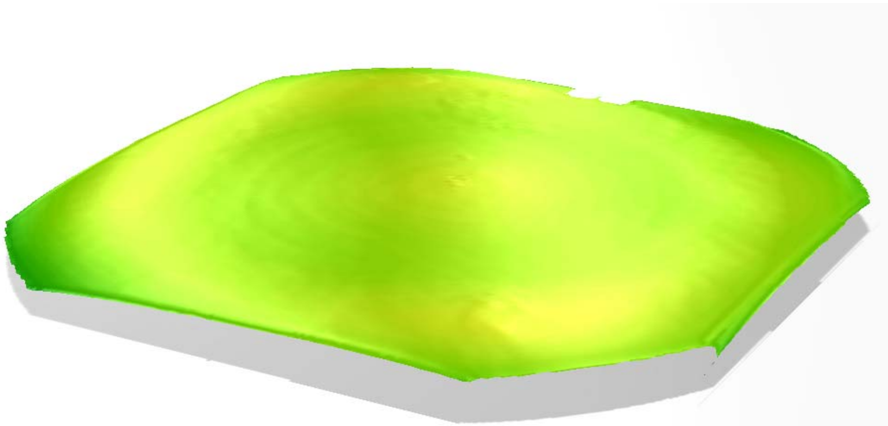

PV_q=0.42 um

Thin Workpiece (26 x 26 x 0.8 cm^3)
FBB (E1019)

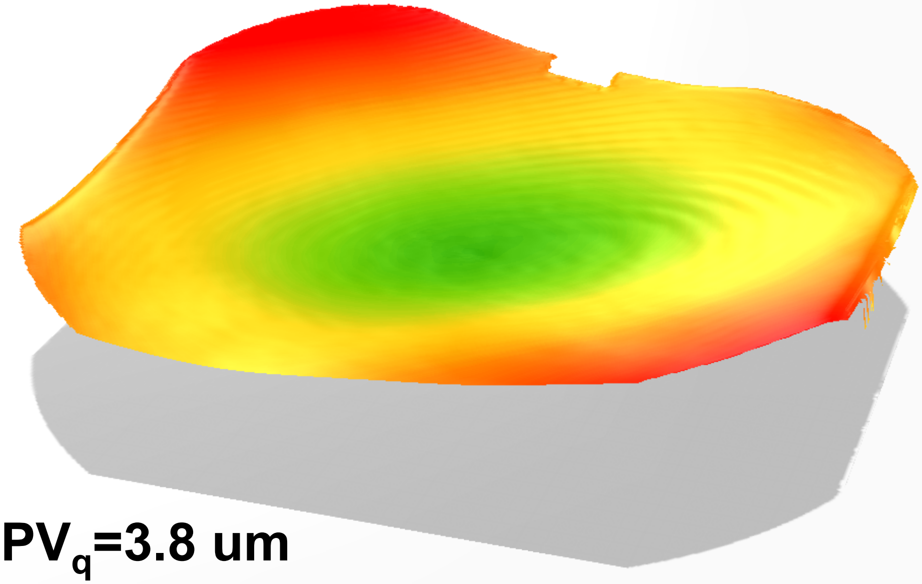

PV_q=3.8 um

Pitch button blocking (PBB) technique prevents workpiece from bending during polishing

265 mm (side) x 8 mm (thick) Fused Silica PBB

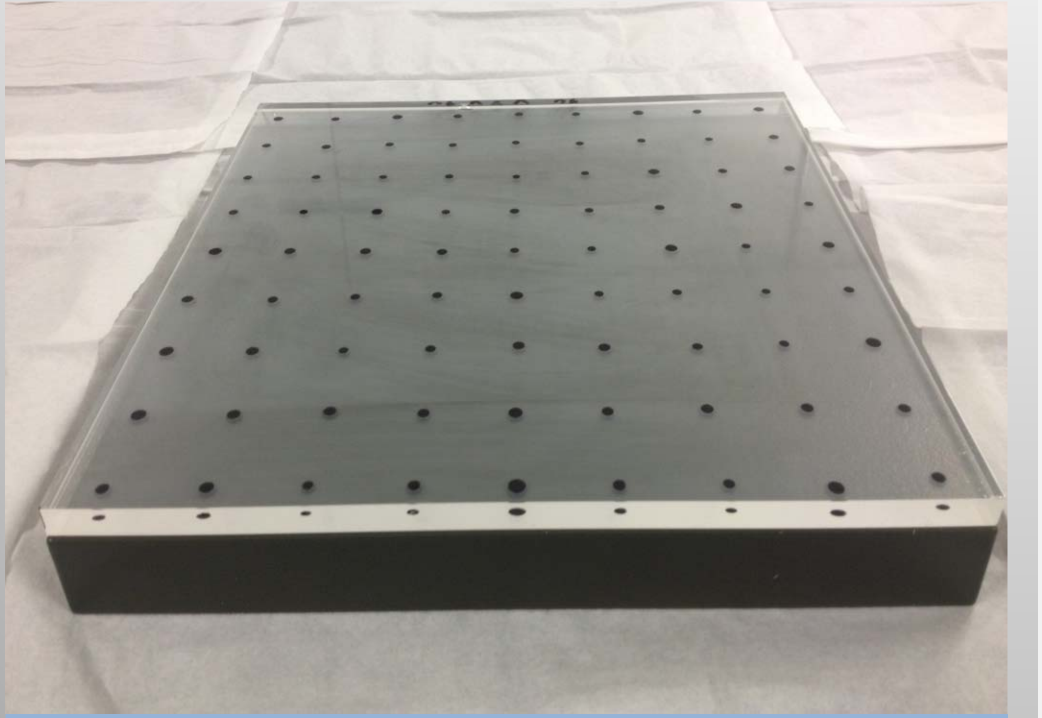

FS	**ΔPV=0.003 μm**
Phosphate	**ΔPV=0.035 μm**

Model vs Experiment: ΔPV as fn of pitch button area fraction

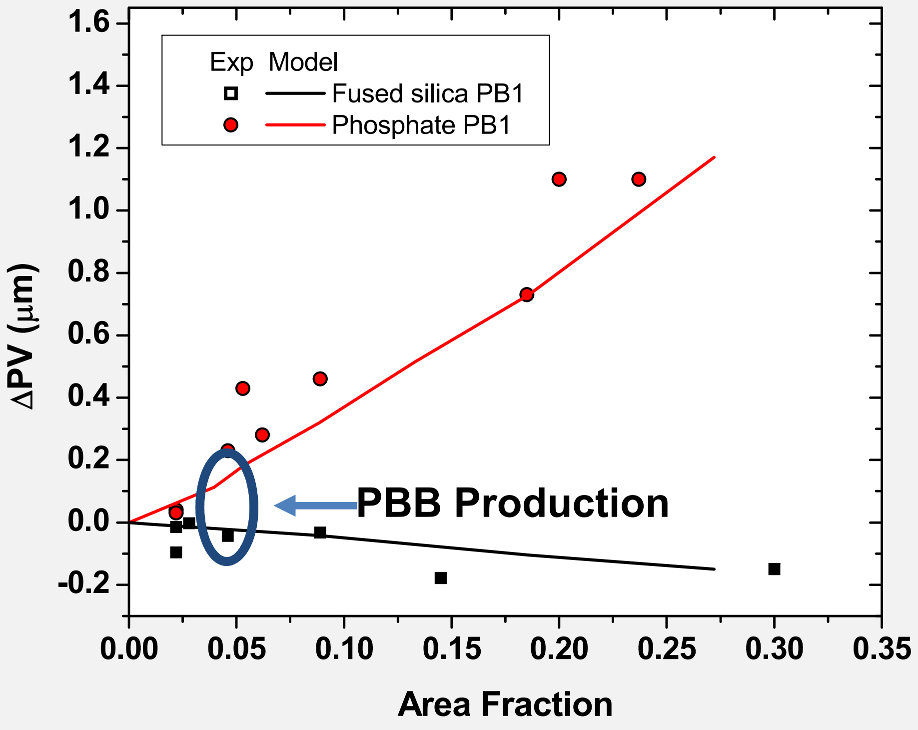

M. Feit et. al., *Applied Optics* 51(35) (2012) 8350-59

Fine scale radial material non-uniformity is caused by local islands of slurry on the pad

Schematic representation of islands of slurry on pad

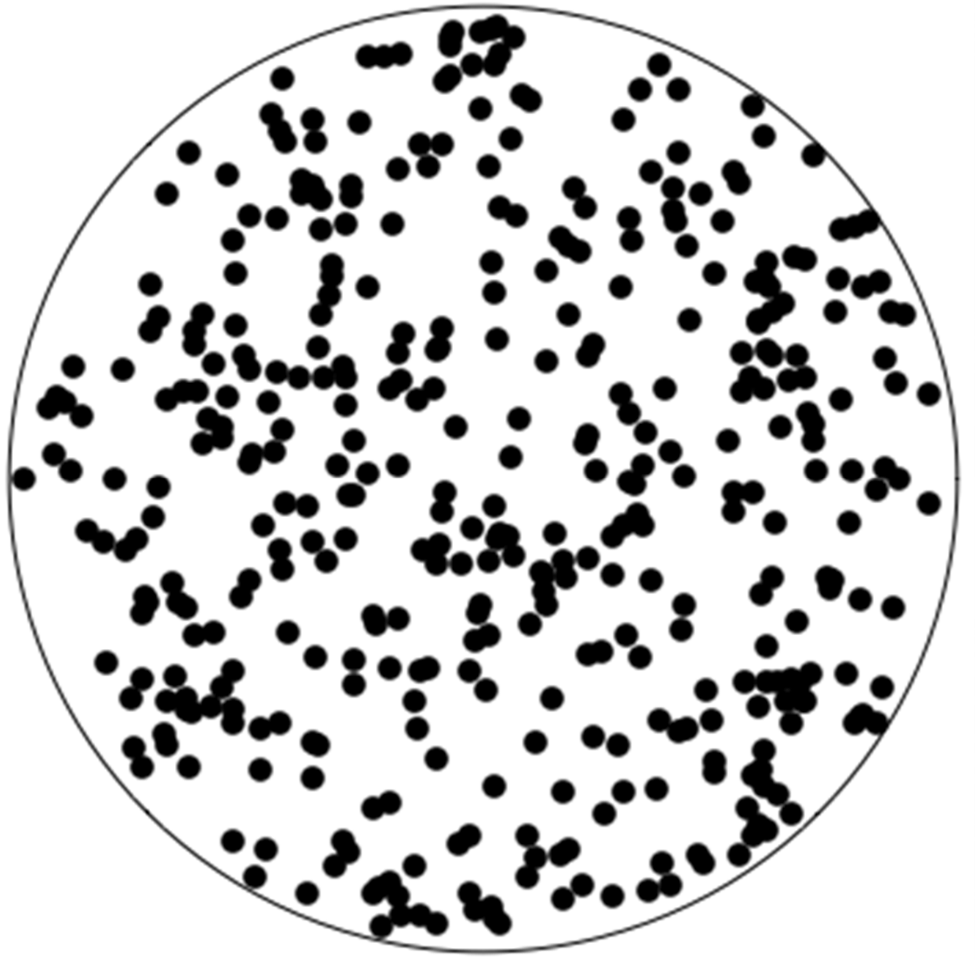

Optical micrograph of grooves observed on non-rotated workpiece

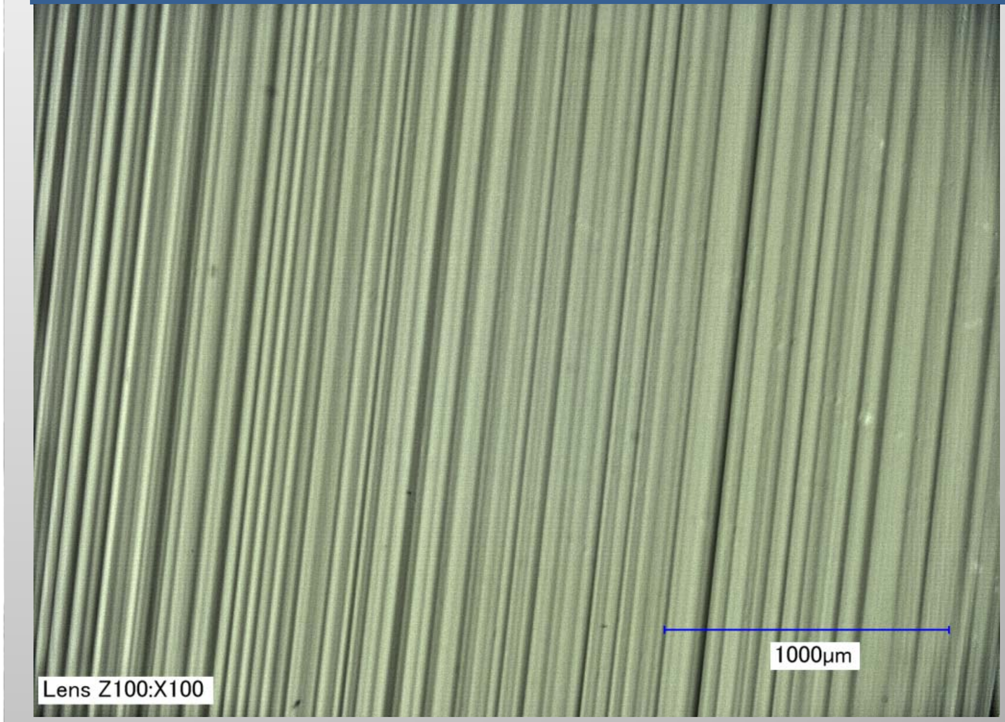

J. Am. Ceram. Soc., 97 [6] 1720–1727 (2014)

Fine scale radial material non-uniformity is caused by local islands of slurry on the pad

Schematic representation of islands of slurry on pad

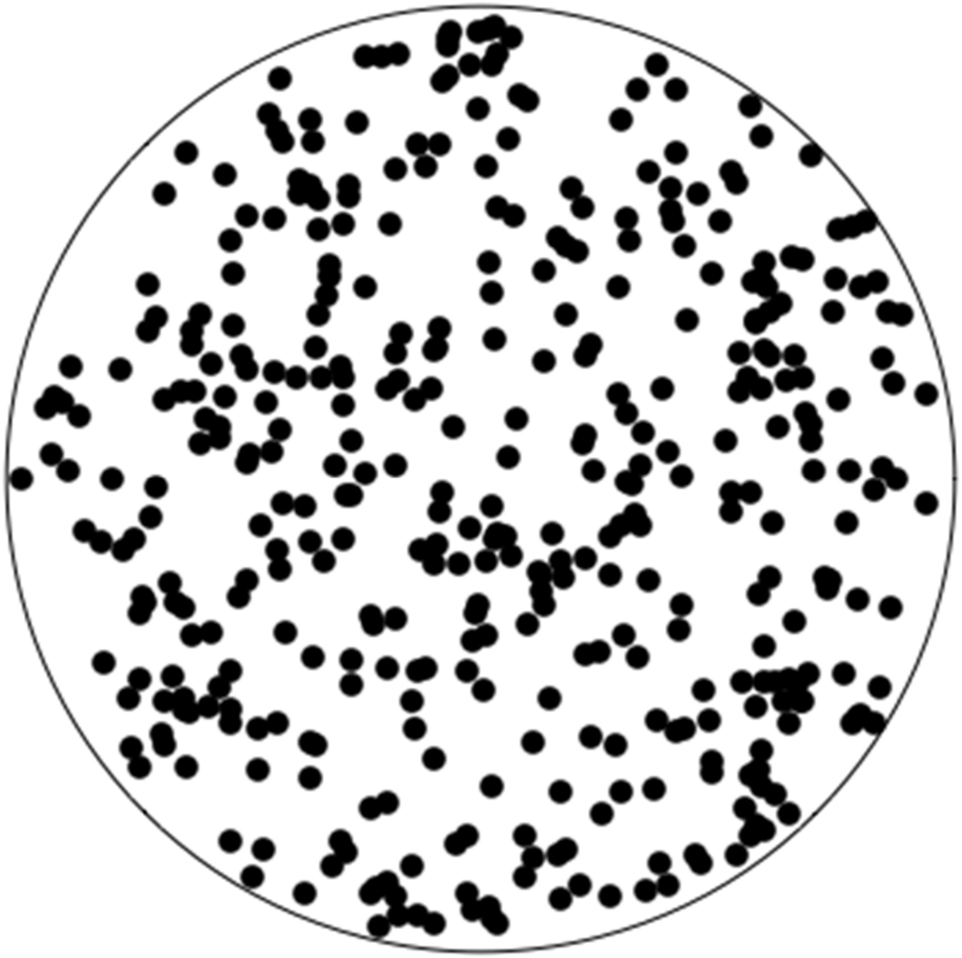

Optical micrograph of grooves observed on non-rotated workpiece

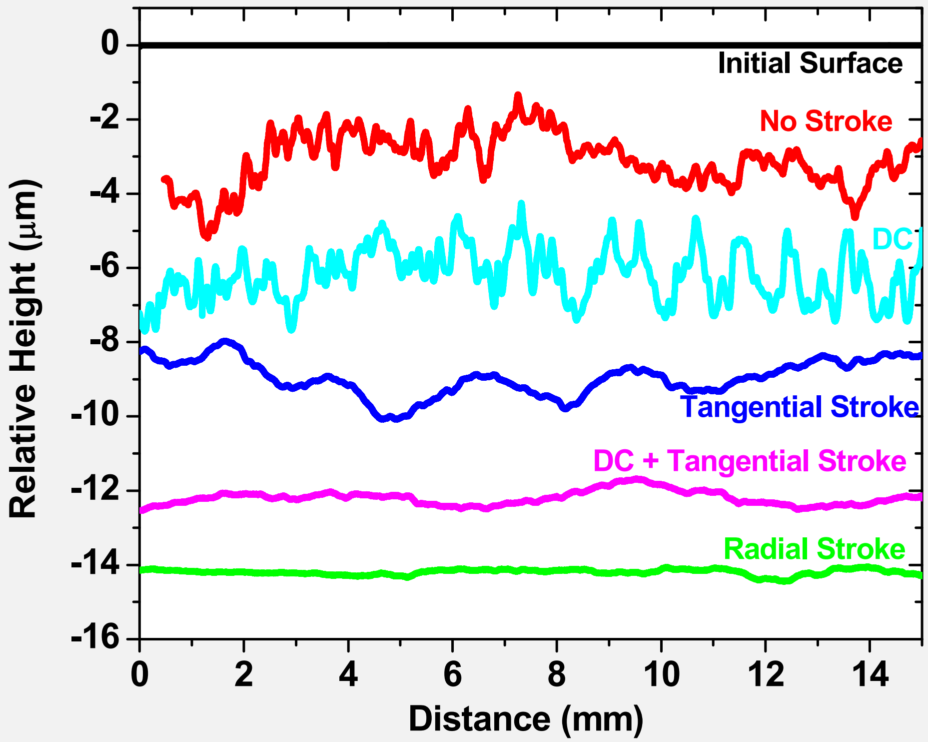

Radial stroke motion dramatically reduces this non-uniformity

J. Am. Ceram. Soc., 97 [6] 1720–1727 (2014)

Residual grinding stress causes a high aspect ratio workpiece to bend

Surface Figure of S2 (Initial)

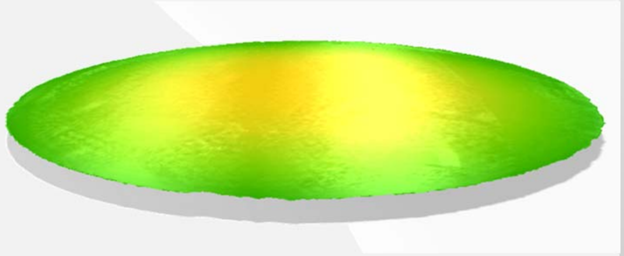

PV_q= -1.29 μm

Surface Figure of S2 (After Grinding S1)

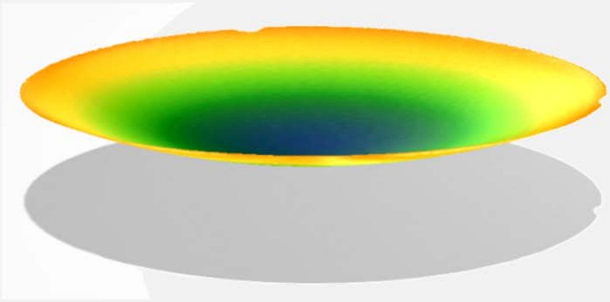

PV_q= 3.65 μm

Surface Figure of S2 (After Grinding/Etching*)

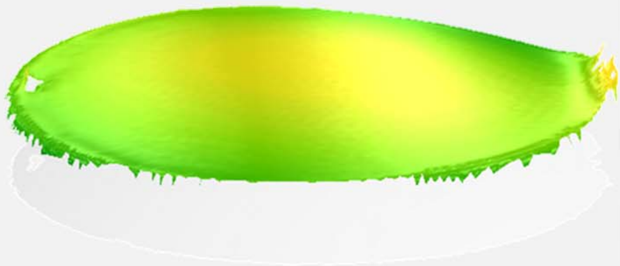

PV_q= -1.16μm

Chemical etching can effectively remove the residual stress and any complications to workpiece-lap mismatch

T. Suratwala, IJAGS 3(1) 14-28 (2012)

Material removal on a workpiece is governed by a large number of phenomena

$$\frac{dh}{dt}(x,y,t)=\underbrace{k_p}\,\underbrace{\mu(x,y,t)}\,\underbrace{v_r(x,y,t)}\,\underbrace{s\,(x,y,z,t)}$$

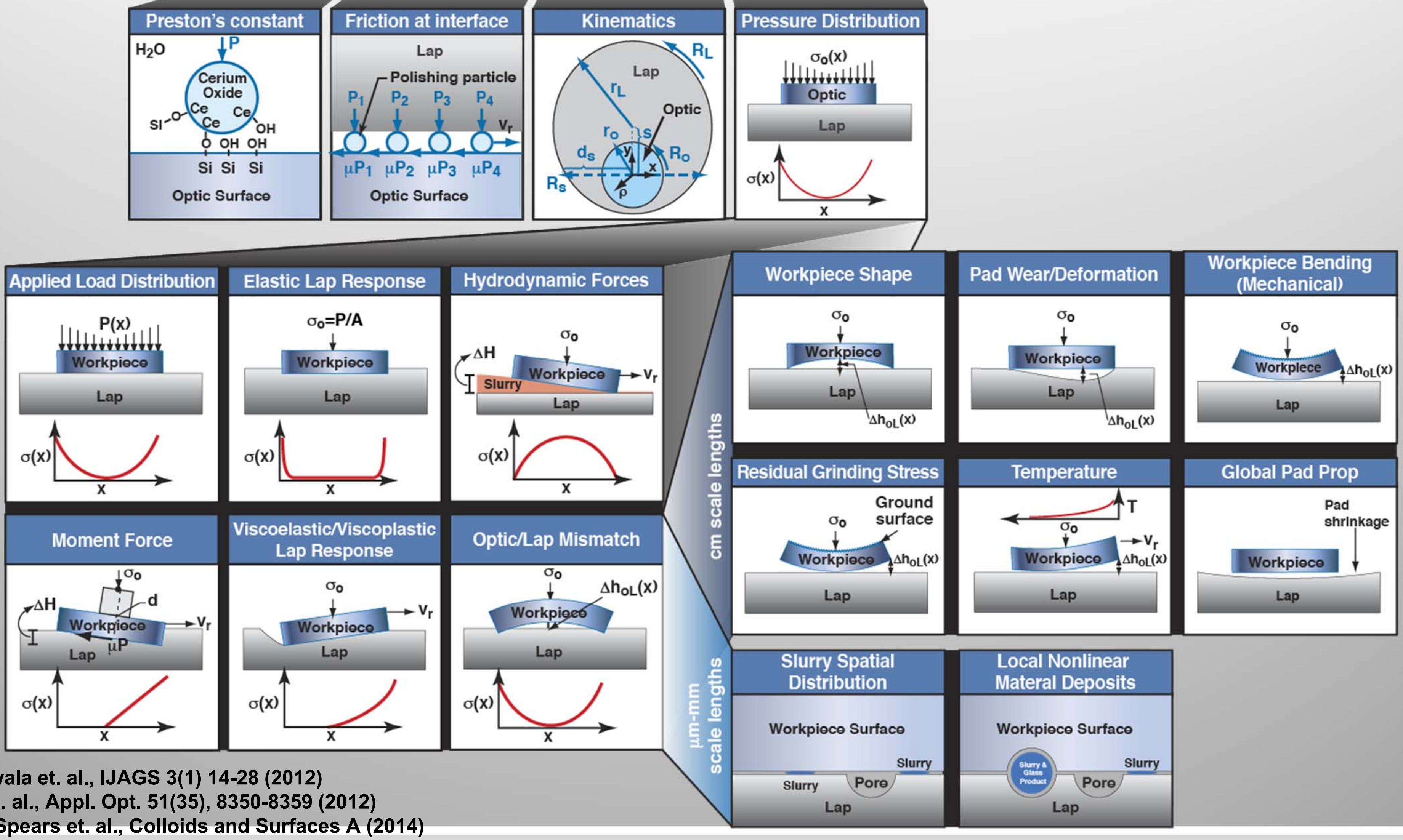

T. Suratwala et. al., IJAGS 3(1) 14-28 (2012)
M. Feit et. al., Appl. Opt. 51(35), 8350-8359 (2012)
R. Dylla-Spears et. al., Colloids and Surfaces A (2014)

The materials science behind grinding & polishing

1. **Sub-surface Damage (scratch/dig)**
2. **Roughness**
3. **Surface Figure**